

Thubalenkosi Vuadens

Dominic Ziegler

November 2025

SILENCE

Seismic Investigation in the Lunar Environment for Cosmic Events



Supervision Team Yara Luginbühl Kirthihan Gobe Simon Stähler Elias Hohl Pascal Kaufmann Ella Villiger

Mission Summary Table

SILENCE		
Mission objectives Detection of gravitational waves with ultra-high precise measurements of the Moon's surface vibrations		
Overall mission profile	bile Deployment of 4 seismic stations on the lunar surface; placed in a 1 km scale array at a distance from a central lander. Communication and power transmission through aluminum cables	
Mission requirements	L0-1: Measure gravitational waves on the lunar surface in the un- observed frequency band L0-2: The payload shall survive in a PSR for at least 10 years	
Payload	4 seismic stations, laser generation module and fiber cables for laser transmission	
Deployment site	Permanently shadowed region (PSR) near a lunar pole	
Power system	Solar array with lithium-ion battery	
Communication	CAN bus powerline communication and double-redundant (Kaband, S-band, UHF) up- and downlink via orbital relay	
Thermal design	Two-stage-compression Joule-Thomson cryocooler for each seismic station	
Mission drivers	Maximum shade time and total power consumption PSR temperature Distance between solar array and seismic stations Data uplink frequency Deployment strategy	
Cost	Estimated to be 1.1 billion EUR	
Schedule	L-class mission, expected to launch in early 2040s, operation for at least 10 years	

Table 1: Mission summary for the SILENCE/LGWA mission

Authorship and Acknowledgements

This report was written by Kirthihan Gobe, Elias Hohl, Pascal Kaufmann, Ella Villiger, Thubalenkosi Vuadens, and Dominic Ziegler as part of the Space Systems Engineering course at ETH Zurich. We thank everyone who was involved in the process, be they friends, colleagues, or others who provided opinions, new ideas, or support. Our special thanks go to our coach Yara Luginbühl, who supported us throughout the process and many of our discussions, and to Dr. Simon Stähler for his feedback and suggestions. We also thank our scientific partner Prof. Jan Harms from the Gran Sasso Science Institute for his insights into the research and development of the Lunar Gravitational Wave Antenna's stations and considerations on their deployment; Dr. Joris van Heijningen from VU Amsterdam for his inputs on station design; Dr. Michiel van Limbeek from the University of Twente for inputs on thermals; and Dr. Philipp Gläser from TU Berlin for his support with site selection and for providing the simulation data on the illumination conditions at the landing site.

Contents

\mathbf{A}	bstra	act	2
Li	\mathbf{st} of	Tables	6
Li	st of	Figures	8
1	Executive Summary		13
2	Mis	sion Objectives	14
	2.1	Mission Statement	14
	2.2	Primary Objectives	14
		2.2.1 Measuring gravitational waves	14
		2.2.2 Show feasibility of a mission in a PSR	14
	2.3	Secondary Objectives	15
		2.3.1 Find out about seismic activity on the Moon	15
		2.3.2 Strengthen European scientific presence in space	15
	2.4	Constraints	15
	2.5	Stakeholder Analysis	16
3	Mis	sion Requirements	18
	3.1	Overview	18
		3.1.1 Requirements L0 to L2	18
	3.2	Environment	21
		3.2.1 Key environmental requirements	21
		3.2.2 Radiation, charging, lunar dust and micrometeorites	21
	3.3	Deployment	22
		3.3.1 Lander	22
		3.3.2 Rover mobility	22
	3.4	Power	22
	3.5	Communication	23
	3.6	Computing	23
	3.7	Thermal	23
		3.7.1 Lander	23
		3.7.2 Measurement stations	24
		3.7.3 Rover	24
	3.8	Key and Driving Requirements	24
4	Pay	load Description	26
	4.1	Payload Mass, Volume, Power and Data Generation Budgets	26
	4.2	Payload Measurement Principle and Architecture	29
		4.2.1 Laser	29
	4.3	Payload Estimated Performance	30

4 Contents

	4.3.1 Background noise estimates
4.4	Cable Configuration
5 Mis	ssion Design
5.1	Product Tree
5.2	Mission Design Drivers
5.3	PSR Selection
	5.3.1 Baseline PSR: landing and solar panel deployment on "nearby" hill
	5.3.2 PSR for alternative power concept (RTG)
	5.3.3 Landing and solar panel deployment on "nearby" hill: alternative PSR at
	south pole
	5.3.4 RTG power source: alternative PSR at north pole
	5.3.5 PSR selection: summary
5.4	Deployment
0.1	5.4.1 Overview
	5.4.2 Baseline deployment strategy
	5.4.3 Baseline rover: Venturi Astrolab FLEX
5.5	Power System
	5.5.1 Power generation and storage
	5.5.2 Power control and distribution
	5.5.3 Deployment power
5.6	Communication System
	5.6.1 Deployment operation
	5.6.2 Inter-station communications
	5.6.3 Up- and downlink communications
5.7	Computing
5.8	Thermal Design
	5.8.1 Lander
	5.8.2 Rover
	5.8.3 Measurement stations
	5.8.4 Radiator dust mitigation
5.9	Alternative Mission Design
9.9	5.9.1 Alternative power sources
	5.9.2 Alternative destination and rover sharing
F 10	5.9.3 Alternative deployment strategies
5.10	Budgets
	5.10.1 Data
	5.10.2 Link
	5.10.3 Power
	5.10.4 Thermal
	5.10.5 Mass
	5.10.6 Volume to be transported by rover
5.11	Compliance Matrix
5.12	Interface Descriptions
	5.12.1 Power interfaces
	5.12.2 Data and communication interfaces
	5.12.3 Structural interfaces
	5.12.4 Thermal interfaces
5 12	TRL Assessment
5.15	Risk Assessment
	5.15.1 Thermal risks
	5.15.2 Landing risks

Contents 5

		5.15.3 Deployment risks	78
		5.15.4 Communication risks	80
		5.15.5 Computing risk	80
		5.15.6 Power risk	80
6	Mis	sion Operations & Ground Segment	81
Ŭ	6.1	Concept of Operations	81
	0.1	6.1.1 Deployment phase	81
	6.2	Science Phase	82
	0.2	6.2.1 Payload data flow	82
	6.3	Ground Segment	83
	0.0	6.3.1 Earth link	83
		6.3.2 Data processing	83
		6.3.3 Gravitational wave science	83
		6.3.4 Operations	84
	6.4	Launch Vehicle	84
	0.4	6.4.1 Lander and launch candidate combination: ESA Argonaut and Ariane 64.	85
		6.4.2 Starship; launch and landing candidate	86
		17	87
		6.4.4 Conclusion	87
7	Maı	nagement	88
	7.1	Team Management	88
	7.2	Schedule	90
	7.3	Cost Estimation	90
		7.3.1 Assumptions	91
	7.4	Life Cycle Assessment	93
		7.4.1 Goal and scope	93
		7.4.2 Results and discussion	94
٨	Con	nmunication and Computation: Figures and Estimates	96
А		Relay visibility time estimation	97
		Other estimations	98
	A.2	Other estimations	90
\mathbf{B}		litional Material on Deployment	100
		Propellant required for a 6-Minute lunar hover	100
	B.2	FLEX rover aboard an Ariane 6 geometry check	101
\mathbf{C}	\mathbf{LC}	A Additional Plots	104
D	\mathbf{Use}	of Artificial Intelligence	106
Bi	hlio	graphy	107
	~1105	o- ~r/	

List of Tables

1	Mission summary for the SILENCE/LGWA mission	1
2.1 2.2	Mission constraints for the proposed SILENCE mission	16 17
3.1	Traceability between L0 science objectives and L1 mission requirements for LGWA payload	18
3.2	Traceability between L1 Mission requirements and L2 system requirements for LGWA payload	21
3.3	Power requirements	23
4.2	Main characteristics per station. A star * in the reference or comment column indicates that this estimate has been made by Jan Harms based on the current (late 2025) R&D state of the seismic sensors and stations	27
4.4	Mass budget composition per station. A star * in the reference or comment column indicates that this estimate has been made by Jan Harms based on the as of late	
4.6	2025 current R&D state of the seismic sensors and stations	$\frac{28}{28}$
4.7	Comparison of options for laser positioning. Scores: 0–2, 2 is best	30
5.1	Areal summary of temperature, slope, and visibility over selected deployment site with 1 km diameter	38
5.2	Areal summary of temperature, slope, and solar illumination over a circle with $100 \text{ m}/200 \text{ m}$ radius around the selected landing site. Surface Roughness (SR) calculated over an area with 50 m radius around landing site	38
5.3	Areal summary of temperature, slope, and visibility over selected deployment site with 1 km diameter. Temperature data from study with finer seasonal binning (FB) included (6 seasonal bins) [1]. Surface roughness calculated over an area with a	
5.4	radius of 50 m around landing site	40
	100 m/200 m radius around the selected landing site. Surface Roughness calculated over an area with 50 m radius around the landing site	42
5.5	Comparison of estimated characteristics of the Single Station Rover, capable of carrying one station at a time, and the Four Station Rover, capable of carrying all stations at once. Derived by looking at the Perseverance, Endurance, and Viper rovers. While these figures were used for the deployment trades before including the FLEX rover into our baseline, they are still used as a reference value in some chapters, as power consumption of the FLEX rover could not be determined. While the FLEX rover should be self-sustaining given enough illumination, we have no estimate on range in the shade. While we have assumed to have to supply 200 W to the FLEX rover during deployment, this has not driven battery or solar array size	
	section 5.5	48

List of Tables 7

5.7	Comparison of landing site options with respect to various parameters, associated influence factors, and weight of importance. The cross marks the option favorable	
	for the factor on the corresponding row. Weights are are summarized over all factors	
	favoring one variant, according to their impact ¹	50
5.9	Comparison of a scenario where the rover has its own battery and one where its	
	connected via cable to the lander ¹	52
5.10	Comparison of memory and telemetry configurations in seismic stations. Cells marked	
	with "x" signify an advantage of the option in the given aspect ¹	57
5.11	Comparison of direct-to-Earth and lunar orbital relay communication architectures.	
	Cells marked with "x" signify an advantage of the option in the given aspect ¹	58
5.12	Comparison of options for lander thermal system. Scores: 0-2, 2 is best	61
	Data generation, collection and storage. This includes margins as described in Ap-	
	pendix A	67
5.14	Relevant figures of the link budget calculation, together with the transmission pa-	
	rameter estimations. The included margin in these values is explained in Appendix A.	68
5.15	LGWA power budget summary during operation	68
	LGWA power budget summary during deployment	69
5.17	Thermal budget of the lander	69
5.18	Thermal budget of the rover	69
5.19	Thermal budget of the seismic station of the 250K radiator	69
5.20	Thermal budget of the seismic station of the 87K radiator (the power is small compared to the heat capacity of the radiator at cycle timescales, therefore, only the	
	average power is considered)	69
5.21	Thermal budget of the seismic station of the 51K radiator (the power is small compared to the heat capacity of the radiator at cycle timescales, therefore, only the	
	average power is considered)	69
	LGWA mass budget summary	70
	LGWA summary of volume to be deployed by rover	70
	System requirements summary	71
5.26	Technology readiness level (TRL) table of the components of SILENCE. Based on	
	NASA TRL scheme [2]	74
6.1	Data flows between the rover and the ground segment during seismic station de-	
	ployment (chronological order)	82
7.2	L4 Mission timeline	90
7.3	Preliminary cost model for the SILENCE mission	93
A.1	Detailed data generation numbers	96
A.2	Communication link calculation data	99

4.1 4.2	Conceptual Overview of Seismic Station Architecture [3]	30
4.3	Sketch of cable cross-section including glass fiber cable and aluminum cables	32
5.1 5.2 5.3 5.4	Product tree for the SILENCE mission	34 36 37 38
5.5	Fraction of solar disk visible at a height of 2 m above ground at the chosen landing site simulated over the year 2025 with time steps of 2 hours (Image: courtesy of Dr. Philipp Gläser)	39
5.6 5.7	Lunar south pole region in polar stereographic projection	39
5.8 5.9	and maximal angle for incoming radiation from crater walls	41
5.10	cells as power source. Polar stereographic projection	42
5.11	Polar stereographic projection	42
5.12	r=100 m, green: r=50 m). Polar stereographic projection	43 45
5.13	Schematic for landing on a hilltop outside the PSR (Baseline): after landing, the seismic stations need to be moved into the PSR.	46
5.14	The schematic displays the cabling: The four stations are connected to form a chain attached to the lander preflight, such that they can be placed down sequentially on a single drive into the PSR with multiple stops. Each cable link has its own cable drum. It could be considered to deploy the two different cables per segment from	46
5.15	the same drum or even have both connections in the same cable	$\frac{40}{47}$

5.16	Schematic for the landing inside a PSR: after landing either before or after deploying the stations, the solar array structure needs to be moved to the hilltop and deployed	40
	there	49 53
5.19	continuous power generation without a rotating mechanism	54 55
	Schematic of the cooling system of the measurement stations	62
	3D View of the proposed open tapered honeycomb structure for the seismic station radiator panels. The reflective vertical inclined parts honeycomb structure is shown in the figure, the emitting flat plate mounted at the bottom is not shown here	63
5.23	Optical simulation of the open tapered honeycomb radiator (3D view) Optical simulation of the open tapered honeycomb radiator (bottom view) A signal, power, and laser connection diagram of a seismic station. All stations will	64 64
	work the same, but the last station in the chain will not have cable connections for outgoing power, communications, and laser	72
	A signal, power, and laser connection diagram of the lander	72 76
6.1	Concept of operation for the SILENCE mission	81
6.2	Data flow concept while SILENCE is in nominal operation. For clarity, only one out of four seismic stations is pictured	83
6.3	Data flow concept for SILENCE emergency handling. For clarity, only one out of four seismic stations is pictured.	83
6.4	Concept for the mission link architecture, using LunaNet compatible data providers [7]	84
6.5 6.6	Concept Image of the ESA Argonaut Lander [8]	85
	No collisions occurred. Screenshots from Onshape.	86
7.1 7.2	Different roles needed for managing the SILENCE mission	89 91
7.3	Normalized environmental impact comparison between Ariane 64 and NASA SLS across three impact categories for one launcher	94
7.4	Normalized environmental impacts of Ariane 64 and SLS rockets across climate change, abiotic depletion, and ozone depletion. The bars show subcategory contributions, with percentages indicating each subcategory's share of the total impact per rocket	95
A.1	Using Desmos online graphing calculator, it is possible to estimate the coordinates and thus the angle where a relay satellite at altitude 1500 km rises above 20 deg above the horizon.	97
В.1	Illustration showing the FLEX rover with suited humans. The red ligns are all equally long, around 1.7m, hinting that a rover length of 3.8m could be right [5].	101
B.2	Image showing the sketch used to cut a 3.8x2.6x1.8 cuboid to the shape of the rover dummy in Figure 6.6. Screenshots from Onshape	101

В.3	Screenshot from Oneshape showing a 3.8x2.6x1.7m Box (FLEX rover dimensions)	
	inside a 4.6m diameter, 5m high cylinder (dimensions of non-conical part of Ariane	
	6 payload fairing of the single launch short fairing [9]). Red dots represent corners	
	constrained to lie on the cylinder boundary. The part exceeding the 5m cylinder	
	would not collide with the conical part of the Ariane 6 payload fairing [9]	101
B.4	Sketch showing vertical rover mounting inside the payload fairing, appart from the	
	main lever, additional structures supporting the rover until egress could be necessary	.102
B.5	Images showing the FLEX rover dummy inside a model of the dual launch short	
	DLS fairing of the Ariane 6. Only the top fairing bay is shown. The bottom 3m (as-	
	sumption on Argonaut lander height made based on Figure 6.5) of the top fairing	
	bay are assumed to be occupied by the Argonaut Lander. The rightmost graphic	
	includes a sketch of a tiltable telescopic ramp. The payload fairing has been mod-	
	eled according to [9]. A screenshot of the CAD sketch can be found in Figure B.6	
	Screenshots from Onshape.	102
B.6	Sketch used to model the relevant section of the payload fairing in Figure B.5.	
	Screenshot from Onshape	103
C.1	Climate change impact of Ariane 64 and SLS launch system for the chosen functional	
0.1	unit with subcategory breakdown	104
C.2	Abiotic depletion potential of Ariane 64 and SLS launch system for the chosen	
	functional unit with subcategory breakdown	105
C.3	Ozone depletion potential of Ariane 64 and SLS launch system for the chosen func-	
	tional unit with subcategory breakdown	105

Acronyms and Abbreviations

ADCS Attitude determination and control system

ADP Abiotic Depletion Impacts

BER Bit error rate
BOL Beginning-of-life

CAN Controller area network

CC Climate Change

CCSDS Consultative Committee for Space Data Systems

CBE Current Best Estimate
ConOps Concept of Operations

cryo-CMOS Cryogenic complementary metal-oxide-semiconductor

DAU Data aquisition unit
DC Direct current

DEM Digital elevation models
DSN Deep Space Network

DRAM Dynamic random-access memory

DLS Dual Launch Structure

DTE Direct-to-Earth

EDL Entry, descent, and landing
EELV Evolved expendable launch vehicle

EPS Electric power system
ESA European Space Agency

ESPA EELV secondary payload adapter

ET Einstein TelescopeFB Finer binningFoV Field of View

FPGA Field-programmable gate array

FU Functional Unit GaAs Gallium arsenide

GNC Guidance, Navigation and Control

GS Ground Station

GSSI Gran Sasso Science Institute

GW Gravitational wave
GWs Gravitational Wave
IMU Internal measurement unit

ITU International Telecommunication UnionJAXA Japanese Aerospace Exploration Agency

JUICE Jupiter Icy Moons Explorer

Lo
Level 0 (Top-level system requirement)
L1
Level 1 (Derived subsystem requirement)
L2
Level 2 (Component-level requirement)

LEOP Launch and early operations

LGWA Lunar Gravitational-wave Antenna

LIGO Laser Interferometer Gravitational-Wave Observatory

LIGS Lunar Inertial Gravitational-Wave Sensor LISA Laser Interferometer Space Antenna LRO Lunar Reconnaissance Orbiter

LRV Lunar Roving Vehicle
LTO Lunar Transfer Orbit
MCU Microcontroller unit

MRAM Magnetoresistive random-access memory

NASA National Aeronautics and Space Administration

NICM NASA Instrument Cost Model

OBC On-board computer
ODP Ozone Depletion Potential

PCDU Power control and distribution unit

PLC Powerline communications
PSI Plume surface interaction
PSR Permanently shadowed region

PV Photovoltaic

QPSK Quadrature Phase Shift Keying RTG Radioisotope thermoelectric generator

R&D Research and development SBN Seismic background noise

SILENCE Seismic Investigation in the Lunar Environment for Cosmic Events

SLS Space Launch System (launch vehicle by NASA)

SI Solar Illumination
SNR Signal to noise ratio
SoC Statement of compliance

SR Surface roughness

STM Seismic Transient Migration

TID Total ionizing dose

TRL Technology readiness level

TT&C Telemetry, tracking and command

UHF Ultra high frequencyWEB Warm electronics boxWBS Work Breakdown Structure

Chapter 1

Executive Summary

Gravitational waves (GWs) are a relativistic phenomenon caused by ultra-large-scale cosmic events such as interacting binary black holes or spinning neutron stars [11]. These events generate measurable ripples in space-time, and their detection stands at the frontier of modern astrophysics, opening a new observational window into the universe. Measuring GWs is essential for understanding the structure of the cosmos and the nature of interactions on these enormous scales. To detect these perturbations, extremely large and precise measurement facilities are required — such as the existing Laser Interferometer Gravitational-Wave Observatory (LIGO) and proposed missions like the Laser Interferometer Space Antenna (LISA), which will be the first space-based gravitational wave observatory, or the proposed Einstein Telescope (ET) on the ground.

All current and proposed GW observatories are sensitive to specific frequency ranges. However, there remains a significant gap between the high-frequency terrestrial and low-frequency space-based solutions in the deci-hertz range that is not covered by any existing or planned detector. This is where our mission, **SILENCE**, comes into play. The goal of SILENCE is to fill this observational gap by establishing a measurement facility on the lunar surface that uses the Moon itself as a resonant body to detect GWs within this frequency range. The lunar environment offers a unique advantage — the near-complete absence of seismic and atmospheric disturbances — enabling extremely sensitive measurements. By extending GW observations into this intermediate band, SILENCE will complete the GW spectrum and provide valuable data on cosmic events for scientific analysis.

To ensure precise measurements and effectively subtract seismic noise, four seismic stations will be deployed in a kilometer-scale array within a **permanently shadowed region (PSR)** near a lunar pole. These regions, primarily craters, that never receive direct sunlight, offer an exceptionally stable thermal environment characterized by extremely low and nearly constant temperatures. This environment reduces the effort required to further cool the seismometers to their optimal operating temperatures. Nevertheless, operating within a PSR presents significant technical and operational challenges. By successfully implementing SILENCE, we aim not only to advance gravitational wave science but also to demonstrate the feasibility of missions operating within PSRs — paving the way for future lunar exploration endeavors.

Chapter 2

Mission Objectives

2.1 Mission Statement

SILENCE (Seismic Investigation in the Lunar ENvironment for Cosmic Events) aims to detect gravitational waves through ultra-precise measurement of the Moon's surface vibrations. By sensing femtometer-scale displacements induced by passing gravitational waves, SILENCE will transform the Moon into a natural gravitational-wave antenna. Bridging the frequency gap between space-borne observatories like LISA and terrestrial detectors such as the ET, SILENCE will complete the global gravitational-wave spectrum. This will enable scientists to probe the most energetic and elusive cosmic events and and ultimately advance our understanding of the cosmos and fundamental physics.

2.2 Primary Objectives

2.2.1 Measuring gravitational waves

A complete overview of the GW spectrum will yield valuable information about cosmic events as they are happening in the universe [11]. The LGWA works by utilizing the Moon as an elastic resonant body, which is excited by GWs passing through it. This excitement will manifest itself in the celestial body oscillating at its normal mode frequencies (1 mHz - 1 Hz range), which can then be picked up by seismic stations.

Choosing the Moon as a resonant body has various advantages. The Moon, being the closest celestial body to Earth, is comparatively simple to reach, while showing significantly lower background vibrations due to tides and seismic activity. Because it is not known how much background vibration is present on the lunar surface, a pathfinder mission called Soundcheck, planned by the Gran Sasso Science Institute (GSSI), is going to bring a single measurement to the Moon to measure vibrational noise caused by meteorite impacts and seismic activity. Soundcheck is right now in the payload development.

PSRs provide an ideal location for the seismic measurements, as thermal noise can impact GW measurements. The LGWA aims to operate in a PSR for at least 10 years, yielding valuable new data on GWs.

2.2.2 Show feasibility of a mission in a PSR

A PSR offers ideal environmental conditions for the mission, characterized by minimal thermal fluctuations that facilitate the cooling of cryogenic test chambers during operation of the GW antenna. SILENCE, along with its pathfinder precursor Soundcheck, will be the first mission to

explore a PSR. By successfully operating seismic stations—essential for GW measurements—within this challenging environment, the mission will demonstrate our capability to reach and function effectively in any region of the Moon, including the extreme conditions of a PSR. Furthermore, it will serve as a proof of concept, paving the way for future scientific experiments and missions targeting PSRs.

2.3 Secondary Objectives

2.3.1 Find out about seismic activity on the Moon

Placing multiple ultra-sensitive seismic stations on the Moon will provide information about the Moon's seismic activity and frequency, as well as the intensity and locality of asteroid impacts on the lunar surface. This understanding will aid research into astral bodies and the planning of missions to the Moon, which can consider this new data for its own instrument.

2.3.2 Strengthen European scientific presence in space

The LGWA, coming from European scientific communities and institutes, will demonstrate Europe's readiness and presence in extraterrestrial science and research programs on the international stage, providing a boost to the European science and spaceflight community and even inspiring amateur scientists.

2.4 Constraints

The constraints listed in Table 2.1 arise from a combination of mission needs, selected architecture, and external boundary conditions. The scientific objective of detecting femtometer-scale vibrations imposes strict limits on vibration, thermal stability, and long-term operation. The need to operate in a permanently shadowed region and to launch with Ariane 6.4 defines environmental, power, mass, and communication constraints. Finally, ESA L-class mission policies and stakeholder expectations set limits on cost, schedule, risk, and data interfaces. Together, these factors define the fixed boundaries within which the mission must be designed.

Constraint	Description	
Resource constraints		
Time constraint	ESA's L-class schedule (13-18 years after call), foreseen launch 2038 (by GSSI) (section 7.2.)	
Mass constraint	1.5 tonnes due to Ariane 6.4, our launch vehicle, subsection 5.10.5.	
Financial constraint	1.1 billion EUR (typical L-class ESA mission).	
Technical constraints		
Vibration constraint	Ultra-low vibration, few moving parts.	
Thermal constraint	Low temperature variation inside PSR, peak temperature below 60 K.	
Power constraint	Supply adequate power to all stations.	
Communication constraint	Science data downlink only possible during sunlight	
Payload constraint	Low-vibration environment to the Moon.	
Development constraint	Must use provided seismic sensors.	
Interfaces constraint	Data collectable by GW scientists.	
Other constraints		
Environmental constraint	PSR, slope < 15°, reachable by selected station placement system.	
Lifetime constraint	> 10 years.	
Risk constraint	High chance of success, L-class mission.	
Political constraint	Support for European space science.	

Table 2.1: Mission constraints for the proposed SILENCE mission.

2.5 Stakeholder Analysis

The success of the SILENCE mission depends on multiple stakeholders with different roles and interests. All identified stakeholders are shown in Table 2.2.

At this time, no funding for the SILENCE mission is secured. As ESA has selected LGWA's pathfinder mission into its Reserve Pool of Science Activities for the Moon in 2023 [4], it can be assumed that upon success of the pathfinder mission, LGWA will be funded at least partially by ESA.

Stakeholder	Role	Objective		
Primary stakeholders				
GSSI	Coordination, key instrument development, research.	Understand gravitational waves and test novel detection technologies.		
ESA	Funding, mission selection, launch support, potential ground station support.	Support European leadership in space-based gravitational wave research and technology demonstration in PSR environments.		
Secondary stakeholde	ers			
Other space agencies (e.g., NASA, JAXA, ISRO)	Funding, collaboration.	Joint research and technology demonstration in PSR environments.		
Commercial stakehol	ders			
Aerospace companies (e.g., Thales Alenia Space, OHB, etc.)	Develop spacecraft and lander subsystems.	Commercial participation and technological demonstration.		
Launch provider (e.g. ArianeGroup, SpaceX, etc.)	Launch vehicle services.	Commercial participation and technological demonstration.		
Seismometer produc- ers and other high precision manufactur- ers	Profit from research into ultra-high precision devices.	Technology transfer and commercialization of high-sensitivity seismic instruments.		
Lunar relay satellite companies and institu- tions	Provide downlink capabilities.	Commercial participation, technological demonstration of downlink to Earth via lunar relay satellite.		
Regulatory stakehold	lers			
International Telecommunication Union (ITU)	Frequency and communication standards.	Ensure compliance with lunar communication and data transmission regulations.		
Operational stakehol	ders			
LGWA operations	Mission operations and maintenance.	Ensure continuous, reliable data acquisition and system performance, operate initial deployment and setup of LGWA on lunar surface.		
Ground segment	Data reception and monitoring.	Maintain communication with lunar instruments and ensure data integrity.		
End User				
Gravitational wave scientists	Need high-precision seismic data.	Research on gravitational waves in 1 mHz - 1 Hz range.		
Planetary scientists	Need seismic data.	Research lunar internal structure and seismic activity.		

Table 2.2: Stakeholder analysis

Chapter 3

Mission Requirements

The following chapter defines the requirements for our entire system by creating a flow down from the science objectives, listed as L0 requirements. section 3.1 provides an overview of the requirements up to L2. The following chapters discuss the requirements for each subsystem in more detail.

Table 3.1: Traceability between L0 science objectives and L1 mission requirements for LGWA payload.

L0 Science objective	L1 Mission requirement
L0-1: Measure gravitational waves on the lunar surface in the unobserved frequency band	L1-1: Measure vibrations in the 1 mHz to 1 Hz range
	L1-2: Transfer data continuously to Earth
	L1-3: The payload shall consist of at least four stations
L0-2: The payload shall survive in a PSR for at least 10 years	L1-4: Deploy the payload inside the PSR
	L1-5: Operate the payload inside the PSR

3.1 Overview

3.1.1 Requirements L0 to L2

${\rm L}0$ - ${\rm R}01$ Measure gravitational waves on the lunar surface in the unobserved frequency band

Sensing GW on the lunar surface will enable us to complete the measured spectrum of gravitational waves, enabling scientists to research cosmic events more in-depth.

L1 - R01SEI Measure vibrations in the 1 mHz to 1 Hz range

To take advantage of the normal mode frequencies of the Moon, the system shall be capable of sensing the frequency range between 1 mHz and 1 Hz.

L2 - $R01SEI_1$ Keep temperature variation under 50 K

For the instruments to work properly and deliver precise measurements, the temperature variation must be kept as low as possible. If not, the variations

might cause additional noise into the system. 50 K is selected as requirement with respect to temperature variations inside PSRs, adding a 50% margin.

L2 - R01SEI 2 Keep each station at 4.5 K

For the instruments to ensure the above mentioned sensitivity, they must be cooled down to 4.5 K.

L2 - R01SEI_3 Measure with a rate of 20 measurements per second

This high sampling rate is necessary because subsequent filtering will reduce the effective bandwidth of the data. Moreover, capturing higher-frequency signals from moonquakes will provide valuable insights into the local lunar geology.

L2 - R01SEI_4 Measure with 1 pm/ $\sqrt{\rm Hz}$ accuracy at 0.1 Hz and 1 fm/ $\sqrt{\rm Hz}$ accuracy at 1 Hz

Depending on the frequency of the waves, the sensitivity demand changes as well.

L1 - R01DAT Transfer data continuously to Earth

Observing GWs requires the transmission of measured data to Earth. This entails collecting data from all seismic stations, storing it locally, and retaining it until a downlink opportunity becomes available.

L2 - R01DAT_1 Store and process the measured data

Before the measured data can be sent down to Earth, it needs to be stored temporarily. The storage shall be capable of storing the data output of 86.3 Mbits/day per station for at least 24 days. Handling these amounts of data will require sufficient processing power onboard.

L2 - R01DAT_2 Collect data from seismic stations

Collect time-synchronized data at set intervals from the seismic stations, without interrupting the sensor readout. This includes data transmission from the outer stations to the inner hub.

L2 - R01DAT_3 Communicate with Earth

Communication to and from Earth should be reliably available in between defined time slots for down-link of gathered data and for up-link of commands and firmware updates from ground station.

L1 - R01PAY The system shall consist of at least four stations

To measure GWs and effectively distinguish them from seismic background noise (SBN), a minimum of four seismic stations shall be deployed to form a spatial array. Three stations shall be positioned along the arc of a circle, with one station located at the center of that arc. This configuration enables seismic transient mitigation (STM), a technique used in ground-based GW detectors to subtract seismic disturbances and enhance GW signal extraction.

L2 - R01PAY_1 The stations shall be placed in a circular plane with a diameter of 1 km

To achieve effective STM performance, the deployed seismic stations must span a sufficiently large area to resolve spatial variations in seismic background noise.

3.1. Overview

L0 - R02 The payload shall survive in a PSR for at least 10 years

Aside from the mission's dependence on PSRs, operating within these extreme environments remains a significant engineering challenge. The 10-year mission duration is designed to ensure long-term operation and data collection under these harsh conditions, allowing for the local seismic activity to be studied in detail. Moreover, maintaining functionality over such an extended period will serve as a crucial demonstration of technological resilience and sustainability, proving that human exploration and research within PSRs are feasible in the future.

L1 - R02DEP Deploy the payload inside the PSR

First major challenge of operating inside a PSR is the deployment of the instruments inside it. The deployment system must navigate and access the PSR fully autonomously.

L1 - R02OPS Operate the payload inside the PSR

After deployment, the instruments must be continuously operated for 10 years.

L2 - R02OPS_1 Power seismic stations and communication devices adequately

Continuous usage requires continuous power. The payload power requirement, in addition to the communication, is estimated at 40 W. Powering also means distributing the power to the four stations and storing excess energy as backup if needed.

L2 - R02OPS_2 Operate all subsystems in their optimal thermal environment

The thermal requirements for the instruments are already listed above. The rest of the systems must be kept in operating temperatures, which is hard on the lunar surface, since the temperature can vary up to 300 K.

L2 - $R02OPS_3$ Protect all subsystems from incoming radiation

The radiation on the lunar surface can be harmful to electronics, even inside a PSR and therefore need to be protected from it.

Table 3.2: Traceability between L1 Mission requirements and L2 system requirements for LGWA payload

L1 Mission requirement	L2 System requirement
L1-1: Measure vibrations in the 1 mHz to 1 Hz range	L2-1: Keep temperature variation low
	L2-2: Keep the station at $4.5~\mathrm{K}$
	L2-3: Measure with a rate of 20 measurements per second
	L2-4: Measure with 1 pm/ $\sqrt{\rm Hz}$ accuracy at 0.1 Hz and 1 fm/ $\sqrt{\rm Hz}$ accuracy at 1 Hz
L1-2: Transfer data continuously to Earth	L2-5: Store and process the measured data
	L2-6: Collect data from seismic stations
	L2-7: Communicate with Earth
L1-3: The payload shall consist of at least four stations	L2-8: The stations shall be placed in a circular plane with a diameter of 1 km $$
L1-4: Deploy the payload inside the PSR	_
L1-5: Operate the payload inside the PSR	L2-9: Power seismic stations and communication devices adequately
	L2-10: Operate all subsystems in their optimal thermal environment
	L2-11: Protect all subsystems from incoming radiation

3.2 Environment

3.2.1 Key environmental requirements

As introduced in subsection 2.2.2, the LGWA mission will operate inside a PSR near a lunar pole. Because the Moon's axial tilt is only about 1.5°, the Sun never rises high above the horizon at the poles. Combined with the irregular terrain and high crater rims that block sunlight, this creates regions that remain in permanent darkness.

Although PSRs are extremely cold, additional cooling will still be required to meet requirement L2-2. The radiators that support this system require a PSR with a maximum surface temperature below 60 K to stay effective.

Selecting a suitable PSR is therefore critical to mission success. The chosen site must be at least 1 km wide to allow proper deployment of the LGWA array, and the slope of the surrounding terrain mustn't exceed 20° (choice based on available PSRs, accessibility, and thermal craterwall reflection), while inside the deployment region slopes below 5-10° are favorable. It must also maintain a maximum temperature below 60 K due to radiator requirements (for derivation, see subsection 5.8.3), with minimal temperature fluctuations over the lunar day. Finally, it should be located far enough from other lunar missions to limit external seismic noise and ensure accurate measurements.

3.2.2 Radiation, charging, lunar dust and micrometeorites

The radiation environment in a PSR is relatively mild because there is no direct sunlight, although scattered light from crater rims and exposure to interplanetary and galactic cosmic radiation still

22 3.3. Deployment

need to be considered when designing electronic systems. According to our research and talking to industry experts, total ionizing dose (TID) is not a concern on the lunar surface [12]. (Taking the $13.2 \pm 1 \,\mu\text{Gy}\,\text{h}^{-1}$ of ionizing radiation measured on the Moon by the Chang'e-4 mission [13], over 10 years results in 13.2×10^{-6} Gy h⁻¹ × 24 h d⁻¹ × 365.25 d y⁻¹ × 10 y = 1.158 Gy = 115.8 rad = 0.116 ± 0.08 krad. which is small compared to the usual TID limit for consumer electronics of 5-10 krad [14].) Radiation analysis for the orbit would need to be performed with special attention in regard to the Van Allen belts, especially given the nowadays common low-energy lunar transfer orbits taking up to around four months [12]. The radiation effects from potential nuclear power sources such as radiation heater units and RTGs shall be mitigated through strategic location within systems and shielding. There is charge separation between the lunar day and nightside as well as between lunar craters and mountains, which needs to be analyzed, especially for solar power solutions electrically connecting systems over a large distance. [12] All systems shall therefore feature mitigation strategies for radiation impact for all mission phases, including the effects of internal radiation sources. Systems shall be robust to the lunar dust environment, especially circuit boards, mechanisms necessary after landing, and potential solar panels [15]. Operations shall be planned such that dust buildup is minimized, as anthropogenic sources are suspected to be a driving factor [16]. Micrometeorites are a threat [17] all subsystems necessary for operation during the science phase shall be robust too. This could especially become a factor in seismic station shroud design if cryogenic electronics were to be used, which would result in little to no thermal isolation material, which for the Apollo seismic experiments also served as shielding against ballistic impacts.

3.3 Deployment

3.3.1 Lander

The lander shall have sufficient volume, structural integrity, and propellant capacity to perform EDL with the LGWA stations and further subsystems for the stations' deployment, power supply, and back-to-Earth downlink aboard. The lander should have a landing accuracy of 50 m independent of lighting conditions to enable precision landing on a terrain with varying slopes and shallow illumination incidence angles to not drastically reduce the already temperature-restricted selection of feasible PSRs. For the same reason of not reducing the set of feasible PSRs, the lander shall be capable of landing on ground tilted by up to 10 degrees. The lander telemetry, propulsion, and control systems shall allow for a soft enough landing without driving shock resistance requirements on components.

3.3.2 Rover mobility

As the uncertainty of the mechanical properties of the lunar regolith in polar regions is big [18], the rover shall be capable of driving on a wide range of surface conditions in terms of how compacted the regolith is. The rover shall further boast high maneuverability and the ability to drive over obstacles up to a certain size. The rover should have an effective driving speed high enough to enable station deployment within 2 months after landing. That way the personnel required only for deployment are not necessary for too long. To not be overly limited by expected terrain slopes and have some margin, the rover shall be capable of driving on slopes of at least up to 20 degrees. The rover should further be capable of autonomous waypoint navigation so as to not drive communication requirements, which for continuous operation are expected to be relatively low.

3.4 Power

The electrical power system (EPS) is a necessity on every space mission, providing power to almost all other subsystems. Power demands are given in subsection 5.10.3. Differentiating between a deployment phase and an operational phase, power requirements are:

Deployment power	334 W
Operation power	$74.8~\mathrm{W}$
Maximum power	$204.4~\mathrm{W}$

Table 3.3: Power requirements

The EPS shall provide 74.8 W continuously for 10 years. The EPS shall provide maximum power during peak power demand times, but not continuously, and the EPS shall provide deployment power at BOL conditions, before the LGWA is fully operational.

The power storage shall have a high enough energy density to compensate for dormant times or power losses and a high life cycle. Power generation, mechanical structure, storage, and distribution subsystems shall have a high radiation tolerance and temperature range or good shielding to survive in the harsh environment on the lunar pole. They shall last ≥ 10 years before significant degradation.

3.5 Communication

Reliable communications are important for long-term data gathering and ensuring mission success. In the SILENCE mission, baseline communications requirements have been determined by Harms et al. [11] in advance. Harms et al. [11] calculates the daily data generation of a single seismic station to be around 62.5 Mbit and the total daily data generation to be around 250 Mbit for experimental readouts. The total telemetry is estimated to consist of 66.4 Mbit per day, where a detailed calculation can be found in Appendix A. The consequence of this is a requirement that the system shall be able to transfer all data, including telemetry, from the seismic stations to the receiving station on Earth without any long-term data backlog. To ensure continuous operation of the seismic stations, data collection shall not impact the sensor readout during transmission. Furthermore, telemetry up- and downlinks shall be possible multiple times per day, including during lunar nights to minimize the risk of data loss during system faults. Concerning link availability, the data link shall work under a minimum elevation angle of 20 degrees above the horizon, given by lunar terrain analysis in Figure 5.3b and a margin.

3.6 Computing

Processing incoming and outgoing data, as well as storing data before transmission or after reception, requires computing hardware on the system. The computing and information processing shall be able to handle all incoming and outgoing data through operations like compression, collection, and distribution. In particular, this means that the system shall be able to process 250 Mbit of data in addition to around 66 Mbit of housekeeping data per day, as well as at most 16.6 Mbit of uplinked data. It shall store the data until an opportunity for downlink is provided, where the data needs to be converted to an analog signal in real-time for wireless communication purposes.

As for uplinked data, the computing power shall further be able to process all uplinked data, such as firmware updates and operational commands, while ensuring non-overlapping operational downtime, which means that no two stations shall be out of order simultaneously and the lander has redundant computing units to prevent any downtime.

3.7 Thermal

3.7.1 Lander

The electronics box inside the lander must be kept at a temperature of approximately 285 K to 305 K to properly operate the laser, the batteries, and the computer. Temperatures on the Moon

can reach about 400 K on the equator. On the poles, a much lower maximum temperature of about 250 K was observed on sunlit crater rims, and the minimum temperatures can be as low as about 60 K. All components that are not inside the electronics box shall be able to withstand the ambient temperature. The thermal system of the radiator must be able to operate for ten years, which requires considering of material degradation and regolith dust.

3.7.2 Measurement stations

A box inside the measurement stations must be cooled down to about $4.5\,\mathrm{K}$ so that niobium becomes superconducting and in order to limit thermal noise of the mass suspension. This is far below the annual maximum temperature of the coldest PSRs that could be used for a kilometer-scale LGWA. Therefore, a sophisticated cooling system (part of which are radiators of significant size) is required. Furthermore, there must be an isolated electronics box inside the measurement stations that is kept between $254\,\mathrm{K}$ and $260\,\mathrm{K}$, without significantly changing the temperature of the cryo components. The thermal system of the radiator must be able to operate for ten years, which requires considering of material degradation and regolith dust.

3.7.3 Rover

In order to deploy the stations from the lander outside the PSR to the inside of the PSR, the rover shall withstand ambient temperatures of as low as 20 K depending on the PSR and season, up to around 330 K [19]. This range is to be refined once the travel path of the rover is defined, with the option of restricting launch windows seasonally. The electronics box inside the rover must be kept at a temperature of approximately 285 K to 305 K. The rover's thermal system shall ensure operability under varying conditions in terms of rover pose, ground tilt, and nearby objects. The rover should operate in the PSR with low heat leakage to reduce energy consumption. Despite the rover subsystem's lifetime being significantly shorter than that of the lander and stations, we recommend careful analysis of dust degradation effects on rover thermals and require that the rover's thermal system shall have a dust mitigation concept.

3.8 Key and Driving Requirements

This report follows the notion of a key requirement being one that relates especially directly to the mission objectives compared to other requirements, whereas a driving requirement is one that has a strong influence on system design. Compared to section 5.2 the here-mentioned requirements follow the SMAD notion of a critical requirement and are not free variables, whereas in section 5.2 we discuss the free variables we observed during mission design to have a lot of impact on mission or system design ("system drivers" in SMAD nomenclature [20]). In our case, many of these requirements derive from the required measurement sensitivity described in L1 - R01SEI in subsection 3.1.1, making this obviously key requirement also an extremely driving one. As described in chapter 4, the main parameters to meet this requirement are ambient ground displacement noise, thermal noise and damping inside the seismometer's IMU, requiring the IMU to be cryogenic [3].

Low ambient ground displacement noise, along with its size and proximity to Earth are some of the main reasons why the Moon is an attractive resonant body to detect GWs and why it is the destination of this mission [11]. Aside from the low seismic noise floor, the Moon features PSRs providing high **temperature stability** compared to periodically sun-exposed areas of the Moon where temperatures vary by around 250 K both for equatorial and polar regions, caused by the strong equatorial solar irradiance and strong impact of the seasons at the poles [19], [21]. The sensitivity-derived need for high temperature stability is the reason for the here proposed conduction of seismic measurements inside a PSR, which impacts many aspects of the mission such as thermal management, power generation, and deployment, making it both a key and driving requirement.

Another sensitivity-derived requirement is the **requirement for the seismic sensors to be cryogenic** to enable low enough thermal noise and high enough Q-factors of the proof mass suspension and actuation using superconducting materials. Associated with this necessity arise stringent requirements on the thermal management system, which have considerable influence on the mass budget of the entire mission, making the need for the seismic sensors to be cryogenic another key and driving requirement of the mission.

Due to the rare (with respect to the observed environment) occurrence of some of the events whose observation is part of the scientific goals of this mission, a mission lifetime of 10 years L0 - 2. subsection 3.1.1 has been selected. The **long mission lifetime** impacts the selection and design of almost all components necessary for operation after initial deployment, making it a driving requirement: It increases the required robustness and shielding of the used electronics to radiation. The power system needs to be heavily over-designed at BOL to account for degradation of the battery(ies) and solar cells. Dust buildup impacts not only the design and dimensioning of the solar cells but also the radiators needed to cool the seismic sensors to cryogenic temperatures.

Chapter 4

Payload Description

4.1 Payload Mass, Volume, Power and Data Generation Budgets

The payload of the LGWA mission consists of four seismic stations and the laser generation module on the lander and the fiber optic cables from the lander to the stations. The key characteristics for each of these stations, driving the design of the power, communication, and deployment subsystems, are summarized in Table 4.2. The station mass composition is given in Table 4.4. The characteristics of the laser and fiber optic transmission cables are given in Table 4.6. Station data generation can be found in subsection 5.10.1. For an overview of station power consumption see subsection 5.10.3.

Figure 4.1 shows one of the stations conceptually with the cryogenic IMU fixed to the leveling system, which compensates for ground tilt.

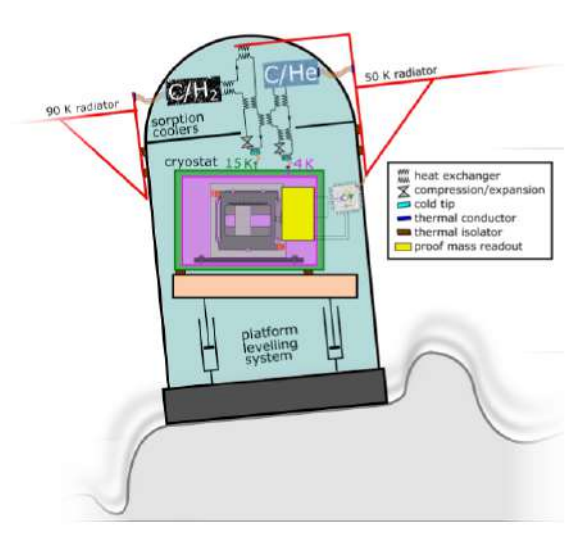


Figure 4.1: Conceptual Overview of Seismic Station Architecture [3]

	Current best estimate	Allocated margin	Total	Reference or com- ment
Mass	47 kg station weight + 43 kg radiation panels	already margined	90 kg	Table 4.4
Power	20 W (acc. to Jan conservative DAU budget, includes DAU control electronics, laser and communication to lunar orbiter or Earth)	5 W	25 W	Based on DAU power model
Data generation rate	73.6 Mbits/day	22.1 Mbits/day	95.6 Mbits/day	[11], section A.2
PSR Temperature	up to 60 K	_	up to 60 K	To be refined after testing
Dimensions station	$400{\times}400{\times}400~\mathrm{mm}$	50 mm in each direction	$^{450\times450\times450}_{\rm mm}$	*Approxima envelope sec- tion 4.1
Volume radiators	$0.3m^{3}$	$0.2~m^3$	$0.5 m^3$	required 9.8m2, panel thickness of 33mm sec- tion 5.8

Table 4.2: Main characteristics per station. A star * in the reference or comment column indicates that this estimate has been made by Jan Harms based on the current (late 2025) R&D state of the seismic sensors and stations.

Component	Mass (CBE) per unit	Total for design	Reference or comment
2x proof mass	10 kg	20 kg	[3]
2x watt's linkages	$6~\mathrm{kg}$	13 kg	* Includes additional structure and fasteners for support within the station, conservative margin applied
Leveling system and sensor platform	$5~\mathrm{kg}$	5.5 kg	*Conservative margin applied
4 K, 15 K cryostats around the linkages	2 kg	$2.2~\mathrm{kg}$	*Preliminary design mass
Sorption cooler, proof mass actuation and readout electronics, shroud	$5~\mathrm{kg}$	$6.3~\mathrm{kg}$	* rough estimate
Radiation panels	43 kg	43kg	subsection 5.10.5 for future iterations TBR based on PSR geometry and max. temperature

Table 4.4: Mass budget composition per station. A star * in the reference or comment column indicates that this estimate has been made by Jan Harms based on the as of late 2025 current R&D state of the seismic sensors and stations.

Component	Details
Glass fiber cables	22.6 kg, diameter of 1 mm [22], subsection 5.10.5
Laser on the lander TESAT NPRO RLU	Around 150x150x60mm, needs to be kept at 300 K, power 9W subsection 5.10.3, weight with necessary electronics assumed 10kg

Table 4.6: Key characteristics of the laser generation and transmission subsystems.

4.2 Payload Measurement Principle and Architecture

The seismic stations of the LGWA each measure the horizontal ground displacement in two directions. This is achieved with an IMU that measures the difference in displacement between an inertially displacing proof mass and the IMU's suspension frame, which is rigidly connected to the lunar surface via a leveling system inside the seismic station attached to the station's base, which is firmly placed on the lunar surface. As GWs deform the Moon, this measurement contains GW signals. The stations have to be deployed in an approximately kilometer-scale array to exploit the difference in phase observed for SBN to subtract SBN from the GW signal, which is roughly the same for all stations. The extremely high sensitivity requirements make cryogenics necessary to reduce thermal noise and proof mass actuation or suspension-induced damping. [4][3]

There are currently two variants of the station subject to R&D: one based on a niobium suspension with interferometric readout, which requires cooling down to 4.5 K, and one based on a silicon suspension with a SQUID readout requiring cooling down to 15 K. The silicon variant would allow us to get rid of one of the second cooling stages of the proposed cooler, significantly reducing the required radiator area. Our baseline assumes the in terms of cooling more demanding niobium variant.

4.2.1 Laser

The payload requires a laser beam for the operation of the interferometer. The laser device (suggested by Jan Harms) is a 1550 nm TESAT NPRO RLU with dimensions of 150x150x60 mm and a power consumption of 9 W. The laser needs to be kept at a temperature of about 300 K. Therefore, its positioning might have a significant impact on the thermal design and the instrument noise and must therefore be carefully considered.

4.2.1.1 Laser positioning options

- **4.2.1.1.1** Laser on the lander One laser could be placed on the lander, and its beam can be guided to the stations using an optical fiber cable. Beam splitters can be used in the stations to split off a part of the beam for local use while allowing the rest of the beam to proceed to the other stations.
- **4.2.1.1.2** Lasers on the stations It would also be possible to place four lasers directly on the stations.
- **4.2.1.1.3** Single laser box Another option would be to use a separate box inside the PSR that has approximately the same distance to all stations and uses a single laser (and beam splitters inside the box) to guide the beam to the stations. The box needs its own thermal management system and potentially also an anti-vibration system.
- **4.2.1.1.4 Multiple laser boxes** Another option would be to position one laser box a few meters next to each station (four boxes in total). The box needs its own thermal management system and potentially also an anti-vibration system.

4.2.1.2 Laser options comparison

A comparison of the advantages and disadvantages of each option is shown in Table 4.7. Placing the laser on the lander is the clear winner, mainly because thermal and vibrational noise are kept to a minimum when using this approach. The other options require less optical fiber cable but more power cable. The separate laser boxes increase system complexity and weight while not offering significant improvements compared to placing the lasers on the stations (we do not know the exact reaction of the lunar surface to temperature fluctuations and vibrations; therefore, placing anything that can cause these near the seismic stations is considered a risk).

	Laser on lander	Lasers on stations	Single laser box	Multiple laser boxes
Vibrational noise	2	0	0.5	1
Thermal noise	2	0	0.5	1
Power consumption	2	2	2	2
System complexity	1	2	0	0
Weight	2	2	1	0
Total	9	6	4	4

Table 4.7: Comparison of options for laser positioning. Scores: 0-2, 2 is best

4.3 Payload Estimated Performance

Payload estimated performance is given in Figure 4.2 below. This mission has been designed for the more conventional niobium variant of the LGWA with higher cooling demand.

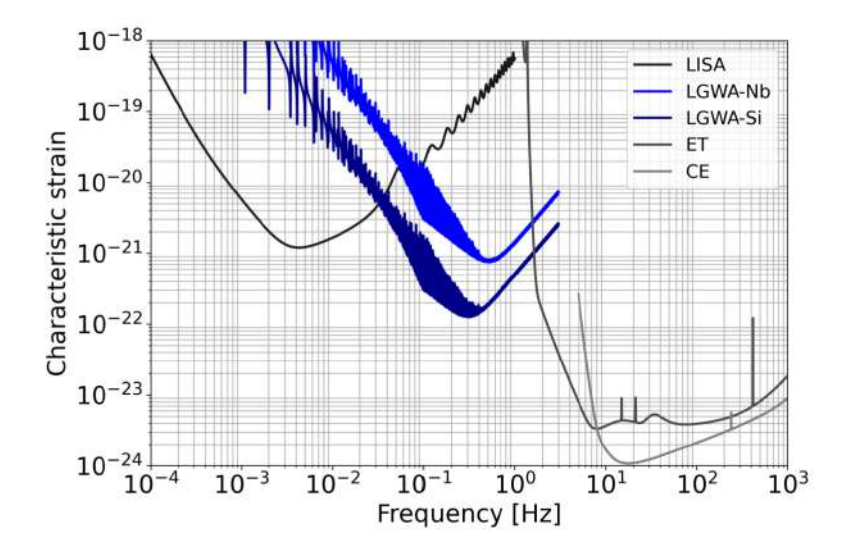


Figure 4.2: Models of characteristic strain sensitivities from [4] showing the estimated sensitivity of the two LGWA variants compared to the future Earth-based Einstein Telescope and Cosmic Explorer and space-based LISA mission, showing the frequency gap in the deci-hertz range where the LGWA would significantly boost the capabilities of the next generation GW detectors.

4.3.1 Background noise estimates

The background noise on the Moon will have a significant impact on whether LGWA can achieve its goal of measuring gravitational waves. Different noise sources will be analyzed here and compared to the instrument noise requirements $1 \, \mathrm{pm}/\sqrt{\mathrm{Hz}}$ at $0.1 \, \mathrm{Hz}$, $1 \, \mathrm{fm}/\sqrt{\mathrm{Hz}}$ at $1 \, \mathrm{Hz}$.

4.3.1.1 CTE mismatch thermal noise

Temperature variations over time will cause a tilt angle if the material below is not perfectly homogenous. Assume a thermal diffusivity of $\kappa=1\times10^{-7}\,\mathrm{m}^2/\mathrm{s}$ and compute the skin depth of the lunar day-night cycle as

$$\delta = \sqrt{\frac{\kappa \tau}{\pi}} = 0.28 \,\mathrm{m}. \tag{4.1}$$

Assume that the shape of T(t) is approximately given by

$$T(t) = \Delta T \max(\sin \omega t, 0). \tag{4.2}$$

This assumption is supported by a simulation received from Philipp Gläser. The Fourier series of this function is given by

$$T(t) = \Delta T \left(\frac{1}{\pi} + \frac{1}{2} \sin \omega t - \frac{2}{\pi} \sum_{n=0}^{\infty} \frac{\cos(2n\omega t)}{4n^2 - 1} \right). \tag{4.3}$$

Therefore, at a frequency f_s measured by the seismic sensor, the temperature amplitude is approximately

$$\Delta T_s = \Delta T \frac{f^2}{f_s^2},\tag{4.4}$$

where f is the frequency at which the Moon rotates around its own axis. Assume lunar regolith has a CTE of $\alpha = 1 \times 10^{-5} \,\mathrm{K}^-1$, and $\Delta \alpha = 0.1\alpha$ across the $L = 40 \,\mathrm{cm}$ length scale of the seismic station. Taking into account expansion in the whole skin depth, this results in a tilt angle of

$$\Delta \theta = \frac{\Delta \alpha \delta \Delta T f^2}{L f_s^2}.$$
 (4.5)

The approximate amplitude is

$$\Delta x = R\Delta\theta = \frac{R\Delta\alpha\delta\Delta T f^2}{Lf_s^2},\tag{4.6}$$

where $R = 20 \,\mathrm{cm}$ is the suspension length. At $f_s = 0.1 \,\mathrm{Hz}$, we get $\Delta x = 4 \times 10^{-17} \,\mathrm{m}$, and at $1 \,\mathrm{Hz}$, we get $\Delta x = 4 \times 10^{-19} \,\mathrm{m}$. This is very small compared to the allowed noise level.

4.3.1.2 Temperature gradient noise

Assume the PSR surface is made of homogenous material, but the spatial temperature gradient ΔT_s changes within a lunar day from 0 to 0.03 K/m (150 K over the the radius of a 5 km PSR). Using the same frequency scaling method as before, the resulting noise amplitude is given by

$$\Delta x = R\Delta\theta = \frac{R\alpha\delta\Delta T_s f^2}{f_s^2}. (4.7)$$

At $f_s = 0.1 \,\mathrm{Hz}$, we get $\Delta x = 3 \times 10^{-19} \,\mathrm{m}$, and at $1 \,\mathrm{Hz}$, we get $\Delta x = 3 \times 10^{-21} \,\mathrm{m}$. These results show that simple temperature expansions are not a problem for LGWA. If there are any problems with noise, this will be more likely due to thermal moonquakes, as observed by the apollo missions. The models above do not consider the cracking of rock and shot noise like effects.

4.3.1.3 Nuclear reactor noise

The nuclear reactor concept proposed by NASA uses stirling converters for energy conversion. These will not generate more noise than any rover. However, the heat conduction into the ground could lead to similar events as natural thermal moonquakes. This would need to be investigated.

4.4 Cable Configuration

The optical fiber cables that transmit the laser light to the seismic stations are coated in acrylate to withstand the cryogenic temperatures and high vacuum [23]. They are laid out together with power transmission aluminum cables (subsection 5.5.2), a cable cross section is sketched in figure Figure 4.3. A double coating of Kapton and Teflon could be used to protect the cables from the harsh lunar environment [24]. Kapton remains stable even at cryogenic temperatures [25], while Teflon is chemically and thermally robust [26]. However, for a mission duration of 10 years, further studies would be required to assess long-term cable survivability under lunar surface conditions.

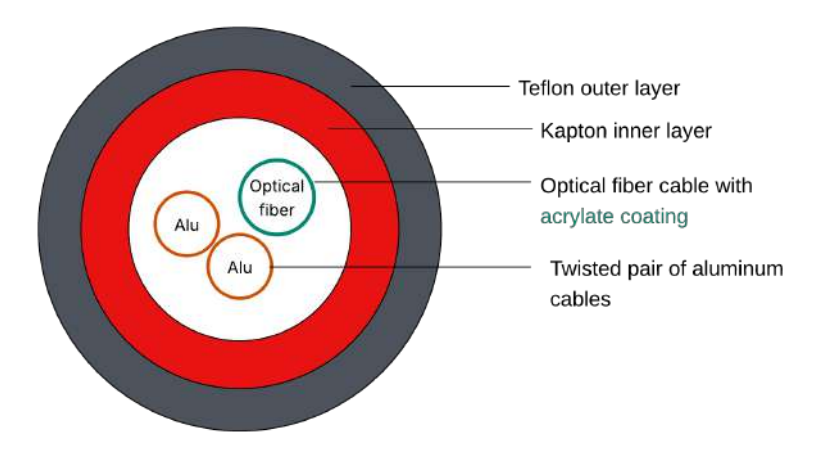


Figure 4.3: Sketch of cable cross-section including glass fiber cable and aluminum cables.

5.1. Product Tree

Chapter 5

Mission Design

5.1 Product Tree

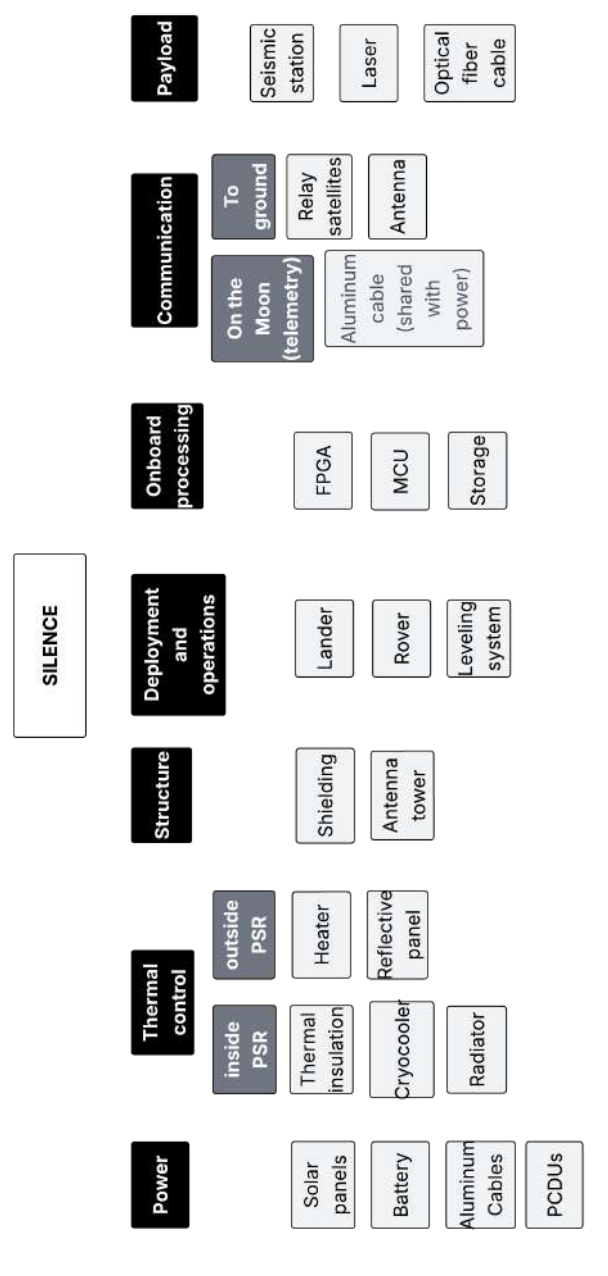


Figure 5.1: Product tree for the SILENCE mission.

5.2 Mission Design Drivers

This section discusses the mission parameters with significant design freedom we observed to have a lot of impact on subsystem designs, summarizing some of the choices discussed in the subsequent sections of this chapter. One such parameter is the broad region the mission plans for. Restricted to polar regions for their PSRs Table 2.1, the North pole offers less predicted space mission activity, potentially causing detrimental vibrational noise, but also fewer opportunities to share infrastructure compared to the South pole, especially regarding the Artemis program and potential rovers and power sources; see subsection 5.4.3 and subsection 5.9.1. Another site selection parameter with significant selection freedom despite constraints such as PSR temperature or accessibility (Table 2.1) is the maximal time in shade for the solar array hilltop site, which drives energy storage solution sizing, which needs to be balanced with other factors such as average solar illumination and distance to the PSR-related cable weight (section 5.5). Despite an upper constraint, PSR maximum temperature can, via PSR selection, be altered strongly, driving seismic station radiator needs, which significantly contribute to mass and volume budget. The data uplink interval is also a mission design driver, as depending on it, power consumption at night, especially in the longest shade periods, drives energy storage sizing. But it also constrains PSR selection by visibility of a lunar relay satellite, especially if, contrary to our baseline, the communications infrastructure is inside the PSR. The deployment strategy is another mission design driver, among others deciding placement of certain assets as the aforementioned communications infrastructure or deciding whether a rover or incorporation into a human spaceflight mission is necessary (subsection 5.4.1). While some of these observations are fairly general in the context of this mission, such as data uplink interval and deployment strategy, some, like the longest interval without sunlight at the location of the solar array, are specific to our mission design baseline.

5.3 PSR Selection

Selecting the right PSR is of essence for this mission, as for the instrument to work, low temperature amplitudes are required, while for the thermal control, very low maximum temperatures are required. As our mission design baseline foresees solar power as the main power source, the PSR not only needs to fulfill strict temperature requirements but also needs to be in the vicinity of a hill or ridge with a high average solar visibility. An alternative approach would be to deploy the solar cells directly out of the PSR with a large enough tower, but large-scale maps of the average sun visibility at different positions above the surface could not be obtained. Moreover, most large-scale PSRs are in deep craters, where the required height of the tower would simply be too large. Additionally, seismic noise coming from the expansion of the tower when illuminated by sunlight and subsequent contraction could influence the measurements. Therefore, we stuck to the first approach and additionally proposed possible deployment sites if an RTG is used instead of solar power.

Gläser et al. [27] investigated solar illumination conditions at 2 meters above the surface for both lunar poles, identifying regions with average illumination levels over 75%, with maximum shadow durations of up to 65 hours. They also located nearby PSRs for further exploration. The best site they identified was on the Shackleton Crater rim at the lunar south pole, which had a maximum average illumination of 85.5% and a maximum shade time of 66 hours. Unfortunately, none of these sites have PSRs nearby that fulfill the temperature requirements needed for the operation of the LGWA.

Therefore, an analysis with the goal of finding PSRs that are suitable for deployment of LGWA had to be conducted. For this analysis multiple publicly available datasets were used, namely topographical data (slope, hillshade, DEM & surface roughness maps) derived from the Lunar Reconnaissance Orbiter (LRO) [28], temperature data from the Diviner Lunar Radiometric Experiment [19], solar illumination of the lunar surface data from a simulation conducted by Mazarico et al.[29] and a collection of all identified PSRs [30]. The temperature data that this analysis is based on came as seasonal data with one dataset (min, mean, max) for winter and one for summer.

36 5.3. PSR Selection

Year-round maps were then produced by taking the maximum of winter and summer temperatures for the mean and average maps and taking the minimum of winter and summer for the minimum temperatures.

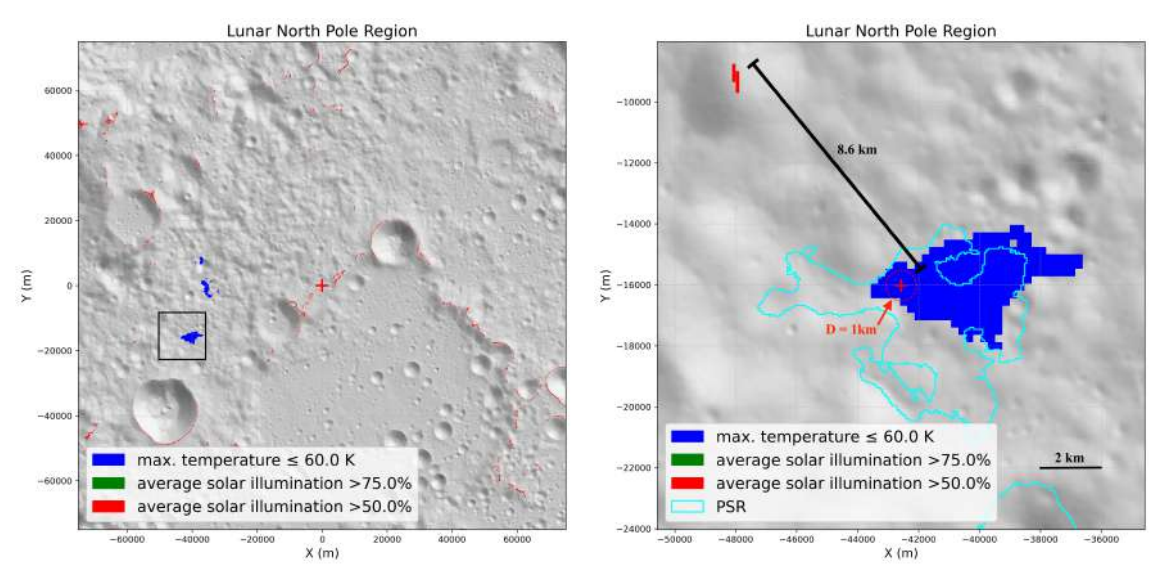
For the LGWA deployment, we are particularly interested in the temperature amplitude over a lunar day (approximately 28 Earth days). No publicly available datasets were found that provide Diviner temperature data binned on this timescale. However, Schorghofer et al. [1] analyzed the same Diviner dataset with an improved temporal resolution by dividing it into six seasonal bins. Unfortunately, their study focused exclusively on the lunar south pole, and no equivalent data products exist for the north pole.

To approximate the temperature amplitude at the north pole, the difference between the maximum and minimum temperatures was calculated for each season. The resulting seasonal amplitudes were then combined by taking the maximum value across the two seasons. This approach provides an upper bound on the possible daily temperature amplitudes for the north pole. For PSRs located at the lunar south pole, the finer binned data from Schorghofer et al. [1] is also displayed. All temperature values are given as bolometric temperatures in kelvin.

5.3.1 Baseline PSR: landing and solar panel deployment on "nearby" hill

5.3.1.1 Method

In the baseline scenario, solar cells need to be deployed at a site with good solar illumination to ensure power supply. From a thermal control perspective, temperatures must be under 60 K as an absolute maximum inside the PSR, while the temperature amplitude should be as low as possible. Therefore, site selection was conducted with a strict focus on sites with maximal temperatures below 60 K (see section 3.2) that had the smallest distance to a point with acceptable average solar illumination (>50%). This value for acceptable average solar illumination is a minimum requirement that the site should be illuminated at least half of the time on average, which is an initial guess.



(a) Overview of the lunar north pole region with solar illumination and regions with max temperature <60 K highlighted

(b) Proposed baseline PSR with LGWA deployment region in red and distance to high illumination site

Figure 5.2: Lunar north pole region in polar stereographic projection

Figure 5.2a shows the PSR selection method illustrated with the north-polar region. PSRs were selected by the nearest patch of surface with good solar illumination.

5.3.1.2 Selected PSR

Figure 5.2b shows the preferred PSR for the LGWA deployment scenario with a rover. It lies at the lunar north pole at the coordinates [88.50°, 290.63°]. The average solar illumination at the spot with the highest value (on the ground) lies between 55 and 60%. With a distance between the PSR and the spot of high illumination of around 8.6 kilometers, this brings its own challenges, namely a power cable needs to be set up over this distance.

The maximum slope inside the selected deployment region is below 7.7° (see Table 5.1), while most of the PSR is rather flat with a slope of less than 5° (see Figure 5.3b). Moreover, the PSR is not surrounded by terrain that is steeper than 20 degrees, which means that no radiation from the crater walls is going to hit the radiators at an angle greater than 20 degrees. As the rover shall be able to navigate terrain with slopes of up to 20 degrees (see subsection 3.3.2), it is feasible to reach the LGWA deployment site, as there is a path with a slope of <15 degrees.

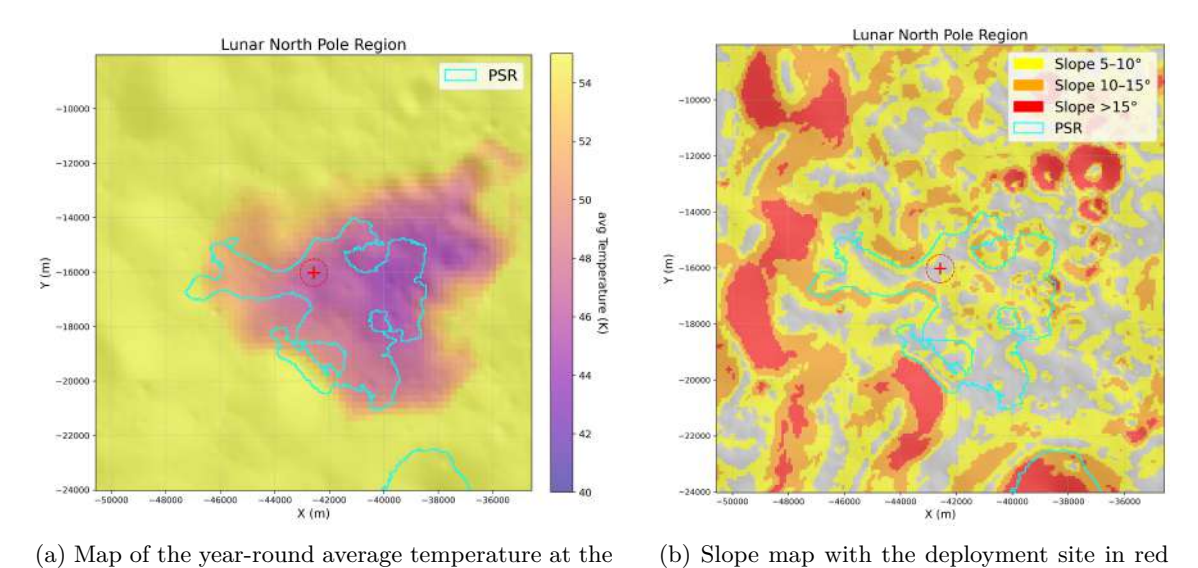


Figure 5.3: Lunar north pole region in polar stereographic projection

and the PSR highlighted in cyan

Table 5.1 summarizes the key variables of the selected PSR, showing the areal statistics over the full deployment site with a diameter of 1 km. The temperature data shows that the PSR remains extremely cold, with a mean minimum temperature of approximately 34 K and a maximum of 59.7 K, reflecting the absence of direct sunlight throughout the lunar day. Overall, the parameters summarized in this table illustrate that the selected PSR offers stable, flat, and cold environmental conditions well-suited for the LGWA's scientific and operational requirements, although with logistical challenges related to the energy supply. As up to now, no other mission targeting the lunar north pole could be found, this site also provides the advantage of having a low risk of anthropogenic noise interfering with the measurements.

5.3.1.3 Landing site environment

deployment site highlighted in red

The selected landing site can be seen in Figure 5.4. It lies on top of a hill with good average solar illumination at the coordinates [88.389°, 280.76°]. Table 5.2 shows the areal statistics of circles around the landing site. With a maximum slope of only 4 degrees within a 200 m diameter area around the landing site, the terrain offers a stable and favorable surface for landing while providing

38 5.3. PSR Selection

Location		Variable	Mean	Min	Max	Unit
Latitude	88.50°	Temperature minimum	34.0	32.1	35.9	K
Longitude	290.63°	Temperature maximum	58.4	57.2	59.7	K
		Temperature average	46.3	45.6	47.3	\mathbf{K}
		Temperature amplitude	32.0	25.9	42.7	K
		Slope	3.7	0.0	7.7	0
		Average solar illumination	0.0	0.0	0.0	%

Table 5.1: Areal summary of temperature, slope, and visibility over selected deployment site with 1 km diameter.

sufficient tolerance for localization uncertainties. Inside a 50m radius around the landing site, the terrain has an average surface roughness (RMS over a plane with diameter 100 meters) of 0.7 meters.

The lander is expected to touch down within \pm 50 m of the designated target, where slopes remain well within the lander requirement of 10 degrees (see subsection 3.3.1).

Furthermore, the site provides robust solar illumination, with an average of 55.8~% and a minimum of 54~% within the 200~m area, ensuring adequate power generation even under small deviations from the nominal landing point. Figure 5.5~shows the fraction of the solar disk visible at the landing site at a height of 2~meters above ground simulated over a time span of a year. It can be seen that in the summer months (April - September) the sun is fully visible almost continuously with a few days of shade in between, while in the winter months (October - February) there are long periods of shadow with roughly one week of continuous solar illumination in between. The maximum period of continuous shade is 538~hours (22.4~days) 1 . The maximum surface temperatures do not exceed 250~K while staying above a minimum temperature of 66~K. As the landing site sits on a hilltop, it has a large enough sky visibility angle needed for communication.

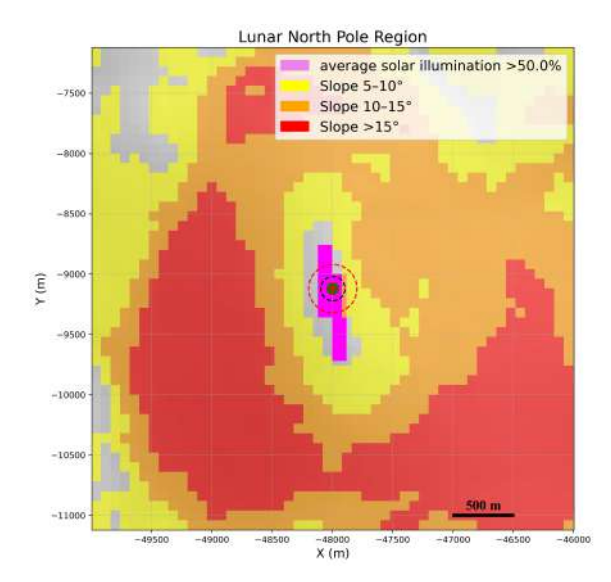


Figure 5.4: Slope map of selected landing site (green) with solar illumination overlaid (violet) and circles for the areal statistics visualized [black: r=100 m, red: r=200 m], polar stereographic projection.

Location	
Latitude	88.389°
Longitude	280.76°

Variable	Mean	\mathbf{Min}	Max	\mathbf{Unit}
200 m radi	us circle	(red)		
T min	68.3	66.7	69.0	\mathbf{K}
T max	244.4	233.0	250.0	K
T avg	166.7	162.6	169.9	K
T amp	182.0	180.8	183.7	K
100 m radi	us circle	(black)	
Slope	2.6	1.1	4.0	0
SI avg	55.8	54.0	59.7	%
50 m radiu	s circle	$\overline{(green)}$		
SR	0.7	0.3	1.1	\mathbf{m}

Table 5.2: Areal summary of temperature, slope, and solar illumination over a circle with 100~m/200~m radius around the selected landing site. Surface Roughness (SR) calculated over an area with 50 m radius around landing site.

¹Value from simulation conducted by Dr. Philipp Gläser

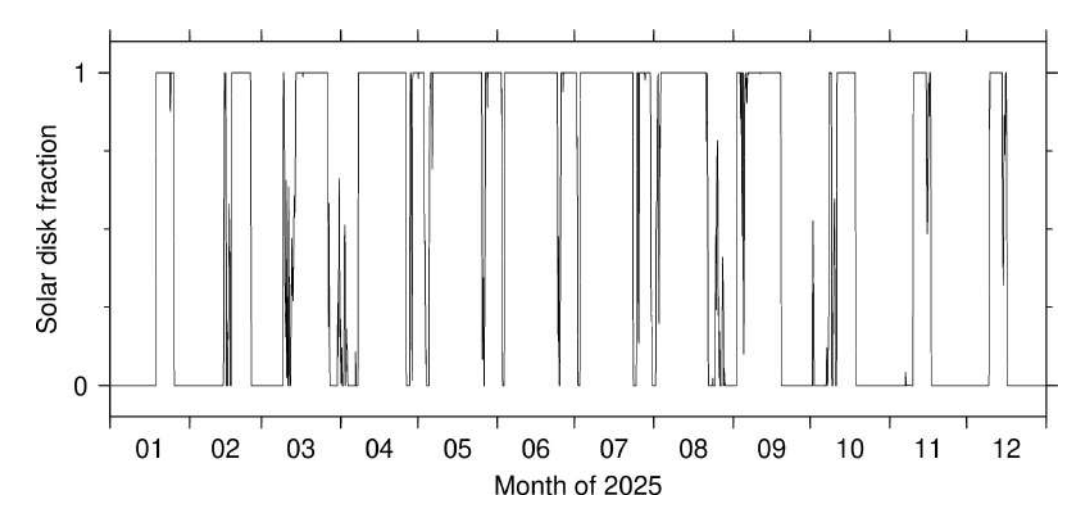
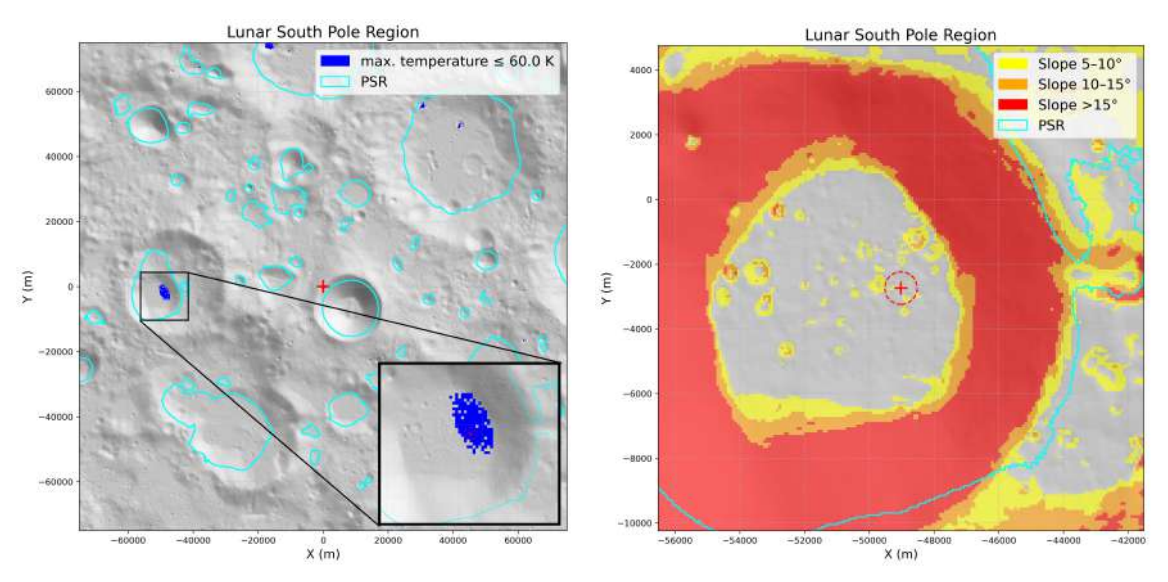


Figure 5.5: Fraction of solar disk visible at a height of 2 m above ground at the chosen landing site simulated over the year 2025 with time steps of 2 hours (Image: courtesy of Dr. Philipp Gläser)

5.3.2 PSR for alternative power concept (RTG)

The landing site proposed for the baseline scenario would obviously also work for the concept with an RTG power source (subsection 5.9.1). The details of deployment in the baseline PSR with an RTG can be found in subsection 5.3.4. However, an additional PSR at the lunar south pole was selected in order to propose an alternative deployment option and to demonstrate the feasibility of the RTG-powered concept at both poles. Moreover, more detailed temperature amplitude data were available for the south polar region, enabling a more accurate site assessment.



(a) Overview of the lunar south pole region with regions with max temperature <60 K highlighted and zoom on selected deployment site

(b) Slope map with the deployment site in red and the PSR highlighted in cyan

Figure 5.6: Lunar south pole region in polar stereographic projection

40 5.3. PSR Selection

5.3.2.1 Method

From a PSR selection point of view, this scenario is favorable, as only the thermal requirements need to be met and no solar cells need to be deployed. Moreover, it is possible to land directly inside the PSR, so only the terrain slope inside the PSR comes in as a selection criterion, and not the slope of the surrounding terrain. Therefore, site selection was done by first selecting all sites with an overall maximum temperature below 60 K (see Figure 5.9a) and then choosing a site with low slope and low temperature amplitudes. The distance to crater walls should be as large as possible to avoid reflected radiation at an angle larger than 20° interacting with the radiators (subsection 5.8.3). Of course, locations in the entire south pole region were considered, but for illustration purposes, Figure 5.9a shows an enlarged view of the south pole region.

5.3.2.2 Selected PSR

Figure 5.8b shows the preferred PSR for the LGWA deployment scenario with an RTG as a power source. It lies at the lunar south pole inside the de Gerlache crater at the coordinates [-88.381°, 266.8°]. The maximum slope inside the selected deployment region is below 7.4° (see Table 5.3), while most of the PSR is rather flat with a slope of less than 5° (Figure 5.6b). As can be seen in Table 5.3, inside the deployment region the temperature never exceeds 60 K with temperature amplitudes below 20 K. The site location was chosen with as large as possible a distance from the crater walls, as both the thermal radiators and the communication system need an unobstructed field of view to space that is as large as possible. Figure 5.7 shows the elevation profile around the deployment site: with a sky visibility angle of over 153° and a maximum angle for radiation reaching the radiators of 13.3°, these values lie well within the requirements (see section 3.5 and subsection 5.8.3).

Location		Variable	Mean	Min	Max	Unit
Latitude	-88.381°	Temperature minimum	27.7	22.4	33.4	K
Longitude	266.8°	Temperature maximum	56.3	52.8	58.2	K
		Temperature average	44.5	43.0	46.4	K
		Temperature amplitude	31.9	24.9	48.8	K
		Temperature amplitude (FB)	19.1	18.5	19.7	K
		Slope	2.3	0.1	7.4	0
		Average solar illumination	0.0	0.0	0.0	%
		Surface roughness (R=50m)	0.6	0.3	0.7	m

Table 5.3: Areal summary of temperature, slope, and visibility over selected deployment site with 1 km diameter. Temperature data from study with finer seasonal binning (FB) included (6 seasonal bins) [1]. Surface roughness calculated over an area with a radius of 50 m around landing site.

Landing site

Inside an area with a radius 100 m from the landing site (black circle in Figure 5.8b), the maximum slope is 2.3 degrees, which presents good conditions for landing. A surface roughness analysis inside an area with radius of 50 m around the landing site shows local variations up to 0.7 m.

The selected deployment site lies fairly close to one of the selected landing sites of the NASA Artemis III mission [31], which provides the advantage of potential serviceability of the LGWA experiment but poses the risk of having anthropogenic noise in the area that could influence the measurements.

In Table 5.3, it can be seen that there is a significant difference between the "daily" temperature amplitudes derived from the Diviner dataset with six seasonal bins by Schorghofer et al. [1] (Temperature amplitude (FB)) and those obtained from the two-bin dataset by Mazarico et al. [29] (Temperature amplitude). This difference highlights the influence of the temporal resolution of the dataset on the derived amplitudes and suggests that the temperature amplitudes shown for the baseline PSR at the north pole are likely overestimated.

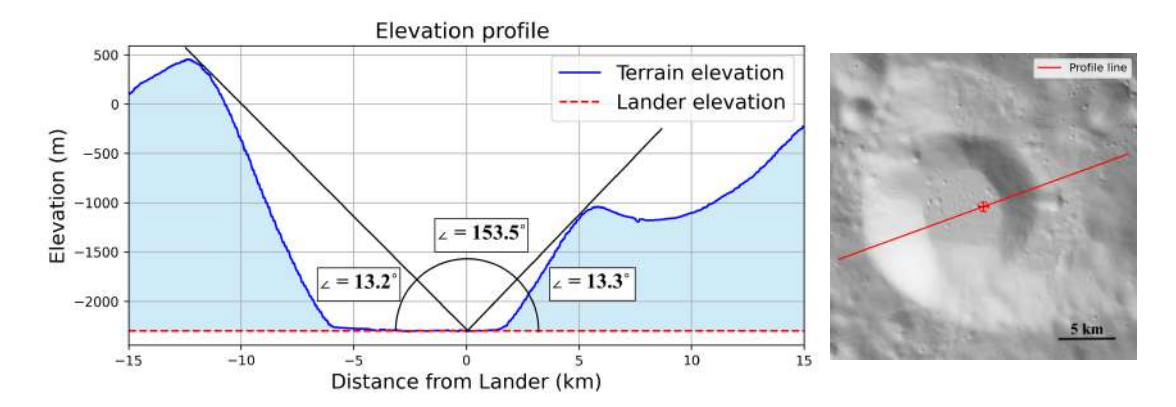
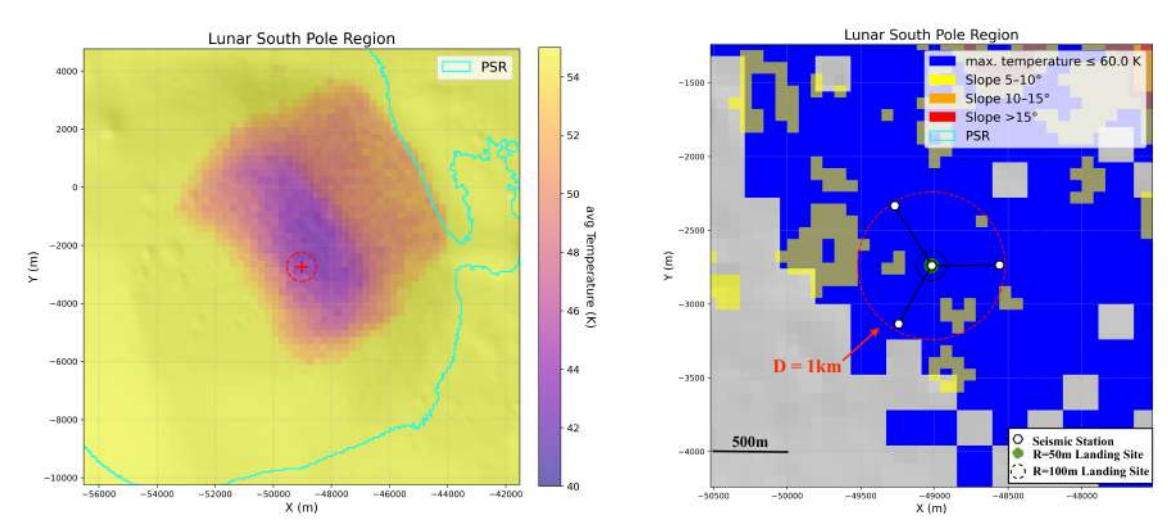


Figure 5.7: Elevation map for deployment site in de Gerlache crater with sky visibility angle and maximal angle for incoming radiation from crater walls.



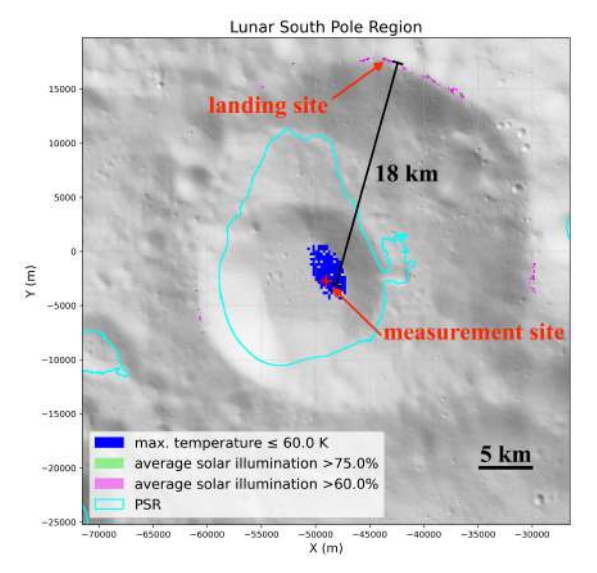
- (a) Map of the year-round average temperature at the deployment site (highlighted in red).
- (b) Proposed PSR with LGWA deployment region in red for a scenario with an RTG power source and circles around the landing site (black: r = 100 m, green: r = 50 m).

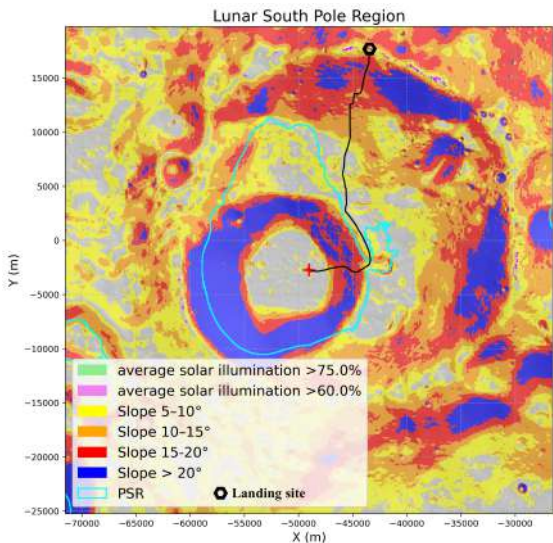
Figure 5.8: Lunar south pole region in polar stereographic projection.

5.3.3 Landing and solar panel deployment on "nearby" hill: alternative PSR at south pole

The same deployment site as the one described in subsubsection 5.3.2.2 could be used as an alternative deployment site for the mission concept using solar cells as a power source, as there exists a site with very good solar illumination on the rim of de Gerlache crater. With a distance of 18 km as the crow flies, this landing site is located way further from the experiment deployment site than in the baseline scenario, more than doubling the amount of cable needed for deployment. In addition, as can be seen in Figure 5.9b, the rover must navigate in steeper terrain close to its specified upper limit of 20°. The slope that the rover needs to navigate and the larger distance that the rover needs to drive both increase the overall risk of the mission during deployment, while the chosen landing site has the benefit of better solar illumination compared to the baseline. In this section the landing site is assessed, while the exact data on the corresponding LGWA deployment site can be found in subsubsection 5.3.2.2.

42 5.3. PSR Selection





- (a) Proposed deployment site at the lunar south pole (red cross) and distance to the landing site.
- (b) Slope map with the landing site (black hexagon), deployment site (red cross), possible rover path avoiding slopes $>20^{\circ}$ and the PSR highlighted in cyan.

Figure 5.9: Alternative deployment site at the lunar south pole region for a scenario with solar cells as power source. Polar stereographic projection.

5.3.3.1 Landing site environment

The selected landing site can be seen in Figure 5.10. It lies north of the deployment site on the rim of de Gerlache crater at the coordinates [88.389°, 280.76°].

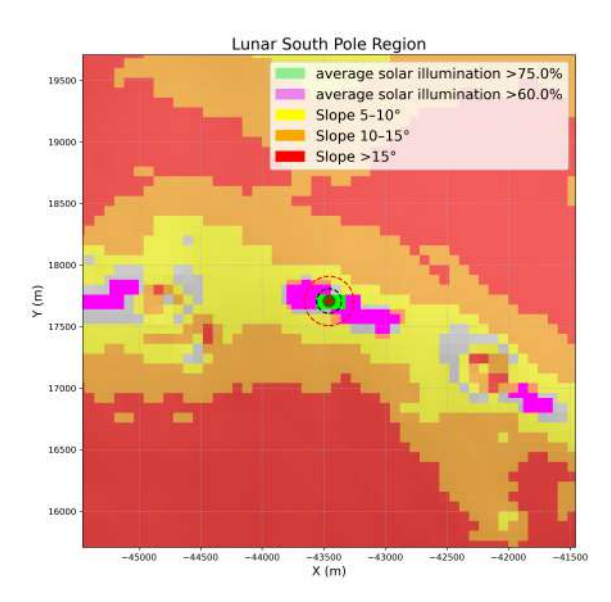


Figure 5.10: Slope map of the selected landing site (green) with solar illumination overlaid (green & violet) and circles for the areal statistics visualized [black: $r=100\,\mathrm{m}$, red: $r=200\,\mathrm{m}$]. Polar stereographic projection.

Location	
Latitude	-88.452°
Longitude	-67.83°

Variable	Mean	\mathbf{Min}	Max	Unit			
200 m radius circle (red)							
T min	71.0	68.2	73.9	K			
T max	242.4	236.9	247.8	K			
T avg	172.6	171.6	173.7	K			
T amp	173.1	168.8	177.4	K			
100 m radi	us circle	(black)					
Slope	1.8	0.3	3.4	0			
SI avg	77.6	76.7	78.5	%			
50 m radius circle (green)							
SR	0.6	0.5	0.7	\mathbf{m}			

Table 5.4: Areal summary of the temperature, slope, and solar illumination over a circle with $100\,\mathrm{m}/200\,\mathrm{m}$ radius around the selected landing site. Surface Roughness calculated over an area with $50\,\mathrm{m}$ radius around the landing site.

Table 5.2 shows the areal statistics of circles around the landing site. With a maximum slope of only 3.4 degrees within a 200 m diameter area around the landing site, the terrain offers a stable and favorable surface for landing while providing sufficient tolerance for localization uncertainties. The lander is expected to touch down within \pm 50 m of the designated target, where slopes remain well within the lander requirement of 10 degrees (see subsection 3.3.1). Furthermore, the site provides very good average solar illumination values, with an average of 77.6% and a minimum of 76.7% within the 200 m diameter area, ensuring adequate power generation even under small deviations from the nominal landing point. As the average illumination is significantly higher than for the baseline landing site, it is very likely that the longest period of continuous shade will be shorter at this site as well.

The maximum surface temperatures are very similar to the baseline landing site: they do not exceed 250 K while staying above a minimum temperature of 68 K. As the landing site sits on a hilltop, it has a large enough sky visibility angle for communication.

5.3.4 RTG power source: alternative PSR at north pole

As mentioned in subsection 5.3.2, the selected LGWA deployment site at the lunar north pole would also be suitable for the alternative mission concept using an RTG as the main power source. In this case the lander would land in the center of the selected experiment deployment site. Therefore the landing conditions in this area are covered in this section, while all the relevant data concerning the deployment site itself can be found in subsubsection 5.3.1.2.

Figure 5.11 shows the LGWA deployment region and the landing site in the center and a possible arrangement of the seismic stations inside the deployment region. The regions with yearly maximum temperatures below 60 K are visualized in blue (and grey). With a maximum slope of 2.3° and a maximum surface roughness of 0.4 m inside an area with a 50 m radius around the landing site, this location has very good conditions for landing.

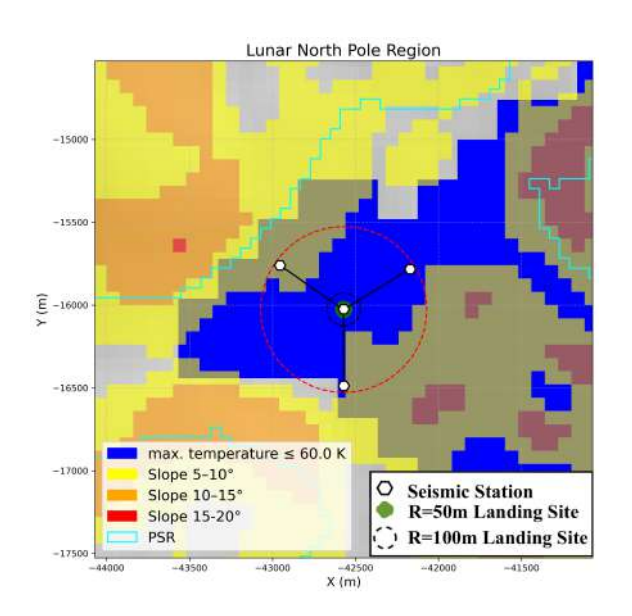


Figure 5.11: Alternative PSR at the lunar north pole with the LGWA deployment region in red for a scenario with an RTG power source and circles around landing site (black: $r=100 \,\mathrm{m}$, green: $r=50 \,\mathrm{m}$). Polar stereographic projection.

5.3.5 PSR selection: summary

Several potential deployment sites were assessed at both the lunar north and south poles to satisfy the thermal and operational requirements of the SILENCE mission. For the baseline scenario, a PSR at the lunar north pole is selected for LGWA deployment, with the corresponding landing site on a nearby hill providing sufficient solar illumination (>55%) for power generation. While the deployment site itself is extremely cold and flat—ideal for scientific measurements—the distance of 8.6 km between the PSR and the landing site introduces logistical challenges, such as the need for long power cables.

Alternative scenarios using an RTG power source allow deployment directly from inside PSRs, removing the need for solar panels and enabling landings directly inside the PSR. A preferred

5.3. PSR Selection

south pole PSR inside the de Gerlache crater was selected due to its low temperature amplitudes and flat terrain. This site benefits from high-quality data availability but carries a potential risk of anthropogenic noise due to proximity to the planned Artemis III landing site. The baseline deployment site is also a very good option for deployment with an RTG as a power source, as it offers very good conditions for landing.

The north-polar baseline was chosen as the most suitable deployment scenario primarily because the availability of an RTG is currently uncertain, and the south-polar solar-powered option poses higher operational risks due to longer distances and steeper terrain. These site selections balance thermal, power, and operational requirements while maintaining a low risk of anthropogenic noise interference for the LGWA experiment.

5.4 Deployment

5.4.1 Overview

This report only considers the deployment of four seismic stations as described in chapter 4. Each of the seismic stations would on their own have sufficient sensitivity to detect gravitational waves [3], but deploying them as an array allows us to filter out the SBN due to the GWs being basically the same at all stations, while the SBN differs significantly in phase from station to station. The size of the array on the first order has to be big enough for the SBN to have a significant phase delay between stations but small enough that the SBN from one station can still be modeled from the data of another one [4]. While further array optimization is still needed, we assume the one-kilometer-diameter star-like deployment pattern proposed in [3], with the idea of having the best SNB cancellation in the central station, depicted in Figure 5.12.

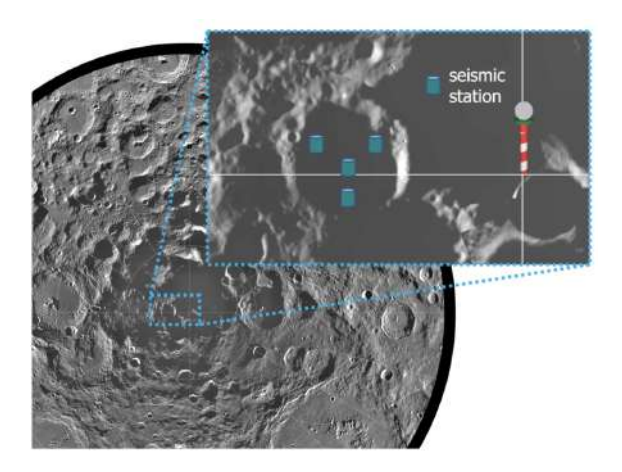


Figure 5.12: Lunar mosaic of about 1500 Clementine images of the lunar south pole region. The inset shows an example crater near the south pole with a star-like deployment configuration of four seismic stations in a kilometer-scale array of seismic stations containing cryogenic inertial sensors. Adapted from [3].

Possible deployment strategies considered in this report are subject to the assumption of having only a single lander and limited to on-ground distribution by (a) rover(s) or astronaut(s), as mentioned in the project description. Nevertheless, we want to mention some deployment strategies that violate these constraints, which are summarized in subsubsection 5.9.3.2. We did our mission design for the case of distribution by rover, as we believe that the additional requirements for human spaceflight would dominate the payload-derived requirements, increasing mission cost for a mission dedicated primarily to the LGWA significantly. However, that does not mean that the deployment of the LGWA as part of a manned space mission could not be an advantageous solution. Our very basic considerations on the scenario of deployment by astronauts can be found in subsubsection 5.9.3.1. We further decided that a wheeled solution makes sense for this mission, as legged robotic solutions have yet to be demonstrated in space [32], while wheeled ones already have heritage [33].

5.4.2 Baseline deployment strategy

Our deployment baseline is that a lander lands outside the PSR on the nearby hilltop with high illumination described for our baseline PSR in subsubsection 5.3.1.3, from which the stations are then all at once driven inside the PSR by a rover, laying aluminum and glass fiber cables on the same drive to establish the connection between the lander and stations. Those will be connected in a chain-like manner, enabling unloading one station after the other from the rover. This baseline has been formulated under the assumption of having a solar array that has to be placed on the highly illuminated hilltop close to the PSR presented in subsection 5.3.1 by first trading one vs.

46 5.4. Deployment

multiple rovers in subsubsection 5.4.4.1, then by trading landing inside the PSR vs outside the PSR in subsubsection 5.4.4.2, and finally deciding whether the rover should carry all stations at once or one after the other in subsubsection 5.4.4.3. Finally, a tradeoff concerning the rovers power provision is made in subsubsection 5.4.4.4. The trades have been performed under the assumption that the rover would be specifically designed for this mission. From the trades, our favorite strategy was the one described above with a rover carrying all four stations on one drive into the PSR while powered by the lander over the same cable that later powers the stations. We picked our baseline rover presented in subsection 5.4.3 because we think opting for a commercially available rover significantly decreases mission cost, and because it has the capabilities to perform the LGWA deployment in a single hilltop to PSR drive, realizing our preferred strategy. We still plan for the rover to be connected via the lander station cable to the lander for communications and possibly power because we have no information on its range in the shade.

Figure 5.13 conceptually displays the baseline deployment strategy, and Figure 5.14 shows how the lander and stations are connected.

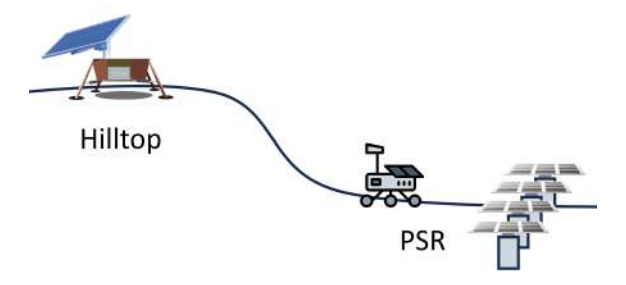


Figure 5.13: Schematic for landing on a hilltop outside the PSR (Baseline): after landing, the seismic stations need to be moved into the PSR.

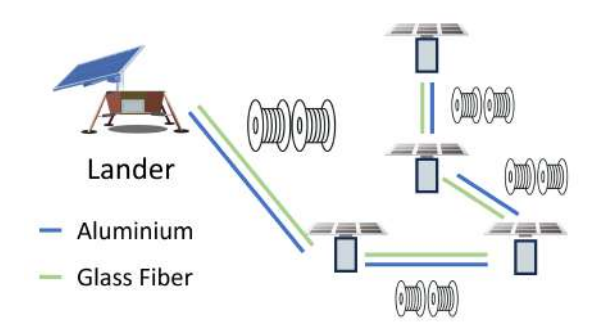


Figure 5.14: The schematic displays the cabling: The four stations are connected to form a chain attached to the lander preflight, such that they can be placed down sequentially on a single drive into the PSR with multiple stops. Each cable link has its own cable drum. It could be considered to deploy the two different cables per segment from the same drum or even have both connections in the same cable.

5.4.3 Baseline rover: Venturi Astrolab FLEX

After first looking at common design elements of current and past rovers, we turned towards commercial solutions that are currently under development and will prospectively be available in time to be integrated into our mission, considering an expected launch in the early 2040s. We specifically looked at the NASA LRV candidates, of which one is planned to first be used on the Artemis V mission in early 2030 [34], namely the Astrolab Venturi's FLEX, Lunar Outpost Eagle, and Intuitive Machines Moon RACER [35]. While the initial NASA request for information stated

that: "mobility systems should accommodate the ability to autonomously load and unload cargo or science packages, including excavation rovers carrying regolith." [36], we only found explicitly stated payload deployment capabilities without human intervention for Venturi Astrolabs FLEX rover[5], which is why we chose it as a baseline. We found no other significantly developed rover we expect to be commercially available in the 2030s, capable of carrying one or more of our seismic stations.

Astrolab's FLEX rover is currently being designed for temperatures ranging from 43 K to 183 K and is set to accommodate up to 1'500 kg [37] with a volume of up to $3\,\mathrm{m}^3$ of payload. It thus meets the rover payload capacity requirements of our mission (around $2.8m^3$ of volume and 600kg of mass for the stations, radiators, and cables section 5.10). The rover is further planned to have a 6-DOF robotic arm with a lifting capability exceeding 25 kg in a 2 m radius workspace and the ability to deploy payloads by lowering its chassis and retracting payload affixing locks [5]. Astrolab's FLEX rover weighs around 500 kg [38][39] and has dimensions of 3.8 m length, 2.6 m width, and 1.8 m height [40]. It features individually turnable and highly deformable wheels [40], enhancing mobility and allowing it to climb slopes of more than 20 degrees [41][42][39]. Venturi's FLEX rover is scheduled to launch aboard a Starship towards the lunar south pole in 2028 [37].



Figure 5.15: Picture of a Venturi Astrolab FLEX rover during field testing [5].

Due to the limited lifting capabilities of the robotic arm and multiple cable drums necessary for the deployment of the LGWA, we think modifications on the FLEX rover may be necessary for this mission. We concretely expect that the payload locking latches may need to be adjusted to securely hold four LGWA stations in place. Further, the height at which the stations are attached on the rover might need to increase in order of deployment, as only the chassis, not the individual stations, can be lowered to the ground. Alternatively, the robotic arm could be replaced with a stronger one. It is possible that these concerns can be adressed via station and cable-laying system design or through a payload adapter. We recommend this to be analyzed in depth, as it strongly relates to the question if this mission needs to fly its own rover to the Moon. The possible necessity of rover modification is one of the reasons why we kept our baseline north pole PSR and planned for having to bring our own rover as discussed in section 5.9.

5.4.4 Deployment trades

The deployment trades were made regarding our baseline PSR presented in subsection 5.3.1 and under the assumption of having to place a solar array on the highly illuminated hilltop nearby presented in subsubsection 5.3.1.3, which we picked as our landing site as a consequence of the trades presented in this section. If landing inside the PSR, the central station is assumed to be placed close to the lander, and the three outer stations each need to be placed 500 m away from the central station. The distance from the highly illuminated hilltop to the PSR is roughly 10 km.

Our assumptions on rover characteristics for the deployment trades were based on the Perseverance rover (1'025 kg heavy, top speed of 152 m/h, power when driving 200 W [43]) for speed and power consumption and on the Endurance (CBE without samples 398.2 kg, average speed of 500 m/h [44]) and Viper (450 kg heavy, up to 720 m/h speed, peak power of 450 W [18]) rovers for mass and are

48 5.4. Deployment

summarized in Table 5.5. There are two versions of the Endurance rover, one capable of carrying 2.2 kg of samples and one capable of carrying 100 kg of samples, with a for-the-concept-phase identically estimated weight of around 400 kg [44], which we then took as the weight estimate for the Single Station Rover, as the station including the radiator weighs around 90 kg (chapter 4). Given the weak influence of carrying capability on unloaded rover mass indicated by the Endurance rover concept study, assuming no unloaded rover weight difference for a carrying capability difference of almost 100 kg, we assumed a 50 kg unloaded rover weight increase going from the Single Station Rover to the Four Station Rover.

Parameter	Single Station Rover	Four Station Rover
Power (W)	150	200
Speed (m/h)	152	152
Mass (kg)	400	450

Table 5.5: Comparison of estimated characteristics of the Single Station Rover, capable of carrying one station at a time, and the Four Station Rover, capable of carrying all stations at once. Derived by looking at the Perseverance, Endurance, and Viper rovers. While these figures were used for the deployment trades before including the FLEX rover into our baseline, they are still used as a reference value in some chapters, as power consumption of the FLEX rover could not be determined. While the FLEX rover should be self-sustaining given enough illumination, we have no estimate on range in the shade. While we have assumed to have to supply 200 W to the FLEX rover during deployment, this has not driven battery or solar array size section 5.5.

5.4.4.1 Single rover vs. per station mobility platforms

Our baseline features a single rover because we believe this is preferred over multiple rovers. For this trade, we have not yet decided whether the single rover could carry only one or all four stations at a time. The multiple rovers were in a first step considered as having essentially the same design as a single rover capable of deploying one station after the other. We decided to increase the rover mass by approximately a factor of four would not be worth the added redundancy and reduction in rover requirements associated with the reduced range and perhaps carrying requirements, regardless of whether we would land inside or outside the PSR and how many stations at a time the single rover can carry. We got to this conclusion by looking at the Viper and Endurance rovers, which indicate that a lunar rover capable of carrying a payload of the same order of magnitude in terms of mass as one LGWA station weighs around 400 kg, and that relative rover mass increase is smaller than relative payload mass increase in this regime (the rover mass without the samples was assumed identical for the 2.2 kg and 100 kg sample versions of Endurance) [44], [18]. So for landing inside the PSR, a single rover doing single-station drives would be favorable compared to multiple rovers, and for landing outside, even if we could not do single-station drives (be that from a risk perspective or), a big rover carrying all four stations would still be less heavy than multiple rovers.

However, we then also considered the "mobile station" case, a variant of the multiple rover case, where rover and lander requirements are reduced by launching the stations pre-attached to a simpler mobility platform, removing the need to pick up the stations from the lander, as well as possibly simplifying the design of the lander. This trade-off was considered under the assumption that the mobility platform would need to detach and move away from the station to not increase the complexity of the station's vibrational response.

While doing this would increase deployment speed, especially if the single rover would only do per-station drives (assuming all variants have the same driving speed), and get rid of the single failure point that is the transportation system between the lander and station deployment location (still being able to deploy 3 stations if one mobility platform fails), it would only allow single transportation system failures at the cost of significantly reduced system performance. We assumed this solution thus does not really bring any benefits in terms of risk reduction, unless the mobility platforms could pick up each other's stations, which would bring us back to the multiple rover

case we have decided against above. The deployment speed advantage is not relevant if landing inside the PSR, as deployment there takes around one Earth day only, considering driving under the assumption of speeds comparable to the 152 m/h of the Perseverance rover [43]. And if landing outside the PSR, mobility platforms wouldn't be significantly faster than a rover carrying all stations at once, as the path to the PSR is longer than the distance that needs to be driven inside the PSR.

In the end, we believe that the requirements for the mobility platforms in terms of operability under the given environmental conditions and the needed sensing and locomotion capabilities necessary to reliably drive on the lunar surface and inspect the stations' sites' local terrain for optimal station placement leads to requirements too close to the ones for a single rover capable of carrying one station at a time to make it the favorable option. However, such an approach could become more attractive if the stations need to be distributed over a larger area if the distances become problematic for a single rover independent of how many stations it carries, be that from an operations or rover energy storage perspective.

5.4.4.2 Landing inside vs. outside the PSR for a solar array outside the crater

We have compared landing inside vs. landing outside the PSR under the following assumptions: We have a single lander and a single rover, and we have a solar array that needs to be deployed outside the PSR as part of the lander or as a module the rover needs to deploy outside the PSR. Laser and communication hardware are in both cases on the lander. This keeps the amount of hardware that needs to be moved around minimally. The lander is connected to the stations via aluminum cables for power and data transmission and a glass fiber cable to transmit the laser signal for the interferometric seismic readout. For the landing inside the PSR case, the rover requirements are reduced to only being capable of carrying a single station at a time, while for the variant where we land outside the PSR, the rover needs to be capable of carrying all four stations while deploying the aluminum and glass fiber cable. The comparison is done this way, as we assume driving several times from the highly illuminated landing site into the PSR should be avoided to reduce risk, while reducing rover carry requirements if landing inside the PSR appears advantageous. This is based on the assumption that the highly illuminated area where the solar panel needs to be deployed is, compared to the size of the array, a significant distance away from the station deployment site inside the PSR. The two scenarios are depicted in Figure 5.16 and Figure 5.13. Our considerations are depicted in the tradeoff matrix in Table 5.7.

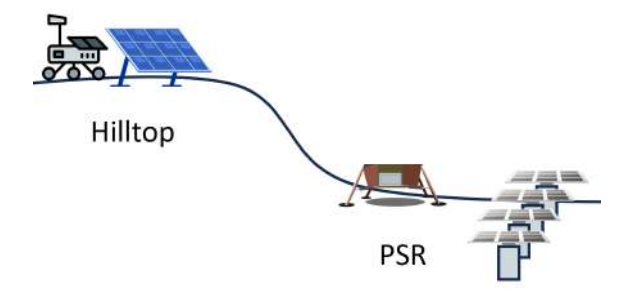


Figure 5.16: Schematic for the landing inside a PSR: after landing either before or after deploying the stations, the solar array structure needs to be moved to the hilltop and deployed there.

Under the above mentioned assumptions, we think landing outside the PSR appears to be the better choice. Landing outside the PSR while adding the need to drive the stations into the PSR and increasing the distances between the stations, thus increasing glass fiber cable length and consequently mass, reduces complexity by allowing the solar array to be part of the lander and not a separately by rover movable and deployable module, which would increase the risk of failing

¹(low, medium, high impact corresponding to weights of 0.5, 1 and 2); a higher total is better

5.4. Deployment

Parameter	Influence factors	Landing inside PSR preferable	Landing outside PSR preferable	Impact
Mass	avoids mass increase due to separable and individually deployable solar module		х	medium
	keeps laser transmission, power, and data connections between lander and stations short	x		medium
Power	power supply quickly available during deployment		X	low
Communication	Communication(easier) DTE		X	low
Complexity	avoids need for solar module that can be separated from lander and moved outside the PSR		x	medium
	avoids need for rover capability to deploy solar array		X	medium
	reduces required landing accuracy	x		low
	avoids permanent lander exposure to high day–night temperature changes outside the PSR	x		medium
Risk	reduces risk of failure to deploy solar panels		x	high
	reduces risk on the station deployment drive	x		low
Total		3	6	

Table 5.7: Comparison of landing site options with respect to various parameters, associated influence factors, and weight of importance. The cross marks the option favorable for the factor on the corresponding row. Weights are are summarized over all factors favoring one variant, according to their impact 1 .

to establish power generation. The main advantage of landing outside the PSR is solar power availability for system status tests after landing, during egress of the rover, and during the drive between the hilltop and the PSR. If landing inside the PSR, solar power would only be available once the rover egressed from the lander and drove to the hilltop site laying the power cable, and deployed the solar array. Despite the lander carrying a battery capable of powering the array for one lunar night, we consider the risk of running out of power before establishing solar power supply significant enough to be the main factor comparing the two strategies. Looking at the examples of Viper [18] and the Endurance rover [44], the weight of the rover is big compared to the payload and does not increase dramatically if payload weight is increased (the endurance concept used the same mass budget for the 100 kg and 2.2 kg sample versions). The increase in payload, going from carrying one to carrying four stations is bigger than going from 2.2 kg to 100 kg of samples for the endurance rover. Nonetheless, we don't anticipate this to increase rover weight from an estimated 400 kg (CBE) for a rover capable of carrying one station or the cables between hilltop and array at a time to more than 450 kg (CBE) for a rover capable of carrying all stations and cables at once. The glass fiber cable to the lander on the hilltop is estimated to weigh around 23 kg, of which around 80% could be saved if the lander is inside the PSR. Having to drive the stations into the PSR does not heavily increase risk, as one drive between the PSR and the hilltop is anyway necessary to establish power supply of the stations under the assumption of using cables. The increase in needed landing accuracy is hard to quantify as it depends on the PSR and nearby sites of high illumination. If there are no obstacles fatal for landing, landing errors inside the PSR can be corrected to some extent during station deployment, but outside the PSR the lander needs to be placed in a high-illumination area, which for our baseline PSR is relatively small.

Variations of the approach of a rover moving the solar array out of the PSR would be a solar array that can detach from the lander and move itself out of the PSR or allocating the power generation via solar function to the rover. A rover equipped with sufficient solar cells and battery capacity could, during station deployment inside the PSR, do charging intervals outside the PSR and after station deployment move with a power connection to the lander to a final position outside the PSR to serve as the long term power source.

The above tradeoff includes factors heavily dependent on various system drivers such as power source or site selection. If an RTG, nuclear fission reactor, or high reaching solar array inside the PSR were to be picked, landing inside the PSR would almost certainly be the better option. Depending on the selected PSR, the risk associated with driving several times into the PSR would need to be weighed differently. There is also the consideration of having solar arrays inside the PSR if a PSR could be found where solar irradiance increases quickly enough with height that solar cells could be deployed inside the PSR while still having low and stable enough temperatures on the ground [11], again vastly increasing the attractiveness of landing inside the PSR.

5.4.4.3 Single rover carrying one vs. carrying all stations

Having a rover carry all stations at once would reduce the risks associated with station deployment, as only a single drive down into the PSR would be necessary. Carrying all stations at once would also allow to get rid of the need to pick up stations from the lander, as they could already be attached to the rover preflight. Having the rover only drive into the PSR once, capable of drawing power from the cable it deploys, would also reduce its battery capacity requirements to a minimum. On the other hand, the requirement for how much payload the rover needs to be capable of transporting massively increases, increasing rover structure size and weight. The requirement on the steepest slope the rover has to be capable of driving would not necessarily decrease due to not having to get out of the PSR again, as slopes on the way from the lander to the PSR might well be steeper than the PSR wall. We estimate the structural weight increase going to the bigger rover at 50kg Table 5.5 to be smaller than the required around 76kg of battery for the small rover for the drives between the PSR and hilltop landing site. This assumes for the smaller rover driving several times, that the cable is laid on the first drive and then detached from the rover and that the rover could recharge inside the PSR when it connects subsequent the stations, only requiring battery capacity for around

5.4. Deployment

11.5km. At the 152 m/h from Table 5.5, this requires $W = Pt = P\frac{s}{v} = 150 \,\mathrm{W} \cdot \frac{11,500 \,\mathrm{m}}{152 \,\mathrm{m/h}} = 11.35 \,\mathrm{kWh}$. At a power density of 150 Wh/kg [45], this results in $m = \frac{11.35 \,\mathrm{kWh}}{150 \,\mathrm{Wh/kg}} = 75.7 \,\mathrm{kg}$. We prefer a single rover carrying all stations for the reduced risks associated with reducing the number of hilltop PSR drives, and alleviating the need for station pickup, given that we do not expect a big mass penalty.

5.4.4.4 Rover powered by battery or cable

Favoring to carry all four stations in one drive, we traded how to power the rover, considering two options: 1) Adding a battery onto the rover 2) Connecting the rover to the power cables it has to lay out.

Parameter	Influence factors	Cable connection	Battery	Impact
Communicatio	n Constant communication with lander and ground	х		medium
Mass	No additional battery mass	x		low
	Second battery needed		X	low
Complexity	Rovers ability to move freely		x	low
	No additional battery heating/shielding	x		low
Risk/Failure	Reduced potential of power loss/failure	x		high
	Potential software error fixable	x		high
Total		4	1	

Table 5.9: Comparison of a scenario where the rover has its own battery and one where its connected via cable to the lander ¹.

 $^{^{1}}$ (low, medium, high impact corresponding to weights of 0.5, 1 and 2); a higher total is better

5.5 Power System

This section describes the EPS that generates, stores, and distributes power for the LGWA. The LGWA will operate in a PSR, so an RTG would be a favorable option for power generation. However, since RTGs are not currently available for small, non-government missions, PV panels are the most favorable option. A dual-panel solar array (Figure 5.18a) and a lithium-ion battery are placed in/on the lander, and power is distributed with aluminum cables to the seismic stations.

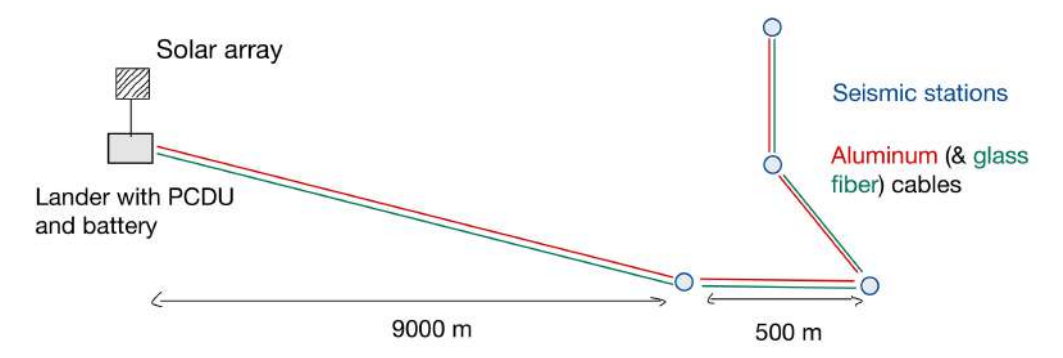


Figure 5.17: Sketch of the cables connecting the stations with each other and the lander.

The average required power of all subsystems and payloads is 74.8 W (subsection 5.10.3). Adding a margin to that, we will size the EPS based on a continuous $P_{required} = 80 W$ power consumption.

The following sections discuss each part of the EPS in more detail.

5.5.1 Power generation and storage

Two solar panels are placed back-to-back forming a dual array [46] to improve solar illumination. A tracking panel is not considered, as the mission's modest power requirement makes the additional complexity, mass, and potential failure risk of a rotation mechanism unnecessary.

AZUR SPACE [47] offers a variation of triple junction gallium arsenide (GaAs) PV cells, ideal for space applications. At a solar irradiance of $P_{Solar} = 1367 \ W/m^2$, triple junction GaAs cells offer the following power at normal incidence [47]:

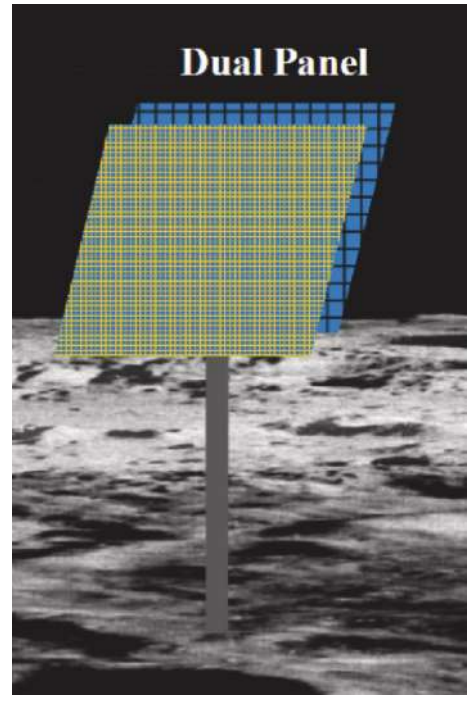
$$P_{BOL} = \eta_{BOL} * P_{Solar} = 403.265 \ W/m^2 \tag{5.1}$$

$$P_{EOL} = \eta_{EOL} * P_{Solar} = 362.255 \ W/m^2 \tag{5.2}$$

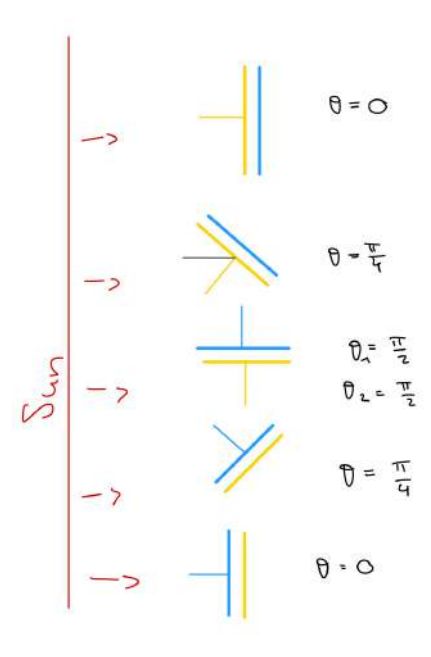
End-of-life efficiency η_{EOL} corresponds to the state after $1*10^{15}~MeV$ fluence [47]. All further calculations assume EOL efficiency and voltage, assuring a margin. Total power output is then given by

$$P_{out}(t) = A * P_{EOL} * \eta * |cos(\frac{2\pi * t}{708h})|.$$
 (5.3)

Where A is the panel area, η the solar illumination, and $\theta = \frac{2\pi t}{708h}$ the incidence angle, which makes a full rotation in one lunar day (708 hours). We can use the absolute cosine value because of the dual array (see Figure 5.18b).







(b) Sun incident angle on panels over 14 days (half a lunar day).

Figure 5.18: The chosen dual-panel array for power generation offers the advantage of close to continuous power generation without a rotating mechanism.

We choose the area of one panel to be A=2 m^2 , ensuring sufficient power generation at only 10% solar illumination. The arrays add up to a mass of 6.8 kg [20], and the support structure is estimated to be 10 kg.

Solar illumination data was difficult to obtain, however, Figure 5.5 shows approximately 20 dark periods (solar disk fraction 0), with the longest one lasting 538 hours. The battery will be sized accordingly:

$$E = P_{required} * t = 40.2 \ kWh \tag{5.4}$$

With a typical energy density of lithium-ion batteries (150 Wh/kg [45]), that is a mass of 268.3 kg and a volume of $0.836 \times 2.896 \times 0.115$ m³. It is assumed that there is no significant battery degradation (charging every 15 days for 10 years), but in further iterations of this process and when more solar illumination data is accessible, that would have to be considered.

5.5.2 Power control and distribution

Power is distributed by connecting the lander (power station) and the seismic stations with aluminum cables as displayed in Figure 5.17. We will use direct current and connect all seismic stations in parallel. For the following calculations we assume the cable connecting lander and first seismic station (or the long cable) to be 10 km long (9 km + depth + margin) and negligible resistance in the shorter cables.

Internal cable resistance is given by

$$R = \rho * \frac{L}{A},\tag{5.5}$$

where L and A are the length and cross-sectional area of the wire and $\rho = 0.0478 * 10^{-8} \ \Omega * m$ is the electric resistivity of aluminum, assumed to be constant at 50 K [48]. A cross-sectional area of $A=4\ mm^2$ yields a negligible power loss.

Given the density of aluminum $\delta = 2700 \ kg/m^2$ [48], the resulting cable mass is $m = 2*l*A*\delta = 248.4 \ kg$.

5.5.3 Deployment power

The power required for deployment of the seismic station is given in Table 5.16 and adds to a total of 334 W.

Given the total driving distance of the rover is 11.5 km, it takes 75.7 hours (roughly 3 days) to deploy all stations. Figure 5.19 displays the generated solar power at BOL in case of total solar visibility. It shows that deployment can be done without additional use of the battery, ensuring no unnecessary degradation.

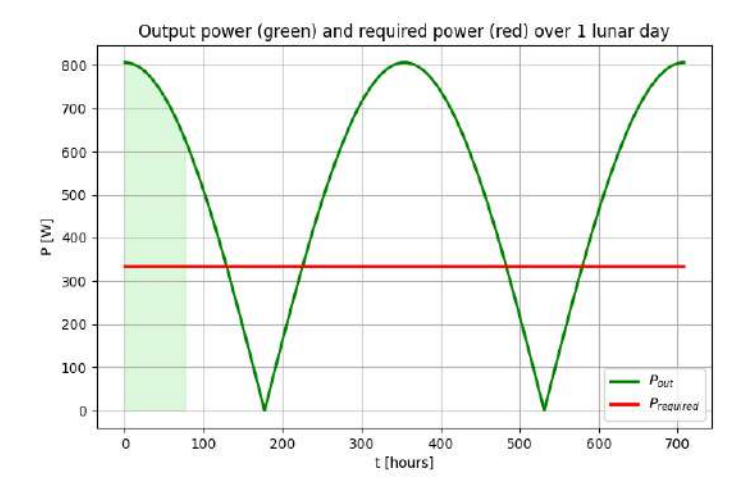


Figure 5.19: Power produced from the solar array and required power during 1 lunar day (29.5 days or 708 hours). The first 76 hours (time to complete deployment) are shaded in green.

5.6 Communication System

The communication system to reliably transmit data from each seismic station to the ground has two almost independent systems that can be identified, namely the down-to-Earth link and the inter-station link. Since detailed calculations have been performed in Appendix A, margins are applied only to the results, which are then indicated by a '-symbol.

5.6.1 Deployment operation

During deployment, a rover will navigate over lunar terrain as concluded in section 5.4. Since a fully autonomous rover is highly complex and impractical, data transmission supports rover operations by downlinking images for more efficient navigation. A heavily compressed (30x) black and white image with a resolution of $1280 \times 720~px$ takes up $D_{img} = 2.5 \times 10^5~bits$ of data. Considering the calculated data rate in Appendix A with margin of $R'_D = 4.3 \times 10^6~bps$, an image would take

$$T'_{img} = \frac{D_{img}}{R'_D} = 0.058 \ s, \tag{5.6}$$

where T'_{img} is the time to downlink an image, D_{img} is the amount of data per image, and R'_D is the downlink data rate. A maximum frame rate of

$$R'_F = \frac{1}{T'_{img}} = 17.3 \text{ fps},$$
 (5.7)

where R'_F is the frame rate and T'_{img} is the time per image. This frame rate is only reached when ignoring other telemetry, tracking, and command (TT&C) signals.

5.6.2 Inter-station communications

The existing concept of routing power to the seismic stations via shielded power cables provides an opportunity for simultaneous communications on the same interface. Instead of opting for another cable, such as an optical fiber for ultrafast communications or a wireless connection between the stations, powerline communications (PLC) provide a balance between speed, simplicity, and reliability that cannot be matched by other suggested methods. To enable a half-duplex PLC that carries data without an additional required wire for a clock signal, a controller area network (CAN) bus is utilized. CAN profits from an established data format that includes useful features for a high-stakes environment, such as built-in error correction and a signal where only 0 and 1 carry data and no intermediate values are used in between. The feasibility of CAN PLC is further explored by Grassi et al. [49], utilizing products from Yamar [50], where the voltage on the powerline has no effect on this protocol. This source also states a data rate of $R_{CAN} = 500 \; kbit/s$, which could be improved with deliberate design to bring it up to the official CAN standard data rate of $R_{CAN,std} = 5000 \; kbit/s$.

Considering that a single seismic station generates $R'_{S,Sci} = 940~bps$ of measurement data [11] and approximately $R'_{S,HK} = 167~bps$ of housekeeping data, a utilization of the CAN bus can be calculated, assuming that the lander and the four stations are all part of the same network.

Sending data from each seismic station to the lander every second ($\Delta T_S = 1 s$) means that $D'_{S,Tx} = (R'_{S,Sci} + R'_{S,HK}) * \Delta T_S = 1107 \ bit$ of data would have to be transmitted per station. Calculating the required transmission time yields

$${\rm T}'_{S,Tx} = {D'_{S,Tx} \over R_{CAN}} = 2.2 \times 10^{-3} \ s \ {\rm or} \ 2.2 \ ms$$
 (5.8)

per station, where $T'_{S,Tx}$ is the required transmission time per station, $D'_{S,Tx}$ is the data volume to be transmitted, and R'_{CAN} is the data rate of the CAN PLC bus, both with an applied margin. A combined transmission time, including $T_{CAN,init} = 0.1 \ s$ as a lump sum of transmitting a data request, lander synchronization command, and PLC delay [49], comes out to

$$T'_{CAN,tot} = 4 * T'_{S,Tx} + T_{CAN,init} = 0.109 \ s \text{ or } 109 \ ms$$
 (5.9)

every second, where $T_{CAN,tot}$ is the total CAN transmission time, $T_{S,Tx}$ is the required transmission time per station, and $T_{CAN,init}$ is the time required for data request and synchronization over CAN.

This very low utilization shows the efficiency of the protocol and the possibility for transmitting more housekeeping data, as well as the capacity for data transmission from the lander to the seismic stations in case of faults or firmware upgrades. A more detailed data budget can be found in subsection 5.10.1, and the various calculations and assumptions are listed in Appendix A.

A hinted-at tradeoff lies in the size and volatility of the data storage on each of the seismic stations and the time between transmissions for instrument and housekeeping data. This tradeoff has been analyzed in Table 5.10, where "Frequent" represents the choice of volatile memory with frequent transmissions and "Occasional" represents occasional transmission with the need for non-volatile storage.

Parameter	Influence factors	Frequent	Occasional	Impact
Power	Power use on seismic stations		X	low
rower	Memory power consumption		X	low
Mass	Storage hardware size	X		low
Complexity	Memory architecture requirement	X		high
Complexity	Transmission frequency		X	low
Risk	Telemetry timeliness	X		high
IUSK	Memory loss on power loss		X	medium
Speed	Capacity of communication wire		X	low
Total		4.5	3	

Table 5.10: Comparison of memory and telemetry configurations in seismic stations. Cells marked with "x" signify an advantage of the option in the given aspect¹.

5.6.3 Up- and downlink communications

The second part of the communications package consists of the downlink from the lunar environment to Earth.

A trade study has been done to determine the feasibility of direct-to-Earth links in Table 5.11. The outcome is that relying on an established relay from a third party shows the most promising results, which is further expanded upon in subsubsection 5.6.3.1. To communicate with the relay, LunaNet standards [51, 7] will be followed in an attempt to make the communication system as universal as possible. Furthermore, downlink will use a common dual-redundant system [20], consisting of a UHF, an S-band, and a Ka-band antenna. The S-band serves as a backup for the Ka-band data antenna, as well as the TT&C antenna during lunar nights. During nominal operations, the Ka-band antenna will serve as a downlink, and the UHF antenna will serve as an emergency communication option. Detailed calculations and assumptions for nominal Ka-band antenna operation can be found in Appendix A, and a more concise link budget can be seen in subsection 5.10.2. The whole up- and downlink system will utilize QPSK as the modulation format, as suggested in [7].

Uplink will also be redundant, since a frequency overlap in both UHF and S-band can be observed in the LunaNet specifications, enabling a simple redundant uplink communication system.

A single, wide-angle Ka-band antenna with a bandwidth of B=6~MHz [51], together with an $P_{Tx}=40~W$ of output power [20], are enough for $R_D'=4.3~Mbps$ of downlink, as calculated in Appendix A with the margin mentioned, meaning that downlink takes less than one minute for one full day of data including telemetry, which is calculated to be $D_{1d}=206~Mbit$ after compression. This enables efficient time sharing of the LunaNet relay network with other applications and an option to increase data collection during mission operation. While S-band will not be as fast due to

¹(low, medium, high impact corresponding to weights of 0.5, 1 and 2); a higher total is better

¹(low, medium, high impact corresponding to weights of 0.5, 1 and 2); a higher total is better

Parameter	Influence factors	DTE	Relay	Impact
Power	Transmission distance		X	medium
Mass	Cable length to reach the required position		X	high
Wass	Antenna dish requirements		X	medium
	System set up		X	medium
Complexity	Antenna pointing		X	low
	Interface with other TRx	X		low
Risk	Risk more under our control	X		medium
Itisk	Less points of failure outside of our control		X	low
Independence	Third-party involved in transmission	X		medium
Total		2.5	6	

Table 5.11: Comparison of direct-to-Earth and lunar orbital relay communication architectures. Cells marked with "x" signify an advantage of the option in the given aspect¹.

the scaling of SNR with bandwidth shown in Equation A.10 and Equation A.7, it will still suffice for data transmission. The overpass frequency of relay satellites will therefore not pose an issue in either data storage or transmission capacity.

Explicit calculations for the overpass time have been performed in section A.1, where a relay connection is assumed to fly overhead at an altitude of 1500 km and transmission requires an elevation of at least $\delta=20$ degrees above the horizon. These restrictions result in an overpass time of $T_{max}\approx 3.6\times 10^3~s$ and a more conservative time of $T'_{overpass}\approx 1812~s$. The maximum time where no transmission can happen is given in subsubsection 5.3.1.3, and with a margin it sums up to $\Delta T_{DL,max}=24~days$. In this time, $D'_{24d}=4.94\times 10^9~bit$ of data is generated. Calculating the time required for a downlink, the overpass duration then turns out to be more than the maximum downlink time, meaning that even after a maximum darkness period of 24 days, all generated data can be downlinked in the first relay visibility interval.

5.6.3.1 Justification for reliance on an orbital relay

Several institutional agencies and private companies, such as NASA [52], ESA [53, 54], and JAXA [55] as institutions and Crescent Space [56] and ArkEdgeSpace [57] as corporations, have announced projects to establish communication and TT&C networks on and around the Moon in the next few years. Considering this mission's need for a pathfinder mission and advanced technologies [11], it can be assumed that SILENCE will not launch before 2035. This gives the aforementioned institutions time to establish a lunar relay service, which can then be assumed to be operational and ready for clients by 2035. Especially with the fact that multiple institutions appear to be hard at work to make this happen, one can be confident that there will be one or another version of a lunar relay service by then.

Furthermore, most of the plans for lunar relays are centered on lunar poles, where it should be mentioned that the south pole seems to be more popular, but that orbital dynamics will work in our favor to bring these relays to the north pole as well. Even if the inclination does not match our PSR exactly and the satellites do not end up passing directly overhead, the figures calculated in subsection 5.10.2 show that a fraction of the visible time in an overhead pass is sufficient to downlink all generated data.

5.7 Computing

The seismic stations shall have a computing system to collect, store, and transmit data. At each station, a microcontroller unit (MCU), together with two CAN PLC transceivers, forms the computing unit, as shown in Figure 5.24. To store small amounts of data, a DRAM is proposed because of its low complexity and volatile behavior as determined in Table 5.10. If the electronics are heated up by the surrounding station and sensor heat dissipation, no thermal control is required. As an alternative, to avoid the need to heat each of the stations, cryo-CMOS is a promising technology that promises to provide working compute power in the two-digit kelvin range [58]. To keep an overview of station operations, each seismic station generates housekeeping data in addition to seismometer readouts.

On the lander, an on-board computer (OBC) with a field-programmable gate array (FPGA) and an MCU is utilized to handle all computation needs and provide high-speed digital signal processing. The entire OBC, as shown in Figure 5.25, is designed to be rad-hard to survive the required time of 10 years under solar radiation. Instead of relying on a single OBC, a redundancy of two more identical OBC units is proposed, which can be switched on on demand, following the cold redundancy paradigm. Additional MRAM units are also present on board, providing a configurable option between majority vote error correction and lifetime extension through cold redundancy. The proposed solution is that all 3 MRAM units are active, providing error correction and hot redundancy for an extra layer of redundancy on valuable seismometer data.

While the MCU is responsible for performing lossless 2x data compression, among other tasks, the FPGA is used to enable high-throughput signal processing for data storage, retrieval, and de- and encoding during up- and downlink, according to Consultative Committee for Space Data Systems (CCSDS) standards [59].

To enable long-term storage on board of the lander, a rad-hard MRAM module is installed, which shows exceptionally low degradation over long periods of time and offers fast data transmission [60].

Sizing the DRAM in each of the stations is performed to ensure that at least $T_{S,store} = 10s$ of measurement and telemetry data can be retained per station, which amounts to

$$D'_{S} = T_{S,store} * (R'_{S,Sci} + R'_{S,HK}) = 1.11 \times 10^{4} \ bits$$
 (5.10)

of data, where D_S' is the data volume per station, $T_{S,store}$ is the time length to store data, $R_{S,Sci}'$ is the data generation rate for scientific data per station, and $R_{S,HK}'$ is the telemetry generation rate per station, and "'" indicates applied margins. When including a further margin of 30%, a DRAM can be as small as 16 kbit or 2 kB. The selected 10 seconds of data ensures that data is not lost if a transmission fails and allows for on-site error detection, which would require more utilization of the CAN bus line to transmit all data two or more times. This would not be an issue as described in subsection 5.6.2.

The MRAM module in the lander requires a much larger capacity, since it should be able to store all generated data and additional uplinked data for 24 days. However, this data storage device does not need to function in the conditions of a PSR, so it does not need any advanced technology, beyond being rad-hard, such as cryo-CMOS. With calculations detailed in Appendix A, $D'_{24d} = 4.94 \times 10^9$ bits of compressed data need to be stored, including a margin of 50%. Therefore, an MRAM with 1 GB of storage, or 8×10^9 bits of storage, is selected. In theory, 1 GB of storage would fill up in $T'_{L,max} = 36 \ days$, which is enough for comfortable operation of the system.

5.8 Thermal Design

While the thermal requirements of the lander are standard for lunar missions, the thermal design of the measurement station is more challenging due to the required operation of a cryocooler that can keep a part of the system at 4.5 K.

5.8.1 Lander

The ambient temperature of the lander is between $60\,\mathrm{K}$ and $250\,\mathrm{K}$. The task of the thermal system is to permanently keep the electronics box (containing the battery, laser, storage, computer, and other electronics) between $285\,\mathrm{K}$ and $305\,\mathrm{K}$. The peak power that the radiator needs to be able to dissipate is assumed to be (Table 5.15) $109\,\mathrm{W}$ (assuming the efficiency of the communication system is 50%). The minimum power is assumed to be $9\,\mathrm{W}$, which corresponds to the power consumption of the laser (depending on the actual power consumption of the computing system, the minimum power consumption might be higher, which reduces the amount of MLI insulation required). During flight and deployment, a resistive heater should be used to provide $9\,\mathrm{W}$ and prevent the system from cooling down too far. The approximate volume of the electronics box is about $0.3\,\mathrm{m}^3$ (mainly occupied by the batteries) and the surface area is approximately $3.2\,\mathrm{m}^2$.

Assuming the radiator is pointing to deep space and heat radiation from the lunar surface is therefore negligible (as well as the ambient temperature of deep space), the required radiator area can be computed as (assume AZ-93 white radiator paint with $\epsilon = 0.91$, $\alpha = 0.15$)

$$A = \frac{P_{\text{peak}}}{\sigma T^4} = 0.24 \,\text{m}^2. \tag{5.11}$$

Therefore, the required radiator area is small, even when adding a generous margin. If the radiator panel is mounted properly, no sunlight can directly hit the radiator panel. At about 88.5 degrees latitude, the incident sunlight has an angle of at most 3 degrees to the horizontal, which can be easily shielded off by using a radiator pointing upwards to deep space with a small sun shield on the side. It is recommended to use a low- α material anyways in case there is reflected sunlight.

When the electronics box is thermally insulated with multiple layers of MLI, the impact of ambient temperature changes can be reduced to a minimum. Even when assuming a heat loss of $1 \,\mathrm{W/m^2}$ (there are many MLI systems that can beat this [61]), only about one third of the laser power is lost to the environment, leaving sufficient margin for heat losses through rigid connections that are required to hold the batteries (these feet need to be made using a high strength, low thermal conductivity material, for example G-10).

However, the remaining impact of that effect as well as the time-dependent heat dissipated by the computing and communication system (these systems do not consume constant power; they try to do work that consumes a lot of power during lunar day only) needs to be considered. During deployment or periods of downlink and data processing, there is an increased risk of overheating if the radiator is designed to keep the electronics warm enough during a period of low power consumption. If the radiator is designed to dissipate peak power, there is a risk of cooling down too far during a period of low power consumption. To solve this problem, the following options can be considered:

- Resistive heater: A resistive heater could be used to heat up the electronics box when it gets too cold.
- Bimetallic louvers or shutters: By mechanically closing / switching the radiator between high- ϵ and low- ϵ values, the dissipated power can be changed.
- Variable conduction heat pipes: These heat pipes can be designed (using a non-condensable gas) to passively decrease convection when the electronics box gets too cold.
- Loop heat pipes: These heat pipes can be controlled using an active or passive valve to adjust convection.

	Bimetallic louver / shutter	VCHP	$_{ m LHP}$	\mathbf{MPFL}
TRL	2	2	2	2
Mechanical system complexity	0	2	2	0
Fluid system complexity	2	0	0	0
Dust risks	0	2	2	2
Power consumption	1	2	2	0
Reliability	1	2	2	1
Lifetime	1	2	2	1
Transport distance	0	1	2	2
Mass	2	2	1	0
Total	8	15	15	8

Table 5.12: Comparison of options for lander thermal system. Scores: 0-2, 2 is best

- Mechanically pumped fluid loop: A cooling fluid is mechanically pumped inside a loop pipe from the hot box to the radiator.
- Variable ϵ materials: There is research being done regarding materials that can change
 their ϵ without mechanical movement.

Obviously bad choices are the resistive heater (it would consume additional power during lunar night, increasing the battery weight significantly) and the variable- ϵ material (low TRL). The remaining options are compared in Table 5.12.

We recommend to use a VCHP, assuming the required transport distance is less than about three meters only. For larger transport distances, we would recommend an LHP.

5.8.2 Rover

Similarly to the lander, the rover will need a heated electronics box. The electronics box radiates a peak heat power of approximately $103.5\,\mathrm{W}$ (Table 5.16; assuming an efficiency of 50% for the communication system and 90% for the motors). The minimum power is $0\,\mathrm{W}$ (when the rover is switched off). Making the same assumptions as for the lander, this requires a radiator panel area of $0.23\,\mathrm{m}^2$ (plus margin). The options for variable heat transfer are fundamentally the same as for the lander. However, the required rover lifetime is much shorter, and - although it might need to be heated in the PSR - the rover is connected to the solar panels during deployment, which happens during lunar day. Therefore, if a customized rover is built, we recommend to use a simple resistive heater with a maximum power consumption of $110\,\mathrm{W}$ (peak dissipated power due to electronics plus margin) in order to be able to keep the flux through the radiators at the designed level at all times (resulting in a stable temperature). This option keeps the weight and complexity of the system at a minimum. However, if a general-purpose rover is used that has a more sophisticated thermal system, this is also acceptable.

5.8.3 Measurement stations

A two-stage sorption-based JT-cooler should be used to cool a box inside the measurement stations to 4.5 K. This type of cooler is chosen because it has no moving parts apart from a few passive valves, which makes it compatible for operation on a seismic station (a low level of vibrational noise is required) and increases the lifetime. The internal setup of the cooler is shown in Figure 5.20. This internal setup has already been designed by the LGWA team as part of the payload and is described in the LGWA payload paper [3]. Therefore, it will not be discussed further here, and we will focus on the radiators instead, which need more attention.

This cryocooler requires two radiator panels: One radiator panel at 87 K (power that needs to be radiated into space: 4.2 W) and one radiator panel at 51 K (power that needs to be radiated into space: 1.925 W) [3]. A quick calculation using the Stefan-Boltzmann law shows that, when

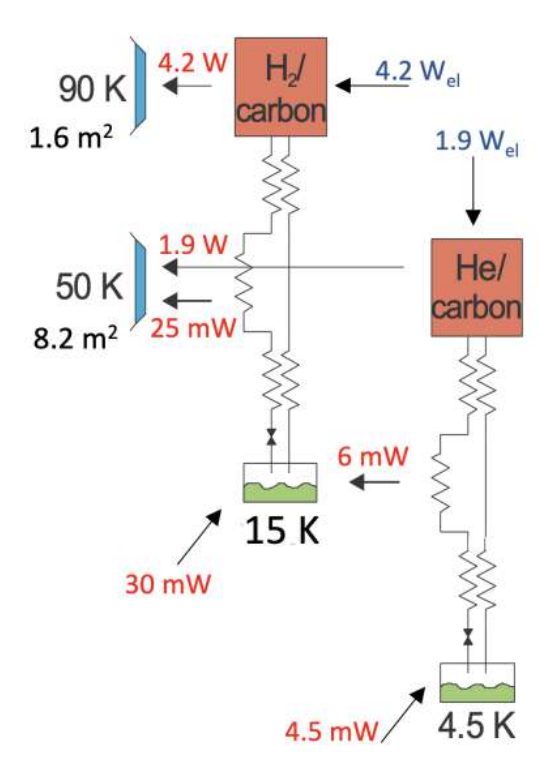


Figure 5.20: Schematic of the cooling system of the measurement stations.

assuming an emissivity of $\epsilon_{rad}=0.98$, the radiators need to have radiating areas of $1.32\,\mathrm{m}^2$ and $5.12\,\mathrm{m}^2$. These radiators are therefore the largest part of the payload, even under these idealized assumptions. They will be drivers of the payload mass requirement, and care should be taken to optimize their design. What makes the situation even worse is that at least sometimes, the 51 K radiator will be colder than the surroundings (no PSR locations were found that are large enough for LGWA and are permanently colder than 51 K. Apart from that, going deeper inside a PSR also means a higher cable length is required and the rover must cover longer distances during deployment. Therefore, it makes sense to build a radiator that has some tolerance towards a higher ambient temperature). In contrast to deployment on flat surfaces, where it is easier to shield off stray radiation from the surface, inside the crater, a significant part of the field of view is covered by the crater walls, and stray thermal radiation striking the top surface of the radiator is unavoidable. The naive way to shield from stray surface radiation is to put vertical shields on the side of the radiator. To shield from the PSR slope and irregularities from the crater structure, we should be immune to all incoming radiation with an angle to the horizontal of 20 degrees or less. When using the computed minimum size for the 51 K radiator, that results in a shield height of

$$h = 2\tan(20^\circ)\sqrt{\frac{5.12}{\pi}} = 0.93 \,\mathrm{m}^2.$$
 (5.12)

This mass of structure and the deployment mechanism could result in a significant torque on the radiator panel, requiring a heavier structure.

To solve the challenges described, we propose using an open tapered honeycomb structure made of aluminum for the top side of the radiators. This structure effectively reflects incoming radiation from the PSR walls away before it can be absorbed by the panel, without requiring a heavy mechanical support structure. The honeycomb should be designed such that light at angles less than 20 degrees to the horizontal is rejected. The bottom side of the panels that points towards the

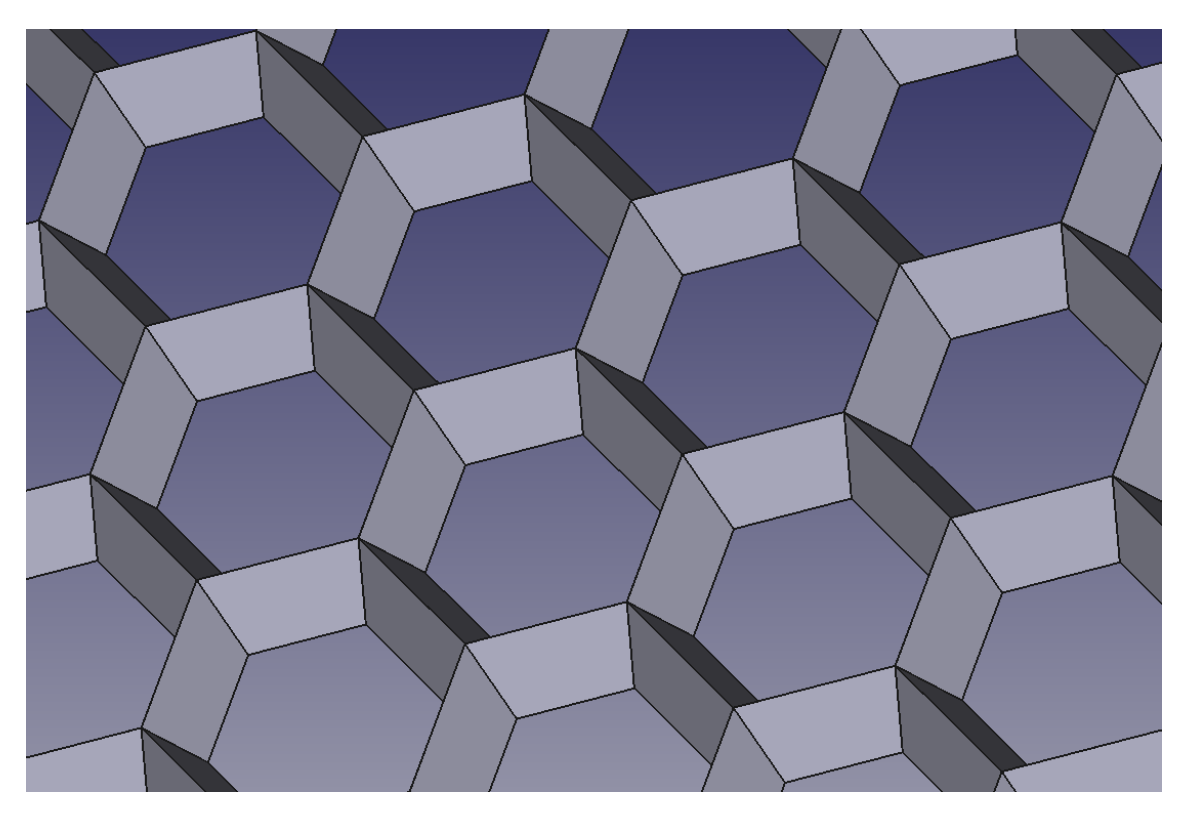


Figure 5.21: 3D View of the proposed open tapered honeycomb structure for the seismic station radiator panels. The reflective vertical inclined parts honeycomb structure is shown in the figure, the emitting flat plate mounted at the bottom is not shown here.

lunar surface should be reflective to absorb as little heat as possible. A 3D drawing of the proposed structure is shown in Figure 5.21.

A possible set of parameters would be a panel thickness of $H = 30 \,\mathrm{mm}$ and an inradius of the upper (larger) hexagon of $r_1 = 40 \,\mathrm{mm}$, with a taper angle of 20 degrees (note: these parameters are not optimized). The taper angle ensures that all incoming rays with angles of less than 20 degrees to the horizontal are reflected away from the emitting panel. The flattest angle under which a ray can pass through the honeycomb is given by

$$\theta_{\min} = \arctan \frac{H}{R_1 + R_2} \tag{5.13}$$

where $R_1 = r_1/\cos(30^\circ)$ is the circumradius of the upper (larger) hexagon, and $R_2 = R_1(1 - H\tan(20^\circ))$ is the circumradius of the lower (smaller) hexagon. Using these equations, we can compute that $\theta_{\min} = 21.7^\circ$. Therefore, we can conclude that this geometry reflects away all incoming thermal radiation with angles to the horizontal of 20 degrees or less.

To estimate the performance of a honeycomb radiator at 51 K, we make the following assumptions:

- To avoid an even larger area, the radiator should not absorb more power from the environment than from the station.
- The reflective material has $\epsilon_{ref} = 0.05$, the radiating material has $\epsilon_{rad} = 0.98$.
- The effective top area of the radiator A is reduced to 0.8A due to the reflective honeycomb parts.

$$P_{\text{ambient}} = 2\epsilon_{ref}\sigma A T_{\text{ambient}}^4 \tag{5.14}$$

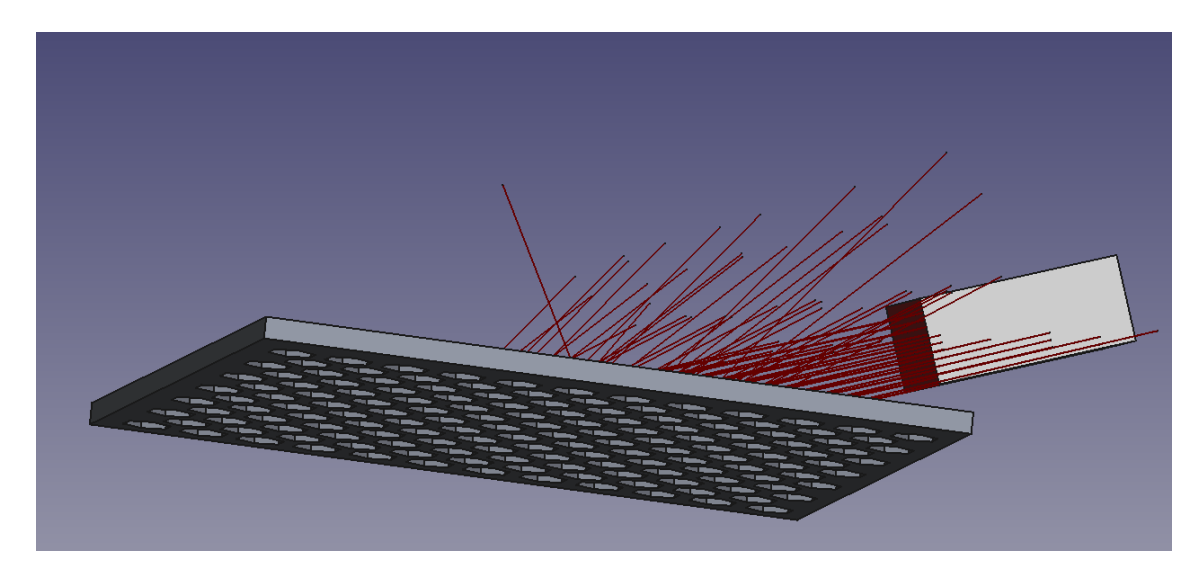


Figure 5.22: Optical simulation of the open tapered honeycomb radiator (3D view).

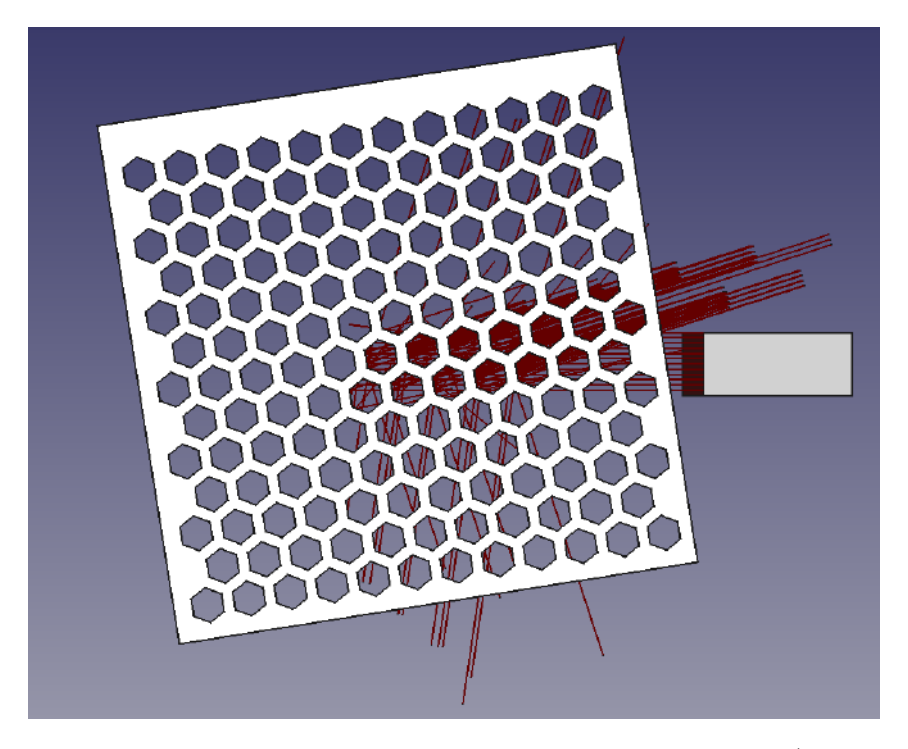


Figure 5.23: Optical simulation of the open tapered honeycomb radiator (bottom view).

$$P_{\text{ambient}} + P_{\text{station},51} = 2P_{\text{ambient}} \approx (0.8\epsilon_{rad} + \epsilon_{ref})\sigma A T_{\text{rad}}^4$$
 (5.15)

Therefore, the maximum ambient temperature where the 51 K radiator can operate properly is approximately

$$T_{\rm ambient} = T_{\rm rad} \left(\frac{0.8\epsilon_{rad} + \epsilon_{ref}}{2\epsilon_{ref}} \right)^{\frac{1}{4}} \approx 1.70T_{\rm rad} \approx 87 \,\mathrm{K}.$$
 (5.16)

Ideally, a PSR with an ambient temperature significantly lower than this is chosen to increase margin and to decrease the required panel size. Site selection has been performed under the assumption that this limit lies closer to 60 K, making a maximal temperature inside the PSR of less than 60 K a requirement. (Station mass and volume estimates in this report were made assuming the $9.8\,\mathrm{m}^2$ of radiators described in [3].) Given the here calculated value, it would make sense to perform a trade study on which maximal PSR temperature favorably balances required radiator area and selectable PSRs with regard to PSR characteristics such as daily temperature amplitude and accessibility but also aspects such as sharing rides, rovers, and power sources with other missions.

The hot electronics box must be well isolated from the rest of the station using MLI. At the temperature differences in question, many MLI setups conduct less than $1\,\mathrm{W/m^2}$. Assuming an isolated electronic box surface area of $500\,\mathrm{cm^2}$, that corresponds to just $50\,\mathrm{mW}$, which could be dissipated easily by the 87 K-radiator or the 51 K-radiator. At the top of the station, there must be a third radiator at $250\,\mathrm{K}$ to radiate away the 4 W generated by the electronics. The radiator should be vertically shielded such that no thermal radiation can hit the crater walls / other objects in the PSR / other radiators. A resistive heater should be used when the electronics do not produce enough heat to stay above the minimum operating temperature. The required radiator area is approximately $0.018\,\mathrm{m^2}$.

5.8.4 Radiator dust mitigation

Regolith dust can damage radiators in two ways:

- Mechanical damage (regolith is abrasive)
- Changing the emissivity (ϵ) and sunlight absorption (α) values

Regolith has an emissivity of about 0.9 [62], so the change of radiator behavior is mainly a problem when the radiator needs to reflect incoming radiation (both sunlight and thermal radiation from lunar surface, in particular from the crater walls). We recommend to deploy an EDS (Electrodynamic Dust Shield) on the lander, the stations and the rover due to its high TRL level [63, 64] and quite negligible size and negligible power requirements (only requires thin electrodes and electronics). The size of a typical EDS power supply is 666 cm³ and is in the process of being miniaturized. EDS systems consume about 2 W-4 W regardless of the size of the EDS. Furthermore, we recommend to consider robustness to lunar regolith when selecting radiator coatings to avoid mechanical damage. It might be possible to not use an EDS system on lander / seismic stations / rover, and instead rely on mechanical shielding or careful mission operations, or accept the rover lifetime reduction due to dust. However, doing so would require a careful simulation of how the systems interact with regolith.

5.9 Alternative Mission Design

5.9.1 Alternative power sources

There are two possible alternatives for power generation. The first one is the use of a **radioisotope thermoelectric generator** (**RTG**), eliminating the need for sunlight and reducing the mass and complexity of the system greatly. Small, non-government missions have practically no possibility of

getting an RTG today; however, that might change in the near future, and at the time of LGWA launch, there might be a higher availability of RTGs. The second option is the use of external power provided by NASA's fission surface power project [65]. This solution also significantly reduces system complexity, eliminating the need for its own power system completely.

5.9.2 Alternative destination and rover sharing

An obvious alternative mission design would be to fly to the south pole, with the idea of using a FLEX rover that might anyway be there in support of the Artemis missions, drastically reducing mission cost. We at some point decided not to alter our baseline with this motivation for the following reasons: Our main motives were the overall favorable conditions and comparably lower risk aspects of the baseline PSR, as discussed in subsubsection 5.3.1.2. We further expect more space mission activity at the south pole, associated not only with resource sharing opportunities but also potential vibrational noise endangering our measurements. The potential need to modify the mechanical interfaces of the FLEX rover, discussed in subsection 5.4.3, together with the reduced post-landing complexity enabled by launching with pre-mounted payloads, as noted in subsection 5.4.4, also contributed to this decision. However, that does not mean that we think the north pole or making the launch of a rover part of the mission is necessarily the better solution. On the contrary, we think looking for opportunities to share resources is important to mission design activities for the LGWA.

5.9.3 Alternative deployment strategies

5.9.3.1 Deployment by astronauts

Cooperation with a lunar human spaceflight mission for deployment of the LGWA array could be very attractive. Accessible PSRs might, despite technical feasibility, not be an option for human safety concerns. Infrastructure and allowed limits for astronauts to carry the LGWA stations and lay the cables would have to be investigated. PSR temperatures might be a limiting factor, due to spacesuits not being designed for continuous use at such low temperatures. The Artemis Suit Material Project states that suits are required to withstand temperatures of down to 100 K for 8 hours, indicating that this might indeed pose an issue [66]. We recommend an investigation on astronaut deployment of the LGWA array. Due to the extremely high cost and complexity of crewed missions, we believe this option would primarily be attractive in cooperation with another mission but could then open up opportunities to leverage resources already brought to the Moon, possibly making crewed deployment preferable over robotic deployment.

5.9.3.2 Beyond the scope of rovers and astronauts

We thought of or came across the following options outside the here considered scope of a single lander and deployment by (a) rover(s) or astronaut(s) for direct delivery of the seismic stations to the inside of a PSR: A second lander delivering the solar array outside the PSR makes landing inside the PSR more attractive. A platform that would, after delivering the stations and rover to the PSR ground (be that through landing or, less likely, through sky crane-like deployment), land outside the PSR and deploy its solar array.

There also exists a concept called Lunette for flying multiple landers connected to a ring as secondary payloads, which would stay one unit until after the braking burn when the landers split off and perform individual final EDLs, but the application this concept was made for differs from the LGWA: While each of the landers in the Lunette concept was designed to deliver 95 W of continuous power at a polar region [67], which could be enough to meet the power requirements of the entire LGWA array with newer solar panels, the LGWA would need only one such lander and altering the design of the other landers to accommodate a seismic station each would surpass the mass limits per lander at first glance (31.4 kg of payload would be available, assuming the entire mass of the lander power system can be reallocated to the payload), but perhaps a radical redesign

would allow the 6×180 kg, with dimensions $610 \times 710 \times 960$ mm envelopes of the ESPA to accommodate the LGWA. Without having conducted in-depth analysis, we imagine such an approach to be attractive if no further displacement of the stations after landing is necessary (extremely high prior knowledge of the landing sites, as well as landing precision and known effect plume–surface interaction) and if the individually landed assets do not need to be physically connected (no shared laser, individual power sources, or power beaming).

5.9.3.3 Hilltop to PSR hop

The deployment trades in subsection 5.4.4 have been made under the implicit assumption of a single landing. For the single rover capable of carrying only one station at a time, a hop might be interesting, where the lander deploys the rover and solar array on a highly illuminated site, then takes off again and lands in the PSR. The rover could then lay the cable into the PSR, followed by station distribution, alleviating the need for multiple drives or to carry the solar array. In section B.1, fuel consumption for such a hop is crudely approximated as a long hover, indicating that fuel consumption for a hop could be significant. Landers do not usually have reignitable engines. We have not further pursued this idea.

5.10 Budgets

5.10.1 Data

The data budget in Table 5.13 shows data generation, collection and storage, with assumed values for telemetry generation and storage capacities.

Category	${f V}$ alue	\mathbf{Unit}	Source
All stations (Science)	3762	bps	[11]
Individual seismic station (science)	940	bps	
Telemetry per station	167	bps	
Telemetry from lander	333	bps	
Station (science + telemetry)	1107	bps	
Total data (science + telemetry)	4760	bps	
After compression (lossless 2x)	2380	bps	
Uplinked data	192	bps	
Accumulated data, 24 days	4.94×10^{9}	bits	
Storage capacity on lander	8×10^{9}	bits	
Maximum data storage time	36	days	
CAN PLC data rate	5×10^5	bps	[50]
Transmission time every second, per station	2.21×10^{-3}	\mathbf{s}	
CAN bus utilization	0.11		
Data storage per station to store 10 seconds of data	1.11×10^4	bits	

Table 5.13: Data generation, collection and storage. This includes margins as described in Appendix A.

The upper section includes all data generated by the seismic sensors, provided by [11], and an approximation of generated housekeeping data.

To get an estimation of the total data generated across the whole system, the middle section of Table 5.13 provides calculations of storage and downlink data requirements.

The CAN bus utilization figure in the lower section of Table 5.13 includes time for collection of data and telemetry every second and a 0.1 s margin for each transmission to allow for a data request and clock synchronization signal from the lander to the stations before each transmission. It is

5.10. Budgets

apparent that a very large margin exists in CAN bus utilization, which enables the implementation of additional on-site functionality.

The exact equations and any estimations used in generating this data can be found in Appendix A.

5.10.2 Link

The proposed link budget in Table 5.14 shows that Ka-band downlink is possible using a 180-degree antenna without pointing requirements. In order to calculate the provided values in Table 5.14, several estimations were made, which are listed in section A.2.

Name	Value	Unit	Source
Slant range	3.3×10^{6}	m	
Minimum elevation angle	20	\deg	
Seconds of visibility per overpass	1811	\mathbf{S}	section A.1
Seconds of visibility per day	9504	\mathbf{s}	
Center frequency	2.74×10^{10}	Hz	[7, 51]
Bandwidth	6×10^6	Hz	[7]
Antenna transmit gain	6	dBi	[68, 69]
Received signal power	-90.2	dBm	
Noise power	-105.6	dBm	[70]
SNR	15.4	dB	
BER	9.16×10^{-7}		
Bit rate	1.2×10^{7}	bps	
Data rate	4.3×10^{6}	bps	
Accumulated data, 24 days	4.94×10^{9}	bits	
Transmission duration	1142	\mathbf{s}	

Table 5.14: Relevant figures of the link budget calculation, together with the transmission parameter estimations. The included margin in these values is explained in Appendix A.

5.10.3 Power

Component	Power average [W]	Power maximum [W]
Laser	9	9 1
Cryocooler	4*6.125	4*7.1
Station electronics	4*4	4*4
Communication	1.2	102^{-2}
Computing	24.1	49^{-2}
Lander heating ³		
Total power consumption	74.8	204.4

Table 5.15: LGWA power budget summary during operation

5.10.4 Thermal

¹Estimate from Jan Harms.

 $^{^2}$ Assumption that all the data from the longest dark period is transferred at once, taking 19 minutes.

³Rest heat from the laser is assumed to be sufficient to heat the lander and battery.

Component	Power requirement [W]	Reference or comment
Communication	101	Constant, if infrastructure (relay satel-
		lite) allows for constant communication
Computing	33	Same as communication
Rover	200	Perseverance rover, speed 152 m/h
Total power consumption	334	

Table 5.16: LGWA power budget summary during deployment

Component	Power minimum [W]	Power maximum [W]
Laser	9	9
Communication	0	51
Computing	0	49
Total generated heat	9	109

Table 5.17: Thermal budget of the lander

Component	Power minimum [W]	Power maximum [W]
Motors	0	20
Communication	0	50.5
Computing	0	33
Total generated heat	0	103.5

Table 5.18: Thermal budget of the rover

Component	Power minimum [W]	Power maximum [W]
Station electronics	0	4
Total generated heat	0	4

Table 5.19: Thermal budget of the seismic station of the 250K radiator

Component	Power average [W]
H_2 stage	4.2
Total generated heat	4.2

Table 5.20: Thermal budget of the seismic station of the 87K radiator (the power is small compared to the heat capacity of the radiator at cycle timescales, therefore, only the average power is considered)

Component	Power average [W]
He stage	1.9
H_2 stage precool	0.025
Total generated heat	1.925

Table 5.21: Thermal budget of the seismic station of the 51K radiator (the power is small compared to the heat capacity of the radiator at cycle timescales, therefore, only the average power is considered)

70 5.10. Budgets

5.10.5 Mass

Component	Mass [kg]	Reference or comment
4× Stations (excl. radiators, 43 kg each)	172.0	section 4.1
$4 \times$ Station radiators (47 kg each)	188.0	see below
$1 \times FLEX$ rover	500.0	subsection 5.4.3
$1 \times $ Battery	268.3	subsection 5.5.1
$1 \times$ Glass fiber connection	22.6	section 4.4
$1 \times$ Aluminum cables	248.4	subsection 5.5.2
1× Solar array (incl. support structure)	16.8	subsection 5.5.2
1× Laser generation module	10.0	assumption
$1 \times$ Down-to-Earth communications module	34.9	[20]
1x Computation, storage and transmission electronics	2.2	see below
Total mass	1463.2	

Table 5.22: LGWA mass budget summary

Radiator mass

Based on the two sources [71][72], we estimate a radiator mass of $4 \,\mathrm{kg/m^2}$. According to the radiator area requirement of $9.8 \,\mathrm{m^2}$ [3], and assuming a 20% margin, we estimate a per-station radiator mass of $47 \,\mathrm{kg}$.

Computation, storage and transmission electronics

4x Seismic Station MCU (0.4 kg) + 4x DRAM (0.2 kg) + 3x Lander OBC and storage (1 kg) + 1 Telemetry sensors (0.6 kg) = 2.2 kg These estimates are upper limits given from practical experience and estimations with high margins.

Glass fiber connection

The glass fiber has a density of approximately $\rho = 2.5\,\mathrm{g/cm^3}$ [73]. Assuming a fiber diameter of 1 mm and a total length of 11.5 km (approximately 10 km outside the PSR and 1.5 km within it), with cross-sectional area A, volume V, and mass m:

$$A = \pi \left(\frac{0.05 \,\mathrm{cm}}{1}\right)^2 = 0.00785 \,\mathrm{cm}^2.$$

$$V = A \times (11.5 \times 1000 \times 100 \,\mathrm{cm}) = 9.0 \times 10^3 \,\mathrm{cm}^3.$$

$$m = \rho V = 2.5 \,\mathrm{g/cm^3} \times 9.0 \times 10^3 \,\mathrm{cm^3} \approx 2.26 \times 10^4 \,\mathrm{g} = 22.6 \,\mathrm{kg}.$$

5.10.6 Volume to be transported by rover

Component	Volume $[m^3]$	Reference or comment
4× Stations	0.4	margined section 4.1
$4 \times$ Station radiators	2	margined section 4.1
$1 \times \text{Glass fiber connection}$	0.009	unmargined section 4.4
$1 \times$ Aluminum cables	0.092	unmargined subsection 5.5.2
$1 \times$ margin for cables	0.3	assumption
Total Volume to be transported by rover	2.801	

Table 5.23: LGWA summary of volume to be deployed by rover

5.11 Compliance Matrix

The L2 requirements mentioned in section 3.1 are listed in the matrix below, marked with their statement of compliance (SoC), the verification method, and the subsystem they are part of.

ID	Requirement description	Subsystem	T/A/R/I	SoC
R01SEI_1	Keep the temperature variation low	Thermal/EPS	T/R	C
$R01SEI_2$	Keep the stations at 4.5K	Thermal/EPS	\mathbf{R}	\mathbf{C}
R01SEI_3	Place stations in one plane with diameter of 1 km $$	Deployment	Т	TBD
R01SEI_4	Measure with a rate of 20 measurements per second	Communication	Т	С
$R01DAT_1$	Store and process measured data	Communication	T	\mathbf{C}
$R01DAT_2$	Collect data from seismic stations	Communication	T	\mathbf{C}
$R01DAT_3$	Communicate with Earth	Communication	\mathbf{R}	TBD
R01PAY_1	Place stations in a circular plane with a diameter of 1 km	Deployment	A	TBD
R02OPS_1	Power seismic stations and communication devices adequately	EPS	R	С
R02OPS_2	Operate all subsystems in their optimal thermal environment	Thermal	R	С
R02OPS_3	Protect all subsystems from incoming radiation	-	Τ	С

Table 5.24: System requirements summary

5.12 Interface Descriptions

5.12.1 Power interfaces

Power system interfaces ensure efficient power distribution between the components of the LGWA. Power lines are shared with communication and depicted in Figure 5.24 and subsection 5.12.3. DC-to-DC converters, which are part of the PCDU, are used at the stations and the lander to satisfy voltage requirements of the components while keeping a high bus voltage (120 V). The lander and rover are connected via cable over an interface between the stations and rover.

5.12.2 Data and communication interfaces

Data from the seismometer has to be transmitted to the lander. For this, measurements and telemetry are saved and sent via CAN PLC as shown in Figure 5.24. When arriving at the lander given in Figure 5.25, data is compressed and stored until a downlink window presents itself. All collected data is processed by the antenna into a transmit signal and then passed through the digital-analog converter before exiting the lander through the antenna. Through the rover station interface, the rover is connected to the lander station CAN bus during deployment.

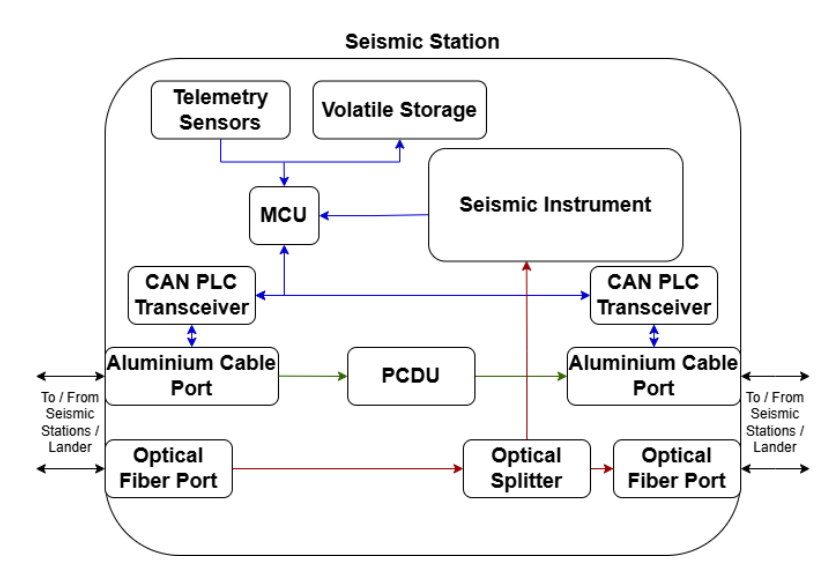


Figure 5.24: A signal, power, and laser connection diagram of a seismic station. All stations will work the same, but the last station in the chain will not have cable connections for outgoing power, communications, and laser.

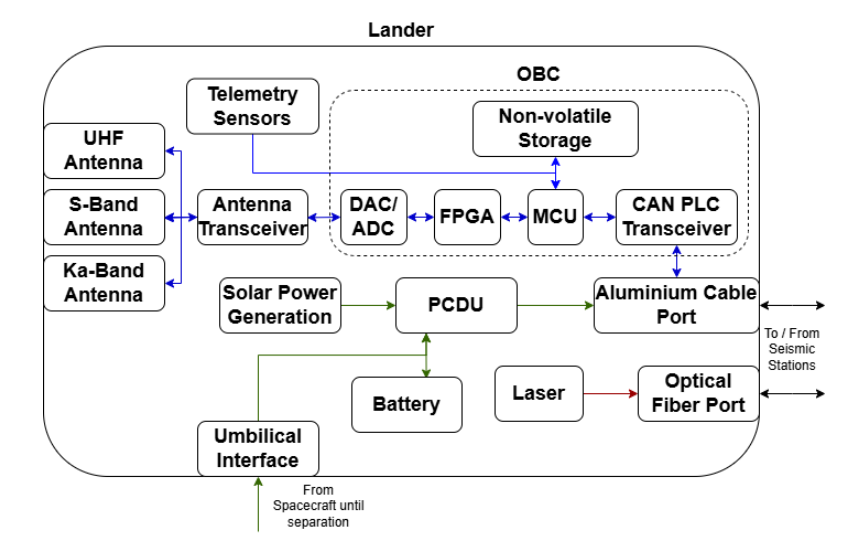


Figure 5.25: A signal, power, and laser connection diagram of the lander.

5.12.3 Structural interfaces

Lander structure ensures stability of all components during flight and operations. Station structure uses a leveling system to keep the payload (seismometer) even. Rover, stations, and cables interfaces for the baseline FLEX rover should be designed going from the rover's standard payload interfaces if possible (given in [74] for the current prototype). This way mechanical design is flexible to change to the scenario where an unmodified FLEX rover already on the Moon is used for deployment. Some of the challenges of these interfaces are outlined in subsection 5.4.3.

5.12.4 Thermal interfaces

5.12.4.1 Lander

There are the following heat sinks on the lander:

• Radiator (approximately 305 K)

There are the following heat sources on the lander:

- Laser
- Communication electronics
- PCB boards with microprocessor, FPGA, microcontrollers, other components
- Resistive heater (only required while the laser is off during traveling and deployment)

All these heat sources should be connected together using thermally conductive material like copper or heat pipes. They should additionally be connected to the batteries to keep them at the operating temperature. The connected heat sources should be connected using a VCHP (variable conductance heat pipe) to the radiator.

5.12.4.2 Rover

There are the following heat sinks on the rover:

• Radiator (approximately 305 K)

There are the following heat sources on the rover:

- Communication electronics
- PCB boards with microprocessor, microcontrollers, other components
- Resistive heater

All these heat sources should be connected together using thermally conductive material like copper or heat pipes. They should additionally be connected to the batteries to keep them at the operating temperature. The connected heat sources should be connected using a heat pipe or conducting material like copper to the radiator.

5.12.4.3 Measurement stations

There are the following heat sinks on the measurement stations:

- Radiator (approximately 250 K)
- Radiator (approximately 87 K)
- Radiator (approximately 51 K)

There are the following heat sources on the measurement stations:

- Cryocooler H_2 stage
- Cryocooler H_2 stage precooling
- Cryocooler He stage
- Electronics
- Resistive heater

The electronics should be connected to the resistive heater and to the 250 K radiator, the H_2 stage should be connected to the 87 K radiator, the He stage and H_2 stage precooling should be connected to the 51 K radiator. All connections should be done using heat pipes or thermally

conductive material like copper. Note that the cryocooler internally cools components down to $4.5\,\mathrm{K}$. This is considered part of the payload design, has already been analyzed $[3,\,75]$ and will not be discussed here further.

5.13 TRL Assessment

Table 5.26: Technology readiness level (TRL) table of the components of SILENCE. Based on NASA TRL scheme [2].

Component	TRL	Notes
Communications		
Ka-band antenna	8	[45]
S-band antenna	8	[45]
UHF antenna	8	[45]
Antenna transceiver	8	[45]
CAN PLC transceiver	5	[50]
Lowest	5	Essential part
Computing		
FPGA	8	[45]
DAC/ADC	8	[45]
Telemetry sensors	7	[45]
Non-volatile MRAM	7	[60]
MCU	8	[45]
DRAM	8	[45]
Cryo-CMOS DRAM and MCU	4	[58]
Lowest	4	Alternative design
Power		
Solar array	7-9	[45]
Batteries	7-9	[45]
PCDU	9	[45]
DC-to-DC converters	5-6	Limited testing data available in extreme environments; the TRL value reflects this
Lowest	5-6	uncertainty. Could be avoided with a different baseline
Seismic stations	5-0	Could be avoided with a different basefine
	4	Proof mass suspension actuation readout
Sensor	4	Proof mass, suspension, actuation, readout [3]
Leveling system	6	Similar to SEIS experiment but cryogenic [76]
Optical Splitter	6	Key component of optical fiber technology
Cooler	5	Absorption-based Joule-Thomson cooler
		previously flown in ESA-Planck;
		non-reversible chemical process limits
		lifetime [3]
Station control electronics	5	No special requirements in radiation-shielded
(non-cryogenic)		warm box
Lowest	5	Key component
Thermal		
Standard radiators, conductors,	9	Standard components
heat pipes		
Resistive heater	9	Standard component
		Continued on next page

Continued on next page

Component	TRL	Notes
Open-honeycomb tapered angle	2	The Open-honeycomb tapered angle radiator
radiator		could significantly reduce weight, and the
		component is simple with no moving parts,
		therefore, this is the preferred solution
		despite low TRL.
VCHP	9	[77]
MLI insulation	9	[61]
EDS system	8	[63, 64]
Lowest	2	
Rover		
Software	6	[74]
Hardware	6	[74]
Lowest	6	Fast TRL advancement expected, see
		subsection 5.4.3
Launch vehicle and lander		
Ariane 6	4	Assumption
Argonaut Lander	4	Assumption
Rover support and egress	4	Other rover egress ramps have already been
structure		designed [78], would probably rely on
		common mechanisms
Lowest	4	Mission critical

5.14 AIT Approach

Communications and processing

Seismic station electronics and telemetry generation testing. Lander electronics and storage testing. FPGA DSP testing. PLC testing using realistic cable lengths. Antenna field of view (FoV) calibration for Ka-, S-, and UHF-band antennas.

Subsystem integration communications and processing

Signal chain from station telemetry and data to lander storage testing. Lander storage to antenna transmission chain testing. Finally, testing of the entire data system, including multi-day data storage and retrieval on the lander. Safe mode with UHF emergency transmission and recovery testing.

Seismic stations

Sensor assembly by GSSI or a partner under supervision of GSSI. Leveling platform development, assembly, and testing by a specialized partner. Integration by an industrial partner, subsequent testing according to ESA standards. Special attention to and testing of the effects of the strong temperature differences and transients during deployment. Modeling and/or testing for vibrations during rover drive.

Rover

Extensive testing of station placement and cable laying with a test unit or a flight model. Testing for the launch loads of the Ariane 64 or comparison with launch loads of a Starship for which the rover is designed (subsection 5.4.3. Extensive testing of the egress system from the Argonaut lander.

Argonaut Lander

Development and assembly of the rover support and egress structure by the Argonaut Lander prime contractor or another party. Integration by the Argonaut Lander prime contractor, collaborative testing.

76 5.15. Risk Assessment

Power system

Power transmission between the solar array, battery, and over long aluminum cables. DC-to-DC converters will have to undergo more testing in cryogenic temperatures and vacuum.

Thermal system

Test the performance of all radiators separately as well as when assembled on the seismic station/-lander/rover. Test the performance also at PSR temperatures. Test the mechanical and thermal robustness of radiators and shields to regolith dust using regolith simulants. Test the performance of thermal systems in extreme situations (large rock directly next to the rover, large mountain in view). Pay specific attention to the new open honeycomb radiator. Carefully simulate the performance of these radiators. Recreate a PSR crater environment on Earth using liquid nitrogen and test the performance of the radiators in this environment. Make sure that the taper angles of the honeycomb radiator are produced with high accuracy and that the mechanical deformation due to the weight of the radiators does not move the outside the allowed range.

5.15 Risk Assessment

Understanding and analyzing risks of a system before its deployment enables assessment and design of potential mitigation strategies in advance. Risks can be classified using Figure 5.26, where a simple analysis provides information on the priority of the risk.

		Impact —				
		Negligible	Minor	Moderate	Significant	Severe
1	Very Likely	Low Med	Medium	Med Hi	High	High
	Likely	Low	Low Med	Medium	Med Hi	High
Likelihood	Possible	Low	Low Med	Medium	Med Hi	Med Hi
]	Unlikely	Low	Low Med	Low Med	Medium	Med Hi
	Very Unlikely	Low	Low	Low Med	Medium	Medium

Figure 5.26: A risk matrix, simplifying the combination of likelihood and impact to compute risk [6].

5.15.1 Thermal risks

Risk: Different temperature / thermal radiation levels than measured before / computed at the position of the seismic stations

Effect: Radiators might be too hot to cool down the superconductors to below the temperature where they become superconducting. This can result in complete system failure

Likelihood: Medium

Risk Categorization: High

Risk Mitigation Plan: Careful simulation and measurement of temperature of the selected PSR, significant margin

Risk: Different temperature / thermal radiation levels than measured before / computed at the position of the lander / rover

Effect: Radiators might be too hot or too cold to keep the electronics in the operating range. This can result in complete system failure

Likelihood: Low

Risk Categorization: High

Risk Mitigation Plan: Careful simulation and measurement of temperature of the selected landing site and PSR, significant margin. Design rover in a way that it can heat itself up even at 0 K ambient temperature. If the rover runs hot, it can be paused, but when it runs cold at full power and computing power, this will likely result in failure

Risk: Failure of new, special electronic components needed to operate at PSR temperatures

Effect: Failure of computing system

Likelihood: High

Risk Categorization: Medium

Risk Mitigation Plan: Not only rely on cryo-electronics, use a warm box for electronics on the seismic station; if cryo-electronics are used, that should be only as technology demonstration

Risk: Open-honeycomb Radiator construction error

Effect: Radiators might be too hot to cool down the superconductors to below the temperature where they become superconducting. This can result in complete system failure

Likelihood: Medium

Risk Categorization: High

Risk Mitigation Plan: Careful calculations, simulations and testing

Risk: Components generating more heat than expected

Effect: System failure or performance degradation due to required shutdown

Likelihood: Low

Risk Categorization: Medium

Risk Mitigation Plan: Careful simulations and testing. Make sure all components that will run at the same time are tested at the same time to stress test the thermal system

Risk: Dust on radiators

Effect: System failure or performance degradation due to required shutdown

Likelihood: Medium

Risk Categorization: Medium

Risk Mitigation Plan: Use EDS (Electrodynamic Dust Shield) system

78 5.15. Risk Assessment

Risk: Seismic background noise (in particular, thermal moonquakes) too high to measure gravitational waves

Effect: Very significant performance degradation, failure at important science goal

Likelihood: High

Risk Categorization: High

Risk Mitigation Plan: Careful simulations, soundcheck mission to test noise on the Moon

Risk: Selected PSR too uneven, many rocks

Effect: Might result in radiator performance degradation or system failure due to higher than expected incident angles of thermal radiation

Likelihood: Medium

Risk Categorization: High

Risk Mitigation Plan: Collect high-resolution data about the surface topography of the target crater, if possible. Otherwise, use data from other nearby craters, if available. If necessary, increase height of the seismic stations to be sure they are above rock level.

5.15.2 Landing risks

Risk: The main risk in terms of landing on the Moon is a PSI. Rocket exhaust interacts with the surface, creating a dust cloud, potentially obscuring clear vision of the landing site or even damaging the lander during descent. [79].

Effect: An unsafe landing will have a disastrous effect on the mission since the entire mission depends on it. In case of crashing into the lunar surface, the entire mission will be over. Even in case of landing safely on the surface, debris might damage the seismometers or "only" the lander, therefore our communication, battery, or other vital subsystem.

Likelihood: Many studies have already been done in this area since PSI occurred in many Apollo missions. So the likelihood is high.

Risk Categorization: Regarding the high likelihood and the disastrous effects, this has to be categorized as a **high** risk.

Risk Mitigation Plan: A way to mitigate PSI would be to predict the behavior of the dust on the floor. The predictions are quite uncertain since they only rely on small-scale vacuum tests and Apollo flight reconstructions. More data from in situ measurements are needed for more precise predictions of PSI. In addition to that, a stereo camera will be used on the descent of the lunar lander to capture more PSI data. For now, the only way to mitigate PSI is to collect more data from possible landing sites and to select the one that might have the least amount of dust/regolith.

5.15.3 Deployment risks

Risk: Lander solar cell deployment failure

Effect: No or reduced power generation, depending on solar array launch configuration, severe impact

Likelihood: Very unlikely, simple solar array

Risk Categorization: Medium

Risk Mitigation Plan: Lander body-mounted solar cells requiring no mechanism, a redundant mechanism, or redundant arrays would be options.

Risk: Rover egress failure

Effect: No station deployment possible, the entire mission fails, severe impact

Likelihood: possible, rover support and egress structure design are challenging due to rover weight and rover size compared to the payload fairing

Risk Categorization: Medium-High

Risk Mitigation Plan: Extensively test rover egress, build a redundant egress structure as far as possible (actuation), and maybe have a backup egress strategy, e.g., on a rope.

Risk: Rover immobilized on the station deployment drive

Effect: No station deployment is possible; depending on the number of already deployed stations, the entire mission fails, with severe impact.

Likelihood: challenging terrain, possible

Risk Categorization: Medium-High

Risk Mitigation Plan: Extensively simulate and test rover operations, limit rover velocity and distance between waypoints, and incorporate manual checks in challenging situations.

Risk: Rover damages cable or cable connection between stations and lander.

Effect: Depending on the location, several or all stations are disconnected from power, communication, and lander-based severe impact.

Likelihood: challenging terrain with obstacles and very likely rover slippage, possible

Risk Categorization: Medium-High

Risk Mitigation Plan: robust cable sheaths, the cable-laying mechanism has lower holdback force than the cable connector limits, investigate cable connectors that can be plugged back in by the rover

Risk: Stations are placed on unfavorable ground.

Effect: Depending on the severity, insignificant station-ground coupling may lead to unusable measurements from concerned stations, significant

Likelihood: potentially high rock density in the deployment area, rocks directly under a few millimeters of regolith, likely

Risk Categorization: Medium-High

Risk Mitigation Plan: Factor this risk into baseline PSR updates, explore the possibility of force feedback during station placement (a big rock would cause a sudden force increase while lowering the station, assuming all DoFs except translation in the vertical direction are restricted), and investigate the possibility of station relocation.

5.15. Risk Assessment

5.15.4 Communication risks

Risk: Cable degradation between stations and lander.

Effect: Communications experience a higher bit error rate (BER).

Likelihood: Likely, given the mission's 10-year lifespan.

Risk Categorization: Medium–High, since the impact of insufficient data on the experiment is significant.

Risk Mitigation Plan: Use a low data rate and ensure communication capacity has a significant margin.

5.15.5 Computing risk

Risk: Lander data storage experiences a fault.

Effect: From data loss to complete inoperability of the storage device.

Likelihood: Very likely, given the system's exposure to solar radiation and lifespan.

Risk Categorization: High, given the mission objective to store data until transmission.

Risk Mitigation Plan: Redundancy in storage devices mitigates this risk almost fully.

5.15.6 Power risk

Risk: Connection/cable failure

Effect: A disconnection in the long cable disrupts power at all stations.

Likelihood: Low to medium with reasonable engineering.

Risk Categorization: High stations don't work without power; cable failure is irreparable without an additional mission.

Risk Mitigation Plan: Armored cables, high-quality connectors, strain relief, and routine monitoring.

Chapter 6

Mission Operations & Ground Segment

6.1 Concept of Operations

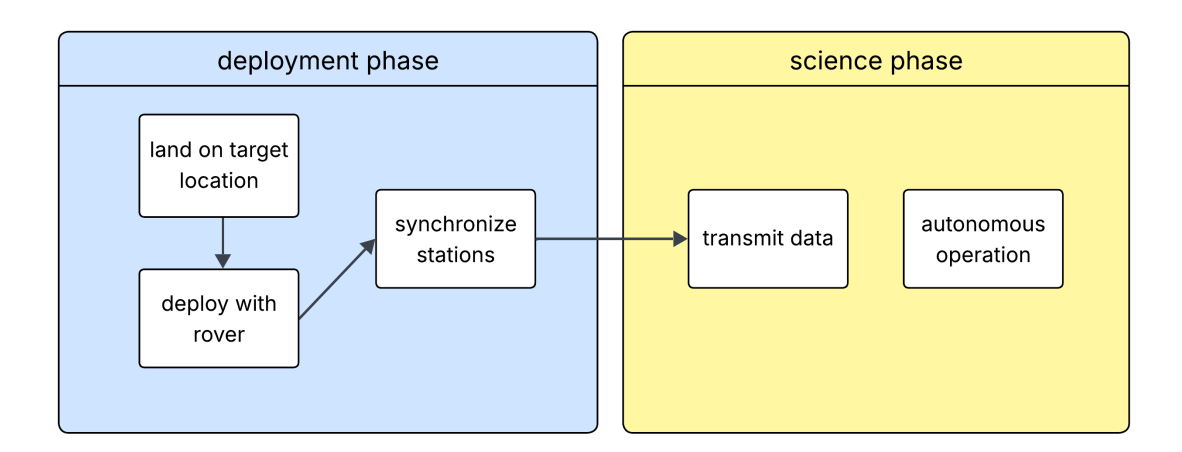


Figure 6.1: Concept of operation for the SILENCE mission.

The concept of operations (ConOps) is illustrated in Figure 6.1. The mission operations can be divided into two main phases: the *deployment phase* and the *science phase*.

6.1.1 Deployment phase

During the deployment phase, the payload will reach the target site with the help of a dedicated lander. Once on the surface, the rover will drive off the lander carrying four seismic stations. These stations are interconnected by two cables — a glass fiber cable for laser data transmission and an aluminum cable for power delivery — forming a single chained connection.

The deployment sequence will proceed station by station. Following an initial health check and position verification by the rover, it will receive the command to begin the mission. It will then descend into the PSR over the crater rim, starting by placing the central (middle) seismic station. Subsequently, it will deploy the remaining stations along a circular arc with a diameter of 1 km.

82 6.2. Science Phase

Each station will be deployed in a semi-autonomous manner, with the ground station (GS) reviewing and approving every deployment site before final placement. The complete data flow for the operation is illustrated in Table 6.1. The "stations deployment" step will be repeated for every seismic station.

During a period of long, constant solar illumination (see Figure 5.5) the PV panels will generate sufficient power to fulfill the rover's energy requirements (subsection 5.5.3). The deployment will take 76 hours.

Table 6.1: Data flows between the rover and the ground segment during seismic station deployment (chronological order)

Step	Direction	Data flow	Purpose	
	$\mathrm{Rover} \to \mathrm{GS}$	Rover health check	Ensure safe deployment	
D., J., J.,		Telemetry	Verify initial position	
Pre-deployment	$\mathrm{GS} \to \mathrm{Rover}$	Command	Approve planned route	
		Command	Authorize crater entry	
	$\mathrm{Rover} \to \mathrm{GS}$	Image of site	Assess terrain suitability	
Station deployment		Telemetry	Update position and track path	
	$\mathrm{GS} \to \mathrm{Rover}$	Target coordinate, command	Specify deployment point and approve action	
	$\mathrm{Rover} \to \mathrm{GS}$	Deployment arm status, image	Verify successful placement	
$Station \rightarrow GS N$		Network handshake	Confirm readiness for sens-	
	$GS \to Rover$	Command	Proceed to next deployment site	

Once deployment is complete, the stations will be synchronized using CAN communication and lasers, marking the start of the science phase. During this phase, the stations acquire data and transmit it to Earth. The lander will host the communication system and onboard processing unit, which is connected to the seismic stations via the aluminum cables. Solar panels on the lunar lander will power the mission. From this point onward, nominal mission operations will be conducted fully autonomously.

6.2 Science Phase

In the science phase, each station begins continuous acquisition of GW data, recording local seismic activity from within the PSR. Figure 6.2 shows how data will be passed down from the individual seismic stations to the different parties acting on the ground to acquire GW data and monitor system health.

6.2.1 Payload data flow

If for any reason SILENCE encounters unexpected behavior, such as errors in the code or hardware issues that it cannot resolve on its own, the system enters emergency mode, and data flow is severely restricted to conserve power in case of a power generation issue. The flow of data in emergency mode is pictured in Figure 6.3, where the most noticeable change is a suspension of GW data acquisition.

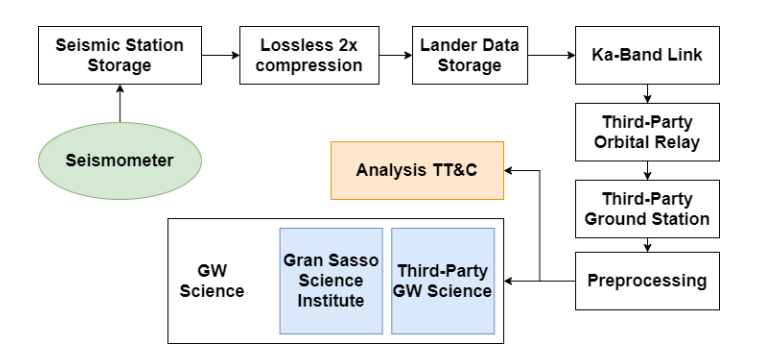


Figure 6.2: Data flow concept while SILENCE is in nominal operation. For clarity, only one out of four seismic stations is pictured.

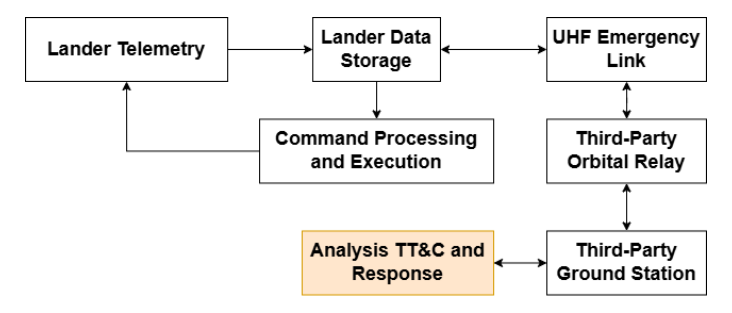


Figure 6.3: Data flow concept for SILENCE emergency handling. For clarity, only one out of four seismic stations is pictured.

6.3 Ground Segment

6.3.1 Earth link

In the LNIS [7], a section is dedicated to ground station standards. Data created by the SILENCE mission will therefore be uplinked to a LunaNet relay and received on the ground by the LunaNet GS network , which includes existing infrastructure such as the NASA Deep Space Network, as shown in Figure 6.4.

Once on the ground, the data will be passed from the GS operators to various data users.

6.3.2 Data processing

Received data is sent to the primary mission operator, where decoding, error correction, and separation of the data happen to distinguish between telemetry and instrument data. After some processing to ensure coherent and time-synchronized seismic data, it gets passed on for GW analysis.

Telemetry is sent to mission operators for status reports and device fault identification.

6.3.3 Gravitational wave science

Pre-processed seismic data is sent to the GSSI and other interested and invited parties. Extraction of information on potential GWs is performed at the individual science institutions to enable independent conclusions. Data could also be shared for a quicker collaborative approach to gain scientific insight from this mission, together with data from other GW detection systems.

84 6.4. Launch Vehicle



Figure 6.4: Concept for the mission link architecture, using LunaNet compatible data providers [7].

6.3.4 Operations

A dedicated operations team manages incoming housekeeping data and outgoing commands, which involves advanced automated signal processing methods to detect possible emerging risks and faults early. They send commands like updates and resets to the stations while ensuring that no outgoing command has a risk of breaking part of the lunar system.

Especially in landing and early operations (LEOP), this team is responsible for deployment and guidance of the rover and individual stations. For this, the system will downlink images whenever possible and provide and receive accurate telemetry and guidance, navigation, and control (GNC) data until all stations are deployed and active, and the rover can be retired.

6.3.4.1 Daily operation

In nominal operation, telemetry is supervised by a combination of autonomous systems and human guidance and judgment.

6.3.4.2 Emergency support

When in emergency mode, the SILENCE system will communicate either over S-Band or UHF and cease to transmit any scientific data until the issue is resolved. The mission operation team shall be more available during emergency operations to communicate with the lunar system, analyze the reduced telemetry received, request specific reports from the stations for a deeper insight, and attempt a working fix. During emergency operations, the system only sends basic telemetry while storing the rest to send on request in order to save on power consumption and link usage.

6.4 Launch Vehicle

A launch vehicle and lander are necessary to bring the LGWA to the Moon. The LGWA, including the deployment rover, has a mass of 1463.2kg and can either use a dedicated launch and lander or share a launch and/or landing with another mission.

We evaluate our baseline launch vehicle (Ariane 64) alongside a complementing lander in subsection 6.4.1 and briefly discuss some other launch vehicle options that could be used if the baseline approach changes.

6.4.1 Lander and launch candidate combination: ESA Argonaut and Ariane 64

The ESA Argonaut Lander has been selected for its payload capacity of 1'500 kg, which fits our mission's mass budget of a total of 1463.2kg kg (subsection 5.10.5), for its anticipated readiness at our launch date between 2035 and 2040, as it is scheduled to be first used on the ESA ArgoNET mission in 2031 [80] and due to the leading role of ESA anticipated for this mission. The argonaut lander will have a landing accuracy of 50-100 m, which does not necessarily meet our requirement of 50 m subsection 3.3.1, but is sufficient for our baseline PSR subsubsection 5.3.1.3. The Argonaut lander is designed to have a launch mass of 10'000 kg, be 4.5 m in diameter, and be 6 m long [81].

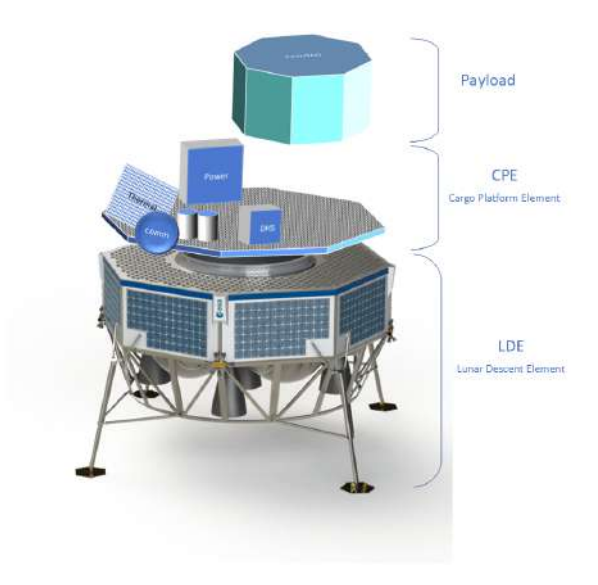


Figure 6.5: Concept Image of the ESA Argonaut Lander [8]

The ESA Argonaut Lander is designed to be brought to the Moon by the four-booster version of the Ariane 6, the Ariane 64. The launch cost of the Ariane 64 is estimated at 135 million[82]. The payload fairing of the Ariane 6 is 4.6 m in diameter, with with a length of 10.15 m before the diameter is reduced for the single launch long fairing and more quickly decreasing diameter for other versions [9]. The diagonal of the horizontal dimensions of the FLEX rover is 4.604 [40]. To fit the FLEX rover inside the Ariane 6 payload fairing, it would have to be placed inside the payload fairing at an angle. It would need to be carefully checked if such a configuration would be possible and would leave enough room for egress ramps. Another option could be to mount the rover like an inverted pendulum vertically onto a tiltable ramp. A sketch of how this could look can be found in Figure B.4. It would have to be checked if the FLEX rover can be put in a vertical position for a prolonged period of time. For both options it would have to be analyzed if said ramp could be designed to sustain the loads during launch, transfer, and landing; keep vibrations of the rover within limits; and allow for reliable, reasonably soft deployment of the rover after landing.

We have performed a CAD check, showing that from a purely geometric perspective the FLEX rover could be launched aboard an Ariane 6 with the Argonaut Lander. We have first considered the single-launch long payload fairing, where the maximum internal diameter of 4.6 m is available over a height of 10.15 m. Figure 6.6 shows that the FLEX rover fits inside a 4.6 m diameter cylinder at an angle of roughly 30 degrees. The single long payload fairing would provide a lot of space for a

86 6.4. Launch Vehicle

rover support and egress structure in the vertical dimension (w.r.t. a rocket on the launch pad). A version of this check with a cuboid rover dummy, showing that the rover would have to be placed at a very high angle if its extent along the long axis is not dictated by the wheel, can be found in Figure B.3. Also for the short dual launch structure (DLS) fairing (the dual launch fairing with the longer top bay), a geometric check has been performed. Under the assumption that the lander takes up the bottom 3 m (assumption based on Figure 6.5) of the top bay, the check shows an even more challenging situation. Nonetheless the check suggests that from a packaging standpoint a shared ride might be possible, see Figure B.5 in appendix IV.

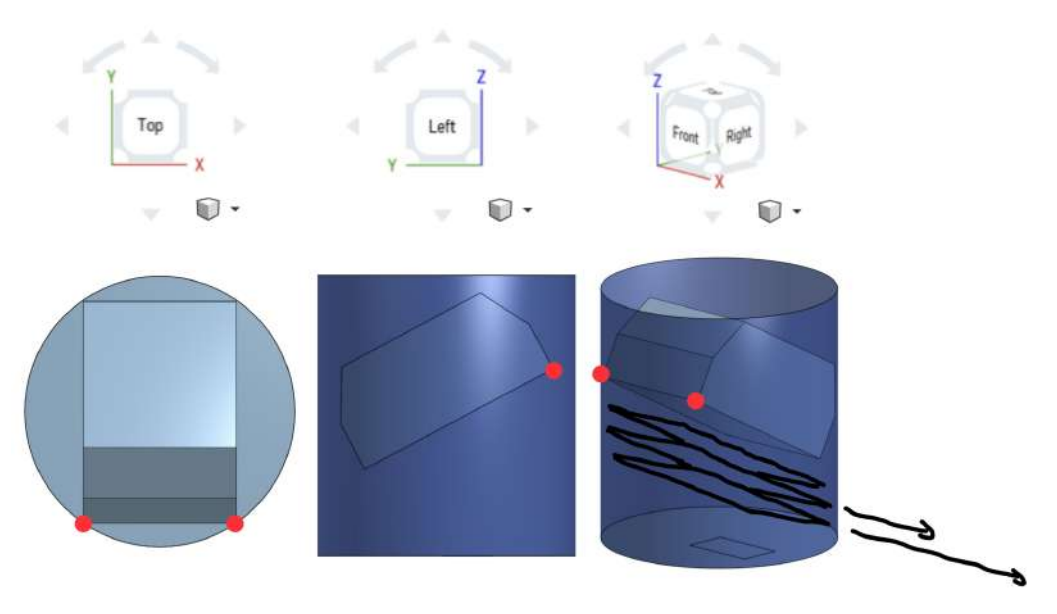


Figure 6.6: FLEX rover CAD dummy inside a 4.6 m diameter cone. The cone length depicted (5 m) is significantly shorter than the Ariane 6 single launch long fairing's 10.15 m long non-conical 4.6 m diameter section [9]. Rover dummy modeled under the assumption that the length dimension is dictated by the wheelbase (bottom dimensions 3.8×2.6 m^2 , extent along the longest side decreases from mid-height to 2.8 m at the top on 1.8 m; see sketch in Figure B.2). A telescopic egress ramp is sketched in the rightmost graphic. Red dots mark the two corners tangent to the payload fairing. No collisions occurred. Screenshots from Onshape.

It is important to point out that the assessment is based solely on the dimensions as reported in a press release (3.8 m length, 2.6 m width, and 1.8 m height according to [40]) under the assumption that the length is dictated by the wheels and that the extent along the longest dimension decreases towards the top. We have contacted Astrolab but as of the writing of this report have not received an answer, but material published by Astrolab seems to confirm these dimensions as shown in Figure B.1. A proper feasibility study would need to be performed with more information on the lander cargo platform and rover geometry, including mechanical analysis for possible egress systems and robustness to the load cases encountered. Thus, currently cannot recommend the combination of the Ariane 64, Argonaut lander, and FLEX rover. However, from a programmatic Europe-centered view, it could make sense to commission a more compact version of the Astrolab FLEX rover or to opt for an alternative in order to conduct the mission with the Ariane 64 and the Argonaut lander. Screenshots from Onshape.

6.4.2 Starship; launch and landing candidate

Another option for launch is SpaceX's Starship, which can deliver payloads directly to the lunar surface without requiring an additional lander and is designed to be fully reusable [83]. Starship offers a payload capacity of 100–150 t to the lunar surface, with an estimated launch cost of around \$100 million [84], resulting in a substantially lower cost per kilogram compared to ESA or NASA

launchers. A lunar landing using Starship is planned as part of the Artemis program in 2032. While this may be slightly early for the LGWA, it is reasonable to assume that additional Starship missions will occur throughout the 2030s, potentially allowing for rideshare opportunities. This, however, would only be feasible if the LGWA is deployed near the lunar South Pole, closer to the anticipated Artemis landing sites, rather than at the current baseline near the North Pole.

6.4.3 Space Launch System

Another option for launch is NASA's Space Launch System (SLS), a super heavy-lift rocket with significantly higher payload capacity and volume. Its Block 1 variant has a payload capacity of >27 t for translunar injection, allowing it to carry either a dedicated lander or additional payloads along. Several Artemis missions planned in the 2030s could provide rideshare opportunities, potentially enabling a smaller, dedicated lander to target a site such as the lunar North Pole, even if primary landers are destined for the South Pole. However, with a total launch cost of \$2.5 billion [85], even with ride-sharing it could come to costs of up to 140 million EUR¹ for the LGWA.

6.4.4 Conclusion

While this section gave different launch vehicles some initial thought, a definite choice can only be made after a more well-defined baseline. Our current baseline option remains Ariane 64 in combination with Argonaut. A definitive launch choice will depend on future mission parameters. If the LGWA were to move to a South Pole location, rideshare options with Starship or SLS could become more attractive, offering higher payload capacity or potential cost benefits. Considering that the LGWA is expected to launch between 2035 and 2040, these systems may be fully operational and more flexible by then, opening opportunities for optimized mission architectures and new deployment strategies.

¹rough guess based on payload mass

Chapter 7

Management

7.1 Team Management

The SILENCE mission is a collaborative effort led by the GSSI in partnership with the European Space Agency (ESA). The organizational structure is designed to ensure efficient coordination between scientific leadership, engineering development, and operational implementation.

At the program level, the project director provides overall leadership and strategic oversight, ensuring alignment with ESA's exploration objectives and GSSI's scientific goals. The project director also acts as the main liaison with precursor initiatives, particularly the SOUNDCHECK pathfinder mission, and oversees major decision-making and stakeholder coordination. In the case of an ESA mission, the project will be executed by a consortium and led by the consortium lead.

Reporting to the project director, the mission management team is responsible for day-to-day coordination, scheduling, budgeting, and resource management. This team maintains interfaces with ESA's programmatic and contractual processes and prepares the project for upcoming design reviews and implementation milestones.

An independent quality and risk management office supports the mission by monitoring compliance with quality standards and performing continuous risk assessment across all technical areas. Given the unique challenges of operating inside a PSR, this office is particularly focused on verification of thermal, power, and communication systems.

The engineering division, under the direction of the chief engineer, leads the design, development, and integration of all technical subsystems. The division is organized into four subsystem teams:

- Thermal system: responsible for ensuring instrument survivability and performance under cryogenic PSR conditions.
- Power system: overseeing energy generation via solar arrays on the lander and power transmission through aluminum cabling to the seismic stations.
- Communication system: managing the glass fiber cable between the seismic network and lander and the relay satellite interface to Earth.
- Deployment system: coordinating with an external rover provider for precise emplacement of seismic stations.

The chief engineer ensures technical coherence across all subsystems, oversees integration with commercial and academic partners, and manages engineering interfaces with ESA's technical boards.

The mission operations team will be responsible for operational planning, post-landing control, and long-term monitoring of the seismic network. The team ensures data integrity, power man-

agement, and communication scheduling, with a focus on maintaining autonomous functionality during extended communication gaps.

The Stakeholder and Communications Office coordinates engagement among GSSI, ESA, supporting space agencies, and commercial entities such as payload and launch providers. It also manages formal interactions with regulatory authorities, including the ITU, and ensures consistent communication and reporting across all stakeholders.

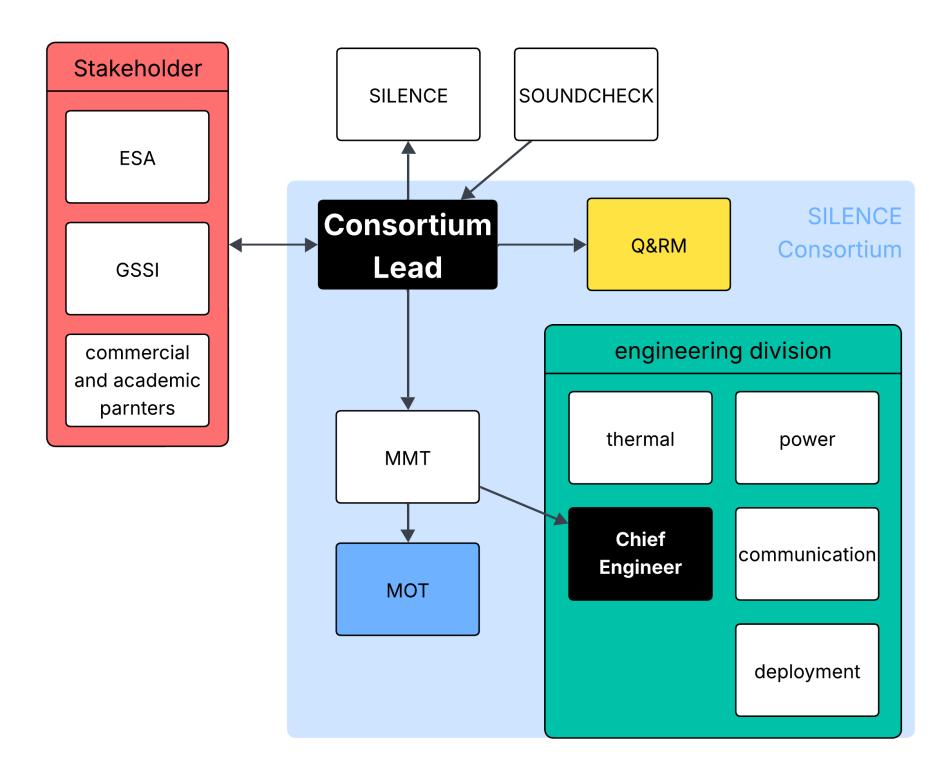


Figure 7.1: Different roles needed for managing the SILENCE mission

90 7.2. Schedule

7.2 Schedule

This mission is using ESA's L-class framework for the scheduling. The schedule is based on the mission call for L3 mission which was used by the LISA mission [86] adjusted for a mission call in oktober 2025.

Activity	Date
Release of call L4	October 2025
Letters of intent submission deadline	November 2025
Briefing meeting	November 2025
Proposal submission deadline	January 2026
Letter of endorsement deadline	March 2026
Proposal evaluation	March-April 2026
Selection of L4 mission concept	April 2026
L4 internal phase 0 studies completed	September 2026
Industrial phase A ITT	Late 2026
End of phase A studies and mission selection review	Second half 2029
Phase B1 completion and mission adoption review	2032 – 2033
Mission adoption	2033 – 2034
Industrial kick-off of phase $\mathrm{B2/C/D/E1}$	2034
Launch	2042–Early 2043

Table 7.2: L4 Mission timeline

According to the current mission call schedule, the launch is planned for 2043. Our partner institute at GSSI, however, suggests that a launch as early as 2038 might be possible (Figure 7.2). Their reasoning is based on the experience from the LISA mission, where the mission call was released only after the successful data return from the Pathfinder mission. Because Pathfinder performed so well, the overall schedule was sped up by about five years, reducing the development time from eighteen to thirteen years.

Using the same idea, GSSI proposes a timeline where the technology development for this mission runs in parallel with the development of the SOUNDCHECK payload. This approach could save roughly four years, moving the expected launch date to 2038–early 2039.

7.3 Cost Estimation

The cost estimation is done based on the framework for an L-class mission of the ESA's science program, comparable to ongoing flagship missions, such as LISA or JUICE.

The SILENCE mission is classified as an L-class mission for several reasons. Its scientific ambition is exceptionally high—measuring gravitational waves on the lunar surface, within a PSR, represents a pioneering and technically demanding objective. Achieving picometer-level seismic measurements in an extremely cold environment poses unprecedented engineering challenges and requires significant technological development, leading to elevated programmatic risk. Furthermore, the mission's scale and international scope—relying on global partners for the payload, rover, and launch services—reflect its flagship nature. The use of a heavy-lift Ariane 6.4 launcher further supports its classification as a large-class, high-complexity mission within ESA's Science Program.

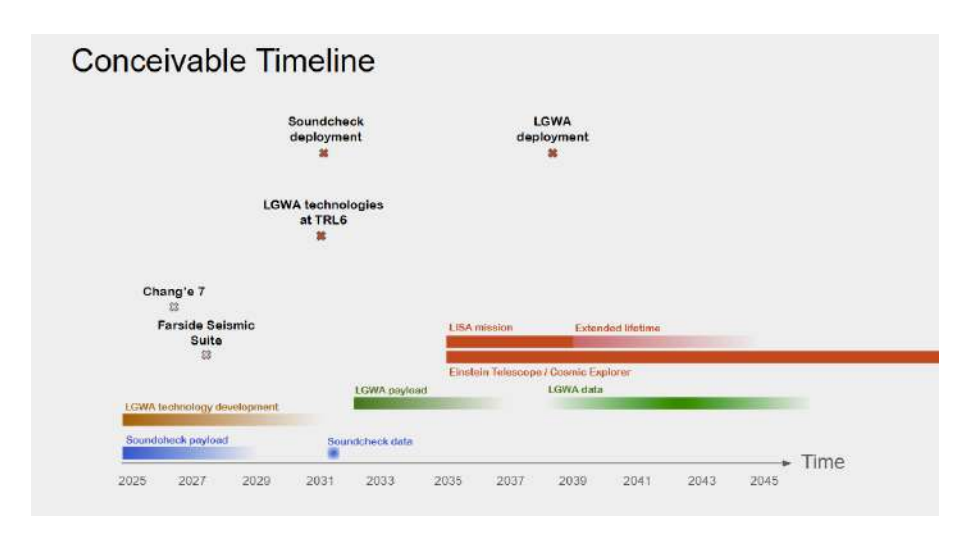


Figure 7.2: Timeline suggested by GSSI [10]

7.3.1 Assumptions

The preliminary cost estimate for the SILENCE mission has been derived by analogy with previous ESA L-class science missions such as LISA [87, 86] and JUICE [88, 89], each with total program budgets in the range of 1.5 billion EUR. Given SILENCE's comparable scientific ambition, technological complexity, and international collaboration model, a similar cost framework was adopted. All figures are expressed in FY2025 euros and rounded to the nearest million.

The payload segment, consisting of four seismic stations operating inside a PSR, is the single most novel element of the mission. Bringing the low-TRL instrumentation (seismic stations, cooler) to flight readiness will require extensive prototype and qualification campaigns. Instrument development—including test articles and environmental qualification—is therefore estimated at 50 million EUR, based on cost scaling from the LISA payload program.

The development cost for the cryocooler has been estimated using the NASA Instrument Cost Model (NICM) [90], given by

Cryocooler Cost (FY04 \$K) =
$$40099 \times \text{LowTemp}^{-0.15}$$

Applying this relation to the target operating temperature yields an estimated 51 million USD (FY04), which, when corrected for inflation (as outlined in *Space Engineering, the New SMAD* [20], (Chapter 11, Table 11-31)), corresponds to approximately \in 60 million under optimistic assumptions. Including production of four flight units and one spare (at 3–7 million USD each), and accounting for qualification and testing, total costs could range from 60 million EUR upward. For the purposes of this preliminary estimate, a mid-case value of 80 million EUR has been adopted. Production of the seismic instruments (four flight models plus one spare) adds approximately \in 16 million, resulting in a payload subtotal of 146 million EUR.

The spacecraft and lander—including structure, propulsion, avionics, and thermal control systems—are estimated at 180 million EUR, scaled from existing ESA lander and probe architectures (JUICE). Integration, testing, and power system elements (solar arrays, harnesses and spares) contribute an additional 50 million EUR, giving a spacecraft and lander subtotal of 230 million EUR.

The deployment **rover** will likely be procured from an external provider (Astrolab) or a similar commercial partner. Depending on partnership agreements, the rover could be supplied in kind or co-funded. A mid-case assumption allocates 80 million EUR for rover procurement and integration, plus 15 million EUR for testing and mission-specific software adaptation, totaling 95 million EUR.

92 7.3. Cost Estimation

The **communications** subsystem, covering the fiber-optic link between the stations and lander, onboard systems, and relay satellite interface, is estimated at 20 million EUR. A further 30 million EUR is allocated for potential relay service procurement (e.g., via LunaNet or equivalent), for a communications subtotal of 50 million EUR.

The **launch segment** includes procurement of an Ariane 6.4 heavy launcher (115 million EUR, per Arianespace list pricing[82]) and associated integration, insurance, and campaign costs (25 million EUR), for a launch subtotal of 140 million EUR.

The ground segment and operations budget, covering mission control, science operations, archiving, and network access over a 10-year lifetime, is estimated at 105 million EUR (of which 90 million EUR is for mission and science operations, and 15 million EUR is for ESA network access).

Program management, systems engineering, and verification testing together account for an additional 110 million EUR, reflecting lifecycle management costs (10% of direct cost) and environmental qualification testing (thermal-vacuum, vibration, and cryogenic campaigns).

A 30% contingency reserve, corresponding to 263 million EUR, has been applied to the total direct costs of approximately 876 million EUR. This accounts for the mission's low technology readiness, the challenging thermal and power conditions within a permanently shadowed region, and the extended operational lifetime. The resulting total preliminary cost estimate for SILENCE is approximately 1.14 billion EUR, positioning it solidly within the ESA L-class mission category.

Table 7.3: Preliminary cost model for the SILENCE mission

Work breakdown structure (WBS) element	Cost [million EUR]
1. Payload development (seismic tations, instruments, cryocoolers)	146
- Instrument development	50
- Cryocooler development	80
- Instrument production (4 flight $+$ 1 spare)	16
2. Spacecraft and lander (bus, avionics, integration, testing)	230
- Lander hardware (structure, propulsion, ADCS, thermal outside PSR)	180
– Integration, testing, harnesses, flight spares, PV	50
3. Rover procurement and integration	95
- Rover procurement / contribution (Astrolab Venturi)	80
 Rover testing and mission integration 	15
4. Communication system and relay service	50
– Communication hardware and lander terminals	20
- Relay service (LunaNet or equivalent)	30
5. Launch service (Ariane 6.4 + campaign)	140
- Ariane 6.4 launch procurement	115
- Launch integration, insurance, operations	25
6. Ground segment and mission operations (10 Years)	105
– Mission and science operations	90
– Ground station access and data archiving	15
7. Program management, systems engineering, and testing	110
 Program management and systems engineering 	80
– Environmental, thermal-vacuum, and vibration testing	30
Subtotal (direct costs)	876
Contingency and reserves (30%)	263
Total estimated cost (mid scenario)	1139

7.4 Life Cycle Assessment

To gain a further potential decision basis for launcher selection (see section 6.4), a very rough life cycle assessment of 2 different launchers was conducted to assess various environmental impacts of launching our mission to the Moon.

7.4.1 Goal and scope

Goal: The goal of this LCA is to model and compare the environmental impacts of two alternative launch vehicles, namely Ariane 64 and NASA's SLS, for transporting the LGWA payload to lunar transfer orbit (LTO). As no final mass of the lander vehicle could be determined, the maximum

payload mass of the Ariane 64 (8.6 tonnes) was used for the payload mass. The results are intended to support decision-making on which launch system to use for the LGWA deployment.

Scope: This screening LCA evaluates the production of the two launchers required to deliver 8.6 tonnes to the Moon. The functional unit (FU) is defined as "transporting 8.6 tonnes of payload to lunar transfer orbit."

The **reference flows** are:

- RF1: One Ariane 64 launch (8.6 t payload capacity)
- RF2: 8.6 kg, roughly one-third of the payload of an SLS launch (27 t payload capacity), assuming mass-based allocation and shared payload capacity.

The system boundaries include launcher production. The launch event, end-of-life processes, mission design phases (0/A), testing, and processing are mostly excluded due to lack of data.

Allocation procedures: For SLS, environmental impacts are allocated proportionally by payload mass (8.6 t / 27 t = 0.3185). For Ariane 64, no allocation is needed, as the full payload capacity is used.

7.4.2 Results and discussion

The comparison between the Ariane 64 and NASA SLS shows distinct differences in environmental performance across the selected impact categories. Because the SLS has a significantly larger total mass (2603 t) compared to the Ariane 64 (860 t), it is unsurprising that the production of the SLS exhibits a much higher climate change impact (see Figure 7.3). Both the normalized and absolute results confirm this trend, with the SLS producing almost four times the climate impact of the Ariane 64. In contrast, abiotic depletion impacts (ADP) are nearly identical between the two systems, showing only minor variation in resource consumption. A notable deviation appears in the ozone depletion potential (ODP), where the Ariane 64 exhibits roughly twice the impact of the SLS. The LCA results showing the unnormalized comparison between the two launchers can be found in the Appendix C.

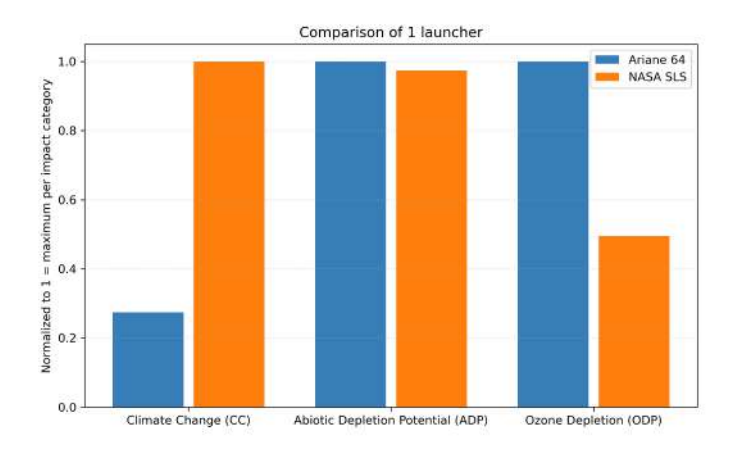


Figure 7.3: Normalized environmental impact comparison between Ariane 64 and NASA SLS across three impact categories for one launcher.

When results are normalized to the functional unit (transporting 8.6 tonnes to lunar transfer orbit), the differences become more pronounced (see Figure 7.4). While the SLS still shows a slightly higher climate change impact, its ADP is nearly three times lower than that of the Ariane 64, and its ODP is more than five times lower. The results also indicate that the boosters of the Ariane 64 are responsible for a dominant share of the environmental burden in these categories. A more

detailed assessment shows that over 97% of the booster ADP value originates from the assumed electronics mass within the boosters. Since this electronics mass was estimated (2000 kg for an Ariane 64 booster and 1000 kg for an SLS booster), the resulting ADP hotspot is highly sensitive to this assumption and may need refinement. For ODP, the booster structure—manufactured from carbon-fiber composite—accounts for more than 73% of the total value. This material choice offers a plausible explanation for Ariane's elevated ODP, since most SLS structural elements are aluminum alloys with considerably lower ozone-depletion impacts during production.

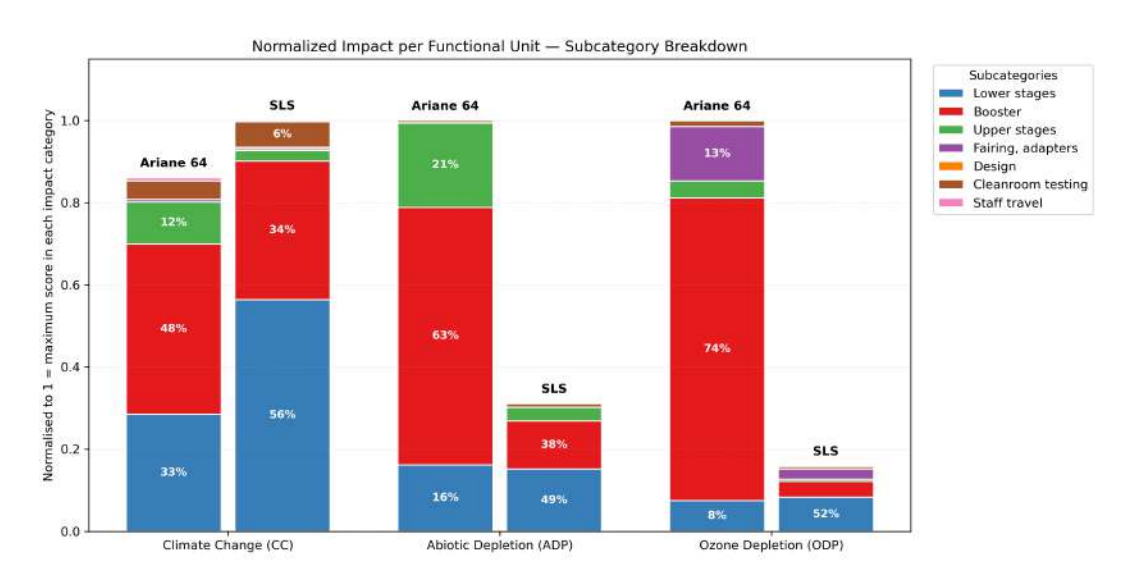


Figure 7.4: Normalized environmental impacts of Ariane 64 and SLS rockets across climate change, abiotic depletion, and ozone depletion. The bars show subcategory contributions, with percentages indicating each subcategory's share of the total impact per rocket.

Overall, the SLS shows a more favorable environmental profile for the defined functional unit. Although its climate impact is slightly higher, the substantially lower ADP and ODP scores result in a comparatively better performance across the three selected indicators. It must be emphasized, however, that this conclusion is shaped by several methodological simplifications and assumptions. The analysis assumes that ridesharing is feasible and that payload-mass-based allocation is appropriate, despite the practical limitations of fairing volume and mission compatibility. These simplifications may bias results in favor of the SLS.

Further uncertainty arises from the use of European datasets to model the production of components predominantly manufactured in the United States. While electricity mixes of Germany and the U.S. exhibit similar climate-change intensities per kWh, differences in industrial energy sources, production technologies, and supply chains remain and may influence the accuracy of the results. Additionally, incomplete subsystem data required the use of generic datasets and engineering estimates, particularly for the SLS, for which detailed component-level information is limited. Similar uncertainties exist on the Ariane 64 side, where assumptions such as electronics mass and material composition significantly influence the outcome of the LCA.

Despite these limitations, the analysis highlights potential opportunities for ecodesign. The significant ODP contribution from composite booster structures of Ariane 64 suggests that reusable or recoverable boosters could substantially reduce the need for new material production, thereby lowering environmental impacts. More accurate, geographically specific datasets, along with refined subsystem inventories—particularly for electronics and composites—would greatly improve the reliability of future assessments.

Appendix A

Communication and Computation: Figures and Estimates

The following calculations and figures are given without margin. They aim to provide a clear overview over the steps used to arrive at a particular value or expression. In section 5.6 and section 5.7, as well as in subsection 5.10.2 and subsection 5.10.1, the following margins are applied:

Data generation 30%, due to uncertainty of measurement frequencies and housekeeping data.

Uplinked data 50% due to high uncertainty of required uplink data volume.

Slant range 50% due to absence of defined figures by relay providers.

Relay visibility time 100% (half the time) due to unknown inclination of relay satellite orbits.

Noise Power 10% due to uncertainty in relay system noise and confidence in high-tech receivers.

Data Rate 20% due to uncertainty in transmission protocols.

Description	Formula or Source	Value	\mathbf{Unit}
Data Generation			
Experiment (R_{Sci})	[11]	2894	bps
Telemetry (seismic station, $R_{S,HK}$)	section A.2	128	bps
Telemetry (lander, $R_{L,HK}$)	section A.2	256	bps
Total data per seismic station (R_S)	subsection $5.10.1$	851	bps
Total generated data (R_{tot})	subsection $5.10.1$	3662	bps
Uplinked Data (R_{up})	section A.2	128	bps
Seismic station storage			
Station data storage time $(T_{S,store})$	section A.2	10	\mathbf{S}
Station data storage size	section A.2	1.6×10^{4}	bits
CAN PLC protocol			
CAN PLC data rate (R_{CAN})	[50]	5×10^5	bps
CAN PLC data request delay $(T_{CAN,init})$	section A.2	0.1	S
Total transmission time every second	subsection $5.10.1$	0.11	S
$(T_{CAN,tot})$			
Lander data storage			
Compression efficiency (R_{comp})	section A.2	2	
Data storage capacity	section A.2	8×10^{9}	bits
Data storage time $(T_{L,max})$	subsection $5.10.1$	47.3	days

Table A.1: Detailed data generation numbers.

Equations used in Table A.2.

$$D_{24d} = [\text{data per second}] * 3600 * 24 * 24$$
 (A.1)

$$S = R_L \cdot \left[\sqrt{\frac{(h + R_L)^2}{R_L^2} - \cos^2(\delta)} - \sin(\delta) \right]$$
 (A.2)

$$T_{orbit} = \sqrt{\frac{4\pi^2}{GM_{Moon}}(r_{moon} + h)^3}, \text{ Kepler III}$$
 (A.3)

$$T_{vis} = \alpha_{vis} * 86'400$$
 (A.4)

$$FSPL = 20 * Log_{10}(\frac{4\pi * S * f_{center}}{c})$$
(A.5)

$$P_{Rx} = P_{Tx} - L_{Tx} + G_{Tx} - FSPL + G_{Rx} - L_{Rx}$$
(A.6)

$$P_{\text{noise}} = 10 * log_{10}[k_b(T_{sys} + T_{Moon})B]$$
 (A.7)

$$G_{Rx} = 10 * Log_{10}((\frac{\pi * A_{Rx} * f_{center}}{c})^2) + 10 * Log_{10}(\eta_{Rx})$$
(A.8)

$$R_b = B * log_2(n_{QPSK}) \tag{A.9}$$

$$SNR_{dB} = P_{Rx} - 30 - P_{\text{noise}} \tag{A.10}$$

$$SNR_{linear} = 10^{\frac{SNR_{dB}}{10}} \tag{A.11}$$

$$\frac{E_b}{N_0} = SNR_{dB} + 10 * Log_{10}(\frac{B}{R_b})$$
 (A.12)

$$BER = 1 - \Phi\left(\sqrt{2 \cdot \frac{E_b}{N_0}}\right) \tag{A.13}$$

$$R_D = R_b * R_{code} * (1 - R_{framing}) \tag{A.14}$$

$$T_{DL,max} = \frac{D_{24d}}{R_D} \tag{A.15}$$

A.1 Relay visibility time estimation

To get an estimate of the time a satellite at altitude 1500 km would be visible to a lander at least 20 deg above the horizon, a graphical approach was chosen as shown in Figure A.1. From there, $\gamma = \arctan(\frac{\Im(z)}{\Re(z)})$ provides the elevation angle from the lunar center. Since the altitude is defined as 1500 km, Kepler III $(T^2 = \frac{4\pi^2}{GM_{Moon}}a^3)$ yields a total orbit time of $\approx 1.65 \times 10^4~s$. To get a visibility ratio, $\alpha_{vis} = \frac{3*(90-\gamma)}{360}$ yields around 0.22, which can be easily translated to time, using $T_{max} = \alpha_{vis} * T_{orbit}$ and yielding $\approx 3600~s$, meaning roughly one hour.

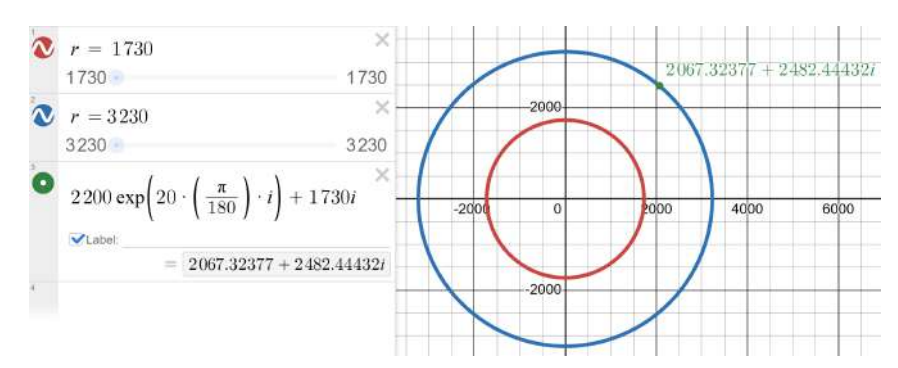


Figure A.1: Using Desmos online graphing calculator, it is possible to estimate the coordinates and thus the angle where a relay satellite at altitude 1500 km rises above 20 deg above the horizon.

98 A.2. Other estimations

A.2 Other estimations

Telemetry (seismic station, $R_{S,HK}$) 128 bps might be four 16-bit values, measured twice per second. This is enough to collect some essential telemetry such as temperatures and voltages.

Telemetry (lander, $R_{L,HK}$) 256 bps might be eight 16-bit values, measured twice per second. Enough to get an overview over the system.

Uplinked Data (R_{up}) 128 bps might be of the form of 3.3×10^7 bits/72h, enough to push small firmware updates or other command and control messages.

Station data storage time $(T_{S,store})$ 10 s are enough to circumvent small outages, while keeping energy consumption and complexity per station minimal

Station data storage size 1.6×10^4 bits is enough to store 10 seconds of data with margin.

CAN PLC data request delay $(T_{CAN,init})$ 0.1 s is a high estimate of what other telemetry and command messages need to be passed over CAN to initiate data collection.

Compression efficiency (R_{comp}) 2x is a comfortable lossless compression efficiency. It causes substantial storage capacity increase while not pushing the limits of compression theory.

Data storage capacity 1 GB is not much in modern data systems, but enough for the SILENCE use case with comfortable margin.

Tx internal losses (L_{Tx}) 0.2 dB has been given as a realistic lecture example. Since a temperature-controlled station might be close to standard, this value has been adapted.

Rx antenna efficiency (η_{Rx}) 0.7 has been given in a lecture as realistic antenna efficiency. Since this concerns a high-tech lunar relay satellite, this value has been deemed representational.

Relay + Lunar Noise Temperature $(T_{sys} + T_{Moon})$ 300 K might include lunar noise temperature of 160-230K [70] with the addition of some unknown relay system temperature, presumably below 100 K for lunar orbit.

Rx internal losses (L_{Rx}) 0 dB might be realistic for very high-tech systems, provided in a lecture. Since lunar relays have to be high-tech to operate effectively, this value was chosen.

Altitude (h) 1500 km is a compromise. Lunar gravity is low and the moon has no atmosphere, so orbits could be lower, but the Lunar Gateway station has a planned periapsis of around 1500 km [93].

Bandwidth (B) $6 \times 10^6 \ Hz$ seems to be a cutoff frequency between low and high bandwidth in LunaNet specifications [7]. This is enough to comfortably downlink data while not falling into high bandwidth territory that is not allowed to use S-band transmissions anymore.

Code Rate (R_{code}) $\frac{1}{2}$ is a common coding rate, together with $\frac{2}{3}$. $\frac{1}{2}$ is lower and has greater error correction capability over the channel.

Framing Overhead ($R_{framing}$) 0.1 is an upper bound for overhead such as headers, routing and CRC (cyclic redundancy checks). With a BER of below 10^{-6} , occasional retransmission also fits into this margin.

Description	Formula or Source	Value	Unit
Transmitter			
Generated Data after 24 days (D_{24d})	Equation A.1	3.80×10^{9}	bits
Antenna Output Power (P_{Tx})	[20]	40	W
Transmit gain (G_{Tx})	[69]	6	dBi
Tx internal losses (L_{Tx})	section A.2	0.2	dB
Minimum elevation angle (δ)	Figure 5.3b, section 3.5	20	\deg
Receiver			
Rx aperture size (A_{Rx})	[53]	1.25	\mathbf{m}
Rx antenna efficiency (η_{Rx})	section A.2	0.7	
Relay + Lunar Noise Temperature $(T_{sys} +$	[70], section A.2	300	K
$T_{Moon})$			
Rx internal losses (L_{Rx})	section A.2	0	dB
Channel			
Altitude (h)	section A.2	1.5×10^{6}	\mathbf{m}
Slant Range (S)	Equation A.2	2.2×10^{6}	\mathbf{m}
Orbital Period (T_{orbit})	Equation A.3	1.65×10^{4}	S
Orbital visibility fraction (α_{vis})	section A.1	0.22	
Maximum overpass visibility time (T_{max})	section A.1	3623	S
Seconds of visibility per day (T_{vis})	Equation A.4	1.9×10^{4}	S
Signal values of QPSK (n_{QPSK})	[91]	4	
Carrier center frequency (f_{center})	[7]	2.74×10^{10}	Hz
Bandwidth (B)	section A.2	6×10^{6}	Hz
CMB noise temperature	[92]	2.7	K
FSPL	Equation A.5	188.0	dB
Code Rate (R_{code})	section A.2	0.5	
Framing Overhead $(R_{framing})$	section A.2	0.1	
Channel Metrics			
Received power (P_{Rx})	Equation A.6	-86.7	dBm
Noise power (P_{noise})	Equation A.7	-106.01	dBm
$\operatorname{Rx} \operatorname{Gain} (G_{Rx})$	Equation A.8	49.5	dB
Bit Rate (R_b)	Equation A.9	1.2×10^{7}	bps
SNR_{dB}	Equation A.10	19.3	dB
SNR_{linear}	Equation A.11	85.7	
E_b/N_0	Equation A.12	16.3	dB
BER	Equation A.13	5.56×10^{-9}	
Data Rate (R_D)	Equation A.14	5.4×10^{6}	bps
Downlink duration $(T_{DL,max})$	Equation A.15	759	\mathbf{s}

Table A.2: Communication link calculation data.

Appendix B

Additional Material on Deployment

B.1 Propellant required for a 6-Minute lunar hover

Assuming a lander mass of 5'000kg for the Argonaut lander after EDL and a 10km hop at roughly 100km/h approximated as a 6-minute hover, relative exhaust velocity of 2'000m/s [94] the amount of fuel used for the hop is derived below hover: thrust equals lunar weight,

$$T = mq$$
.

$$\dot{m} = \frac{T}{c} = \frac{mg}{c}.$$

$$\frac{dm}{dt} = -\dot{m} = -\frac{g}{c} \, m.$$

(g is negative) initial mass

$$m(t) = m_0 e^{-gt/c},$$

 m_0

For a $t = 6 \min = 360 s$ hover

$$\Delta m = m_0 \left(1 - e^{-g \cdot 360/c} \right).$$

$$\Delta m = 5000 \text{ kg} \left(1 - e^{-(1.62 \text{ m/s}^2)(360 \text{ s})/(2000 \text{ m/s})} \right) \approx 1,265 \text{ kg}.$$

B.2 FLEX rover aboard an Ariane 6 geometry check



Figure B.1: Illustration showing the FLEX rover with suited humans. The red ligns are all equally long, around 1.7m, hinting that a rover length of 3.8m could be right [5].

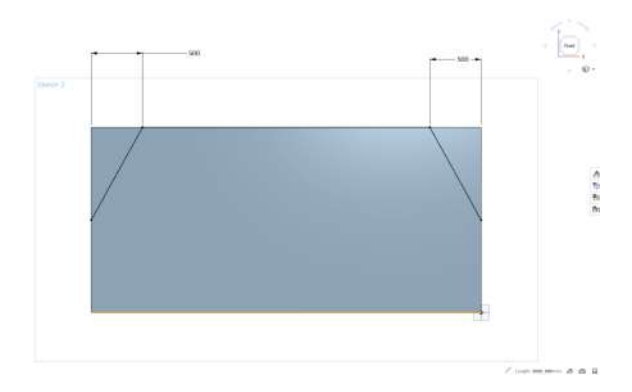


Figure B.2: Image showing the sketch used to cut a 3.8x2.6x1.8 cuboid to the shape of the rover dummy in Figure 6.6. Screenshots from Onshape.

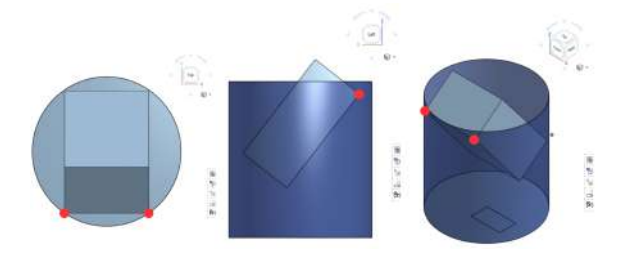


Figure B.3: Screenshot from Oneshape showing a 3.8x2.6x1.7m Box (FLEX rover dimensions) inside a 4.6m diameter, 5m high cylinder (dimensions of non-conical part of Ariane 6 payload fairing of the single launch short fairing [9]). Red dots represent corners constrained to lie on the cylinder boundary. The part exceeding the 5m cylinder would not collide with the conical part of the Ariane 6 payload fairing [9].

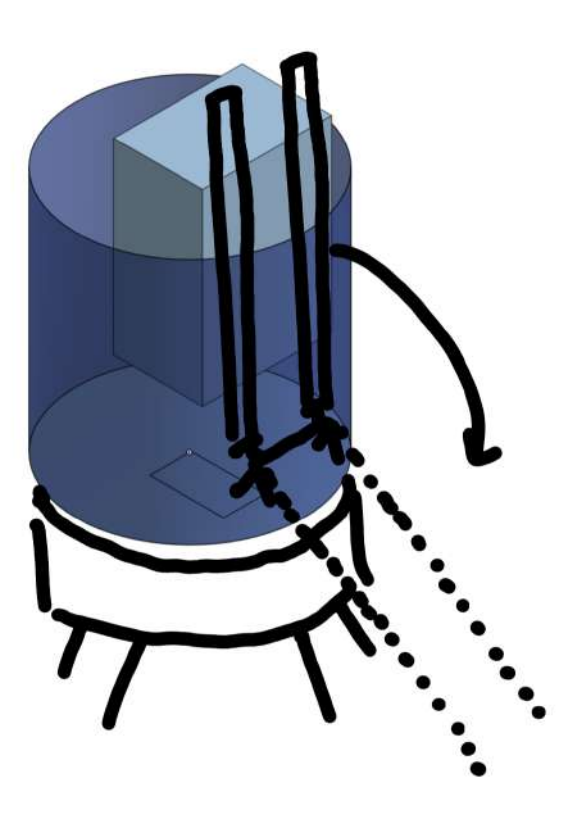


Figure B.4: Sketch showing vertical rover mounting inside the payload fairing, appart from the main lever, additional structures supporting the rover until egress could be necessary.

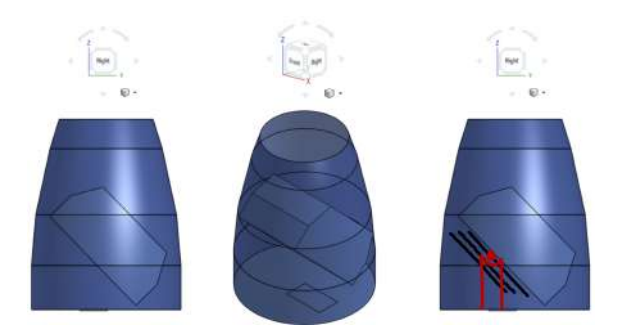


Figure B.5: Images showing the FLEX rover dummy inside a model of the dual launch short DLS fairing of the Ariane 6. Only the top fairing bay is shown. The bottom 3m (assumption on Argonaut lander height made based on Figure 6.5) of the top fairing bay are assumed to be occupied by the Argonaut Lander. The rightmost graphic includes a sketch of a tiltable telescopic ramp. The payload fairing has been modeled according to [9]. A screenshot of the CAD sketch can be found in Figure B.6 Screenshots from Onshape.

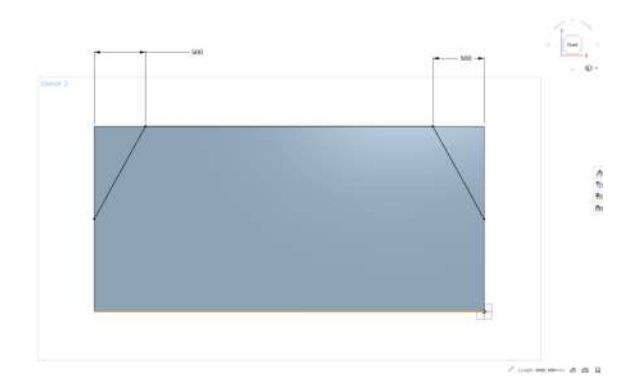


Figure B.6: Sketch used to model the relevant section of the payload fairing in Figure B.5. Screenshot from Onshape.

Appendix C

LCA Additional Plots

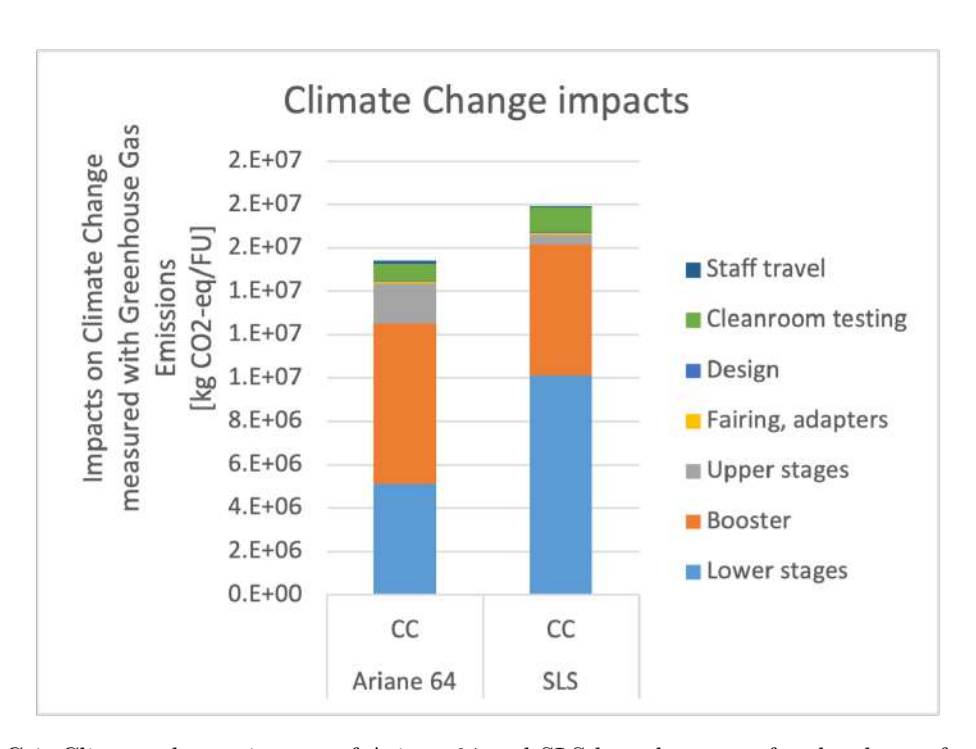


Figure C.1: Climate change impact of Ariane 64 and SLS launch system for the chosen functional unit with subcategory breakdown

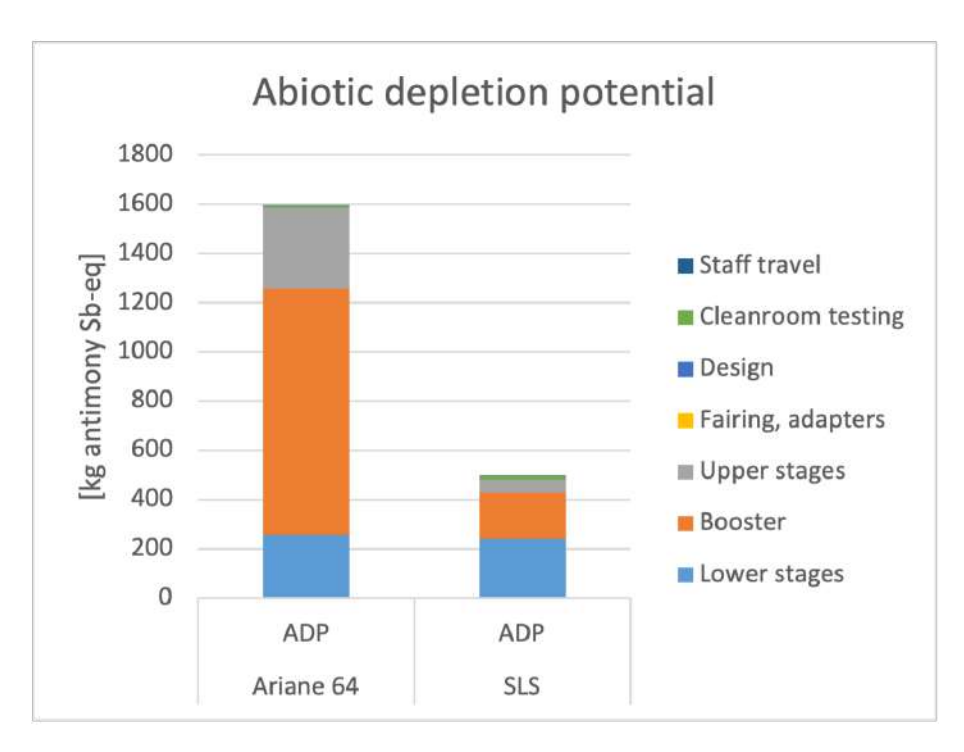


Figure C.2: Abiotic depletion potential of Ariane 64 and SLS launch system for the chosen functional unit with subcategory breakdown

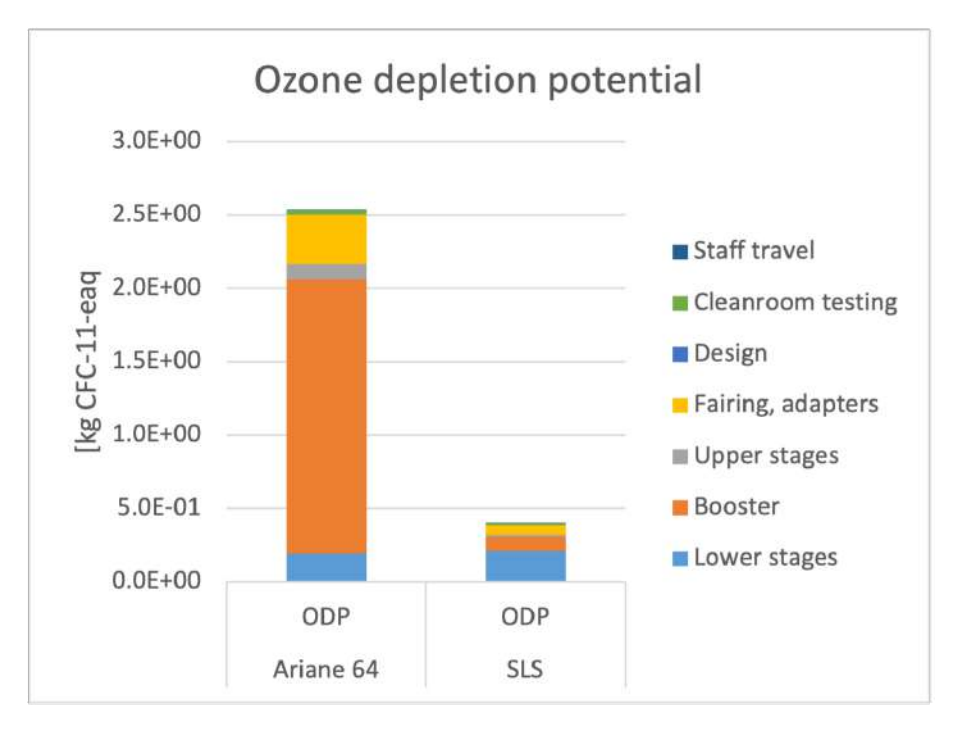


Figure C.3: Ozone depletion potential of Ariane 64 and SLS launch system for the chosen functional unit with subcategory breakdown

Appendix D

Use of Artificial Intelligence

In this work, LLMs and other AI tools were used to quickly explore concepts, perform surface-level research, assist in coding, and aid report creation through text refinement and suggestions.

- [1] N. Schorghofer and J.-P. Williams, "Mapping of ice storage processes on the moon with time-dependent temperatures," *The Planetary Science Journal*, vol. 1, no. 3, p. 54, 2020.
- [2] N. Catherine G. Manning, "Technology readiness levels," accessed 14.11.25. [Online]. Available: https://www.nasa.gov/directorates/somd/space-communications-navigation-program/technology-readiness-levels/
- [3] J. V. van Heijningen, H. J. M. ter Brake, O. Gerberding, S. Chalathadka Subrahmanya, J. Harms, X. Bian, A. Gatti, M. Zeoli, A. Bertolini, C. Collette, A. Perali, N. Pinto, M. Sharma, F. Tavernier, and J. Rezvani, "The payload of the lunar gravitational-wave antenna," *Journal of Applied Physics*, vol. 133, no. 24, Jun. 2023. [Online]. Available: http://dx.doi.org/10.1063/5.0144687
- [4] P. Ajith, P. A. Seoane, M. A. Sedda, R. Arcodia, F. Badaracco, B. Banerjee, E. Belgacem, G. Benetti, S. Benetti, A. Bobrick *et al.*, "The lunar gravitational-wave antenna: Mission studies and science case," *arXiv* preprint arXiv:2404.09181, 2024.
- [5] Astrolab, "Flex rover astrolab," accessed 14.11.25. [Online]. Available: https://www.astrolab.space/flex-rover/
- [6] G. D. Felice, "What is a risk matrix, how to prioritize risks in project management," accessed 14.11.25. [Online]. Available: https://www.gustavodefelice.com/p/what-is-a-risk-matrix-how-to-prioritize-severity
- [7] N. S. C. B. Secretariat, "Lunanet interoperability specification document version 5," accessed 14.11.25. [Online]. Available: https://www.nasa.gov/wp-content/uploads/2025/02/lunanet-interoperability-specification-v5-baseline.pdf
- [8] ESA, "Argonaut: a first european lunar lander," accessed 14.11.25. [Online]. Available: https://www.esa.int/Science_Exploration/Human_and_Robotic_Exploration/Argonaut_a_first_European_lunar_lander
- [9] G. D. Felice, "Ariane 6 user manual as of february 2021," accessed 14.11.25. [Online]. Available: https://ariane.group/app/uploads/sites/4/2024/10/Mua-6_Issue-2_Revision-0_March-2021.pdf
- [10] J. Harms, "Lgwa; presentation of mission concept, science case, and payload." [Online]. Available: lgwa.unicam.it
- [11] J. Harms, F. Ambrosino, L. Angelini, V. Braito, M. Branchesi, E. Brocato, E. Cappellaro, E. Coccia, M. Coughlin, R. Della Ceca et al., "Lunar gravitational-wave antenna," The Astrophysical Journal, vol. 910, no. 1, p. 1, 2021.
- [12] K. L. Ryder and M. J. Campola, "The lunar radiation environment, nasa gsfc conference,code 561 4/27/2022," https://ntrs.nasa.gov/api/citations/20220007070/downloads/20220007070-Kaitlyn-Ryder-2022-LaRC-Presentation_v2.pdf, August2022, accessed14.11.25.

[13] S. Z. et al., "First measurements of the radiation dose on the lunar surface | science advances," *Science Advances*, 2020.

- [14] Wikipedia, "Radiation hardening," accessed 14.11.25. [Online]. Available: https://en.wikipedia.org/wiki/Radiation_hardening
- [15] NASA, "Moon dust," accessed 14.11.25. [Online]. Available: https://science.nasa.gov/moon/moondust/
- [16] —, "Lunar dust considerations for vertical solar arrays volume 1: Lunar environment and dust interactions," accessed 14.11.25. [Online]. Available: https://ntrs.nasa.gov/api/citations/20240003496/downloads/TM-20240003496.pdf
- [17] p. f. M. S. F. C. M. Rais-Rohani, Mississippi State University, "On structural design of a mobile lunar habitat with multi-layered environmental shielding," accessed 14.11.25. [Online]. Available: https://ntrs.nasa.gov/api/citations/20050185204/downloads/20050185204.pdf
- [18] NASA, "Viper in depth," accessed 14.11.25. [Online]. Available: https://science.nasa.gov/mission/viper/in-depth/
- [19] J.-P. Williams, B. Greenhagen, D. Paige, N. Schorghofer, E. Sefton-Nash, P. Hayne, P. Lucey, M. Siegler, and K. M. Aye, "Seasonal polar temperatures on the moon," *Journal of Geophysical Research: Planets*, vol. 124, no. 10, pp. 2505–2521, 2019.
- [20] J. R. Wertz, D. F. Everett, and J. J. Puschell, Eds., Space Mission Engineering: The New SMAD. Microcosm Press, 2011.
- [21] Nasa, "Weather on the moon," accessed 14.11.25. [Online]. Available: https://science.nasa.gov/moon/weather-on-the-moon/
- [22] A. Biradar, S. Arulvel, and J. Kandasamy, "Significance of ballistic parameters and nanohybridization in the development of textile-based body armor: A review," *International Journal of Impact Energy*, vol. 180, 2023.
- [23] A. J. Christiansen, M. Popelka, B. G. Gom, D. A. Naylor, and A. A. Stolov, "Characterization of optical fiber at cryogenic temperatures," 2023. [Online]. Available: https://www.ofsoptics.com/wp-content/uploads/Characterization-of-optical-fiber-at-cryogenic-temperatures.pdf?srsltid= AfmBOopvBVOyLW5zgPfEbnsQz4iSeSjOVH2FqE66VNETRkFp3AR3ulHa
- [24] A. Saha and M. Ghassemi, "Developing an mvdc bipolar coaxial cable system for lunar power transmission," in 2024 IEEE Conference on Electrical Insulation and Dielectric Phenomena (CEIDP), 2024, pp. 1–4.
- [25] Wikipedia contributors. (2025) Kapton. Accessed 14.11.25. [Online]. Available: https://en.wikipedia.org/wiki/Kapton
- [26] —. (2025) Polytetrafluoroethylene. Accessed 14.11.25. [Online]. Available: https://en.wikipedia.org/wiki/Polytetrafluoroethylene
- [27] P. Gläser, J. Oberst, G. Neumann, E. Mazarico, E. Speyerer, and M. Robinson, "Illumination conditions at the lunar poles: Implications for future exploration," *Planetary and Space Science*, vol. 162, pp. 170–178, 2018.
- [28] M. K. Barker, E. Mazarico, G. A. Neumann, D. E. Smith, M. T. Zuber, J. W. Head, and X. Sun, "A new view of the lunar south pole from the lunar orbiter laser altimeter (lola)," *The Planetary Science Journal*, vol. 4, no. 9, p. 183, 2023.
- [29] E. Mazarico, G. Neumann, D. Smith, M. Zuber, and M. Torrence, "Illumination conditions of the lunar polar regions using lola topography," *Icarus*, vol. 211, no. 2, pp. 1066–1081, 2011.

[30] H. Brown, A. Boyd, A. Sonke, A. Huft, M. Robinson, and E. Cisneros, "Lunar reconnaissance orbiter camera permanently shadowed region images: Updates to psr atlas and psr mosaics," in *Lunar Polar Volatiles Conference*, vol. 2703, 2022, p. 5033.

- [31] NASA, "Nasa identifies candidate regions for landing next americans on moon," https://www.nasa.gov/news-release/nasa-identifies-candidate-regions-for-landing-next-americans-on-moon/, National Aeronautics and Space Administration, August 2022, accessed 14.11.25.
- [32] L. L. Team, "Lunarleaper," accessed 14.11.25. [Online]. Available: https://www.lunarleaper.space/
- [33] Wikipedia, "Rover(space exploration)," accessed 14.11.25. [Online]. Available: https://en.wikipedia.org/wiki/Rover_(space_exploration
- [34] —, "Artemis program," accessed 14.11.25. [Online]. Available: https://en.wikipedia.org/wiki/Artemis_program
- [35] NASA, "Nasa selects companies to advance moon mobility for artemis missions," accessed 14.11.25. [Online]. Available: https://www.nasa.gov/news-release/nasa-selects-companies-to-advance-moon-mobility-for-artemis-missions/
- [36] U. G. S. Administration, "Lunar terrain vehicle (ltv) request for information," accessed 14.11.25. [Online]. Available: https://sam.gov/opp/46cd587dcba34a8e96792f26d3c7a8d8/view
- [37] V. Space, "Venturi space|our rovers," accessed 14.11.25. [Online]. Available: https://venturi.space/en/rovers/
- [38] Venturi, "Venturi 2023 facebook post," accessed 14.11.25. [Online]. Available: https://www.facebook.com/photo.php?fbid=685329760304847&id=100064834862741&set=a.455647223273103
- [39] J. Space, "Everything we know about the rover nasa's artemis astronauts will drive on the moon," accessed 14.11.25. [Online]. Available: https://jatan.space/what-we-know-about-artemis-ltv/
- [40] A. C. International, "Flex: a monegasque astromobile on the moon," accessed 14.11.25. [Online]. Available: https://aircosmosinternational.com/article/flex-a-monegasque-astromobile-on-the-moon-3792
- [41] NASA, "Lunar logistics frequently asked questions," accessed 14.11.25. [Online]. Available: https://ntrs.nasa.gov/api/citations/20210019235/downloads/2021-7-28%20FAQ--Data%20Package.pdf
- [42] F. in Space, "Astrolab venturi," accessed 14.11.25. [Online]. Available: https://www.factoriesinspace.com/astrolab
- [43] NASA, "Mars 2020 perseverance rover," accessed 14.11.25. [Online]. Available: https://science.nasa.gov/mission/mars-2020-perseverance/rover-components/
- [44] J. E. J. James Tuttle Keane (JPL), Sonia M. Tikoo (Stanford), "Endurance lunar south pole–aitken basin traverse and sample return rover mission concept study report for the 2023–2032 planetary science and astrobiology decadal survey," https://science.nasa.gov/wp-content/uploads/2023/11/endurance-spa-traverse-and-sample-return.pdf, Nasa, Tech. Rep., 2023.
- [45] C. Ames Research Center, Moffet Field, "State-of-the-art small spacecraft technology," NASA, Tech. Rep., 2024. [Online]. Available: https://newspaceeconomy.ca/wp-content/uploads/2024/02/soa-report-2023.pdf
- [46] W. Sun, Q. Wang, J. Zhang, B. Zhao, L. Shi, M. Hu, M. Li, H. Yang, X. Ao, and G. Pei, "Comprehensive assessment of photovoltaic designs and power generation potential at lunar south pole," Energy, vol. 335, p. 137922, 2025.
- [47] A. S. P. GMBH, "30
- [48] P. D. Desai, H. M. James, and C. Y. Ho, "Electric resistivity of aluminum and manganese," *Journal of Physical and Chemical Reference Data*, vol. 13, 1984.

[49] F. Grassi, S. A. Pignari, and J. Wolf, "Assessment of can performance for powerline communications in dc differential buses," in 2009 IEEE International Conference on Microwaves, Communications, Antennas and Electronics Systems. IEEE, 2009, pp. 1–6.

- [50] Y. E. Ltd., "Redundant can-bus networks using dc-can powerline communication," accessed 14.11.25. [Online]. Available: https://yamar.com/can-bus-redundancy/
- [51] S. Gersten, "U.s. leadership in lunar spectrumpolicy," accessed 14.11.25. [Online]. Available: https://aerospace.csis.org/wp-content/uploads/2025/03/Lunar-Spectrum-Policy-.pdf
- [52] G. E. NASA and T. Directorate, "Lunar communications relay and navigation systems (lcrns)," accessed 14.11.25. [Online]. Available: https://etd.gsfc.nasa.gov/our-work/lcrns/
- [53] E. S. A. (ESA), "Gateway: Lunar link," accessed 14.11.25. [Online]. Available: https://www.esa.int/Science_Exploration/Human_and_Robotic_Exploration/Gateway_Lunar_Link
- [54] ——, "Esa's moonlight programme: Pioneering the path for lunar exploration," accessed 14.11.25. [Online]. Available: https://www.esa.int/Applications/Connectivity_and_Secure_Communications/ESA_s_Moonlight_programme_Pioneering_the_path_for_lunar_exploration
- [55] M. Murata, "Japan lunar navigation satellite system (lnss) and its contribution towards 'moon gnss'," accessed 14.11.25. [Online]. Available: https://bsgn.esa.int/wp-content/uploads/2024/02/06-Masaya_Murata_JAXA_presentation.pdf
- [56] C. Space, "Introducing parsec," accessed 14.11.25. [Online]. Available: https://crescentspace.com/
- [57] ArkEdgeSpace, "Lunar infrastructure, translating earth infrastructure for the moon," accessed 14.11.25. [Online]. Available: https://arkedgespace.com/en/projects/lunar-infrastructure
- [58] S. TM, "Scaling quantum systems with semiqon cryo-cmos," accessed 14.11.25. [Online]. Available: https://www.semiqon.tech/technology/semiqon-cryo-cmos
- [59] C. T. C. C. for Space Data Systems, "Overview of space communications protocols," accessed 14.11.25. [Online]. Available: https://ccsds.org/Pubs/130x0g4e1.pdf
- [60] A. Technology, "Persistent. instant. radiation-immune. space grade storage," accessed 14.11.25. [Online]. Available: https://www.avalanche-technology.com/products/discrete-mram/storage/
- [61] J. Fesmire and W. Johnson, "Thermal performance data for multilayer insulation systems tested between 293 k and 77 k," 05 2015.
- [62] J. Gaier, K. Street, and R. Gustafson, "Measurement of the solar absorptance and the thermal emittance of lunar simulants," 07 2010.
- [63] C. R. Buhler, M. R. Johansen, M. Dupuis, J. Phillips, J. Malissa, J. Wang, and C. I. Calle, "Current state of the electrodynamic dust shield for mitigation," in *The Impact of Lunar Dust on Human Exploration*. Houston, Texas, USA: Lunar and Planetary Institute, Feb. 2020, conference paper presented at The Impact of Lunar Dust on Human Exploration Workshop, February 11–13, 2020. NASA Technical Reports Server (NTRS) 20200000920, Report No. KSC-E-DAA-TN77159. [Online]. Available: https://ntrs.nasa.gov/citations/20200000920
- [64] S. Plucinsky, "Nasa's dust shield successfully repels lunar regolith on moon," https://www.nasa. gov/image-article/nasas-dust-shield-successfully-repels-lunar-regolith-on-moon/, Mar. 2025, image article, NASA.
- [65] N. G. R. Center, "Nasa's fission surface power project energizes lunar exploration," https://www.nasa.gov/centers-and-facilities/glenn/nasas-fission-surface-power-project-energizes-lunar-exploration/, 2024, accessed 14.11.25.

[66] R. J. Jones, S. McFarland, S. Rodgers-Ahnen, and R. Rhodes, "Artemis suit material project overview," in 54th International Conference on Environmental Systems (ICES), Prague, Czech Republic, Jul. 2025, paper ICES-2025-56.

- [67] J. Elliott and L. Alkalai, "Lunette: A low-cost concept enabling multi-lander lunar science and exploration missions," *Acta Astronautica*, vol. 66, no. 1, pp. 269–278, 2010. [Online]. Available: https://www.sciencedirect.com/science/article/pii/S0094576509003294
- [68] I. SAGE Millimeter, "Sae-2832930645180-28-s1," accessed 14.11.25. [Online]. Available: https://sftp.eravant.com/content/datasheets/SAE-2832930645180-28-S1.pdf
- [69] B. Gravity, "K/ka-band ttc antennas," accessed 14.11.25. [Online]. Available: https://www.beyondgravity.com/sites/default/files/media_document/2025-11/Beyond% 20Gravity%20K%20Ka-band-TTC%20Antennas_Space_Satellites_01-25.pdf
- [70] D. Morabito, "Lunar noise-temperature increase measurements at s-band, x-band, and ka-band using a 34-meter-diameter beam-waveguide antenna," *The Interplanetary Network Progress Report*, vol. 42, p. 166, 2006.
- [71] R. W. Hyers, M. P. C. Briana N. Tomboulian University of Massachusetts, Amherst, and J. R. N. MSFC, "Lightweight, high-temperature radiator for space propulsion," accessed 14.11.25. [Online]. Available: https://ntrs.nasa.gov/api/citations/20130001608/downloads/20130001608.pdf
- [72] M. S. El-Genk, "Esi continuation review: Grant performance summary advanced lightweight heat rejection radiators for space nuclear power systems," University of New Mexico, Institute for Space and Nuclear Power Studies (UNM-ISNPS) and Nuclear Engineering Department, NASA Grant Performance Summary NASA Grant 21-ESI-0049, Nov. 2022.
- [73] Wikipedia, "Glass fiber wikipedia," accessed 14.11.25. [Online]. Available: https://en.wikipedia.org/wiki/Glass fiber
- [74] A. Venturi, "Flex payload interface guide," accessed 14.11.25. [Online]. Available: https://astrolab-images.s3.amazonaws.com/pdf_files/Payload_Interface_Guide.pdf
- [75] J. Burger, M. ter Brake, H. Holland, R. Meijer, T. Veenstra, G. Venhorst, D. Lozano-Castello, M. Coesel, and A. Sirbi, "Long-life vibration-free 4.5 k sorption cooler for space applications," *The Review of scientific instruments*, vol. 78, p. 065102, 07 2007.
- [76] L. Fayon, B. Knapmeyer-Endrun, P. Lognonné et al., "A numerical model of the seis leveling system transfer matrix and resonances: Application to seis rotational seismology and dynamic ground interaction," Space Science Reviews, vol. 214, p. 119, 2018. [Online]. Available: https://doi.org/10.1007/s11214-018-0555-9
- [77] D. Bugby, J. Farmer, and C. Stouffer, "Development and testing of a variable conductance thermal acquisition, transport, and switching system," 07 2013.
- [78] Astrobotic, "Astrobotic lunar landers payload user's guide," accessed 14.11.25. [Online]. Available: https://www.astrobotic.com/wp-content/uploads/2022/01/PUGLanders_011222.pdf
- [79] T. George, B. E. Morales, M. M. Munk, J. M. Carson, E. J. Anzalone, M. A. Rubio, S. Lawrence, R. A. Lugo, and A. M. Korzun, "Safe and precise landing at lunar sites," 2024.
- [80] ESA, "Argonaut: Europe's lunar lander programme," accessed 14.11.25. [Online]. Available: https://www.esa.int/Science_Exploration/Human_and_Robotic_Exploration/Exploration/Argonaut Europe s lunar lander programme
- [81] Wikipedia, "Argonaut(lunar lander)," accessed 14.11.25. [Online]. Available: https://en.wikipedia.org/wiki/Argonaut_(lunar_lander)
- [82] —, "Ariane 6," accessed 14.11.25. [Online]. Available: https://en.wikipedia.org/wiki/Ariane_6

[83] SpaceX. (2025) Starship. Accessed 14.11.25. [Online]. Available: https://www.spacex.com/vehicles/starship

- [84] Wikipedia contributors. (2025) Spacex starship. Accessed 14.11.25. [Online]. Available: https://en.wikipedia.org/wiki/SpaceX Starship
- [85] —. (2025) Space launch system. Accessed 14.11.25. [Online]. Available: https://en.wikipedia.org/wiki/Space_Launch_System
- "Call "13" [86] ESA, for mission concepts for the large-size mission opportunity accessed 14.11.25. [Online]. inesa's science programme," Available: https://www.cosmos.esa.int/documents/1137049/1137100/Call_for_L3_Gravitational+ $waves_missions.pdf/1f0a7dc8-b615-4d09-ba02-9bcda992e4d5$
- [87] P. D. K. Danzmann, "Laser interferometer space antenna," accessed 14.11.25. [Online]. Available: https://www.lisamission.org/wp-content/uploads/2024/01/LISA_L3_20170120.pdf
- [88] Wikipedia, "Jupiter icy moons explorer," accessed 14.11.25. [Online]. Available: https://en.wikipedia.org/wiki/Jupiter_Icy_Moons_Explorer#Background
- [89] ESA, "Selection of the l1 mission," accessed 14.11.25. [Online]. Available: https://www.spektrum.de/fm/976/ESA-SPC.pdf
- [90] NASA, "Nicm: Cryocooler," accessed 14.11.25. [Online]. Available: https://www.nasa.gov/wp-content/uploads/2023/06/14-nicmcryocooler-costsymposium-2017-urs-final-tagged.pdf
- [91] A. Devices, "Qpsk," accessed 14.11.25. [Online]. Available: https://www.analog.com/en/resources/glossary/qpsk.html
- [92] E. S. A. (ESA), "Planck and the cosmic microwave background," accessed 14.11.25. [Online]. Available: https://www.esa.int/Science_Exploration/Space_Science/Planck/Planck_and_the_cosmic microwave background
- [93] S. K. Johnson, D. J. Mortensen, M. A. Chavez, and C. L. Woodland, "Gateway–a communications platform for lunar exploration," in 38th International Communications Satellite Systems Conference (ICSSC 2021), vol. 2021. IET, 2021, pp. 9–16.
- [94] A. O. PROPULSION, "1n, 20n, 400n and heritage thruster -chemical monopropellant thruster family," accessed 14.11.25. [Online]. Available: https://www.space-propulsion.com/brochures/hydrazine-thrusters/hydrazine-thrusters.pdf